

UC Davis

UC Davis Electronic Theses and Dissertations

Title

The Physiological and Evolutionary Implications of Histone PTMs in Mozambique Tilapia

Permalink

<https://escholarship.org/uc/item/8qt5d45g>

Author

Mojica, Elizabeth Ann

Publication Date

2023

Supplemental Material

<https://escholarship.org/uc/item/8qt5d45g#supplemental>

Peer reviewed|Thesis/dissertation

The Physiological and Evolutionary Implications of Histone PTMs in Mozambique Tilapia

By

ELIZABETH ANN MOJICA
DISSERTATION

Submitted in partial satisfaction of the requirements for the degree of

DOCTOR OF PHILOSOPHY

in

Ecology

in the

OFFICE OF GRADUATE STUDIES

of the

UNIVERSITY OF CALIFORNIA

DAVIS

Approved:

Dietmar Kltz, Chair

Hong Ji

Richard Connon

Committee in Charge

2023

TABLE OF CONTENTS

| | |
|--|-----------|
| ACKNOWLEDGEMENTS | V |
| ABSTRACT | VI |
| INTRODUCTION | 1 |
| AUTHOR LIST | 4 |
| CHAPTER 1 | 5 |
| A STRATEGY TO CHARACTERIZE THE GLOBAL HISTONE PTM LANDSCAPE WITHIN TISSUES OF NON-MODEL ORGANISMS | 5 |
| ABSTRACT | 5 |
| INTRODUCTION | 6 |
| EXPERIMENTAL PROCEDURES | 8 |
| <i>Experimental design and statistical rationale</i> | 8 |
| <i>Mechanical single cell suspension</i> | 8 |
| <i>Histone acid extraction</i> | 9 |
| <i>In-solution digestion of proteins into peptides</i> | 10 |
| <i>Construction of histone DIA assay libraries and DIA by LCMS</i> | 12 |
| <i>Strategy for histone PTM quantification</i> | 14 |
| <i>Statistical analyses</i> | 17 |
| RESULTS | 18 |
| <i>Reliable quantification of 503 biologically relevant histone PTMs</i> | 18 |
| <i>Characterization of histone H1</i> | 21 |
| <i>Characterization of histone H2A</i> | 23 |
| <i>Characterization of histone H2B</i> | 24 |
| <i>Characterization of histone H3</i> | 26 |
| <i>Characterization of histone H4</i> | 27 |
| <i>Tissue-specific variation in the global histone PTM landscape</i> | 29 |
| DISCUSSION..... | 31 |
| <i>The use of multiple digestion methods maximizes histone PTM coverage</i> | 31 |
| <i>The global histone PTM landscape distinctly varies by tissue in Mozambique tilapia</i> | 33 |
| <i>Metabolite concentrations in tissues may uphold global levels of histone modifications</i> | 35 |
| FIGURE LEGENDS | 38 |
| FIGURES | 43 |
| <i>Figure 1.1</i> | 43 |
| <i>Figure 1.2</i> | 44 |
| <i>Figure 1.3</i> | 45 |
| <i>Figure 1.4</i> | 46 |
| <i>Figure 1.5</i> | 47 |
| <i>Figure 1.6</i> | 48 |
| <i>Figure 1.7</i> | 49 |
| <i>Figure 1.8</i> | 50 |
| CHAPTER 2: | 51 |
| H3K14AC, H3K18UB, AND H1K16UB IDENTIFIED AS SALINITY-RESPONSIVE HISTONE PTMS IN MOZAMBIQUE TILAPIA (<i>OREOCHROMIS MOSSAMBICUS</i>) | 51 |
| ABSTRACT | 51 |

| | |
|--|------------|
| BACKGROUND..... | 52 |
| RESULTS | 55 |
| <i>Standards established for determining whether histone PTMs are salinity-responsive</i> | <i>55</i> |
| <i>Short-term salinity stress altered one histone PTM in the gills</i> | <i>56</i> |
| <i>Long-term salinity stress altered two histone PTMs in the testes</i> | <i>58</i> |
| <i>Human analogs of the salinity-responsive histone PTMs</i> | <i>60</i> |
| DISCUSSION..... | 60 |
| <i>Three histone PTMs responded to salinity stress in Mozambique tilapia tissues.....</i> | <i>60</i> |
| <i>The intensity and duration of the salinity challenge differentially impacted histone PTMs</i> | <i>63</i> |
| <i>Limitations and Recommendations for Future Studies.....</i> | <i>66</i> |
| CONCLUSIONS..... | 66 |
| METHODS..... | 67 |
| <i>Salinity Treatments and Tissue Collection</i> | <i>67</i> |
| <i>Processing samples for histone PTM analysis.....</i> | <i>69</i> |
| <i>Statistical analyses.....</i> | <i>71</i> |
| FIGURE LEGENDS | 73 |
| FIGURES | 79 |
| <i>Figure 2.1.....</i> | <i>79</i> |
| <i>Figure 2.2.....</i> | <i>80</i> |
| <i>Figure 2.3.....</i> | <i>81</i> |
| <i>Figure 2.4.....</i> | <i>82</i> |
| <i>Figure 2.5.....</i> | <i>83</i> |
| TABLES..... | 84 |
| <i>Table 2.1.....</i> | <i>84</i> |
| SUPPLEMENTAL FIGURES | 85 |
| <i>Supplemental Figure 2.1.....</i> | <i>85</i> |
| <i>Supplemental Figure 2.2.....</i> | <i>86</i> |
| <i>Supplemental Figure 2.3.....</i> | <i>87</i> |
| <i>Supplemental Figure 2.4.....</i> | <i>88</i> |
| <i>Supplemental Figure 2.5.....</i> | <i>89</i> |
| CHAPTER 3..... | 90 |
| ENVIRONMENTAL CONDITIONS ELICIT A SLOW BUT ENDURING RESPONSE OF HISTONE POST-TRANSLATIONAL MODIFICATIONS IN MOZAMBIQUE TILAPIA | 90 |
| ABSTRACT | 90 |
| SIGNIFICANCE STATEMENT | 91 |
| INTRODUCTION | 91 |
| RESULTS | 94 |
| <i>Lifetime exposure to environmental conditions.....</i> | <i>95</i> |
| <i>Long-term exposure to environmental conditions during development.....</i> | <i>96</i> |
| <i>Acclimation to environmental conditions during adulthood.....</i> | <i>97</i> |
| DISCUSSION..... | 98 |
| MATERIALS AND METHODS | 102 |
| <i>Salinity Treatments</i> | <i>102</i> |
| <i>Processing samples for histone PTM analysis.....</i> | <i>104</i> |
| <i>Statistical analyses.....</i> | <i>104</i> |
| FIGURE LEGENDS | 106 |
| FIGURES | 109 |
| <i>Figure 3.1.....</i> | <i>109</i> |

| | |
|---|------------|
| <i>Figure 3.2</i> | 110 |
| <i>Figure 3.3</i> | 111 |
| <i>Figure 3.4</i> | 112 |
| APPENDIX | 113 |
| PHYSIOLOGICAL MECHANISMS OF STRESS-INDUCED EVOLUTION | 113 |
| SUMMARY STATEMENT..... | 113 |
| ABSTRACT | 113 |
| INTRODUCTION | 114 |
| STRESS TRIGGERS MUTAGENESIS THROUGH INCREASED DNA DAMAGE AND DECREASED DNA REPAIR FIDELITY..... | 115 |
| STRESS CAUSES HERITABLE (EPIGENETIC) CHANGES IN HISTONE POST-TRANSLATIONAL MODIFICATIONS..... | 118 |
| STRESS ALTERS HERITABLE (EPIGENETIC) DNA METHYLATION PATTERNS..... | 121 |
| STRESS IMPACTS GENOME STRUCTURE THROUGH CHROMOANAGENESIS | 124 |
| STRESS AFFECTS THE ACTIVITY OF TRANSPOSABLE ELEMENTS..... | 126 |
| LIFE EXPERIENCE AND PHYSIOLOGY SHAPE EVOLUTION | 129 |
| CONCLUSIONS AND FUTURE PERSPECTIVES..... | 132 |
| FIGURE LEGENDS | 133 |
| FIGURES | 134 |
| <i>Figure 4.1</i> | 134 |
| <i>Figure 4.2</i> | 135 |
| TABLES..... | 136 |
| <i>Table 4.1</i> | 136 |
| <i>Table 4.2</i> | 137 |
| <i>Table 4.3</i> | 138 |
| <i>Table 4.4</i> | 139 |
| <i>Table 4.5</i> | 140 |
| BIBLIOGRAPHY | 141 |

ACKNOWLEDGEMENTS

My academic journey has been substantially enriched by the guidance and encouragement from my mentors. I would like to extend my sincerest thanks to my major professor, Dr. Dietmar Kltz, for giving me both the support and freedom to tackle the scientific questions that most fascinated me. Our numerous conversations about the potential of stress-induced evolution motivated me to conduct this research to the best of my ability. I would next like to thank my dissertation committee members, Dr. Hong Ji and Dr. Richard Connon, for their time and effort in reviewing my work. Their invaluable insights into experimental design enabled me to answer the most interesting questions with limited resources. I would also like to thank my qualifying exam committee members, Dr. Andrea Schreier, Dr. Anne Todgham, Dr. Michael Mienaltowski, Dr. Brian Gaylord, and Dr. Andrew Whitehead. They challenged me to think critically about the interconnectedness of scientific fields while appreciating the historical context of each discipline.

I would like to express my deepest gratitude to my Jarett, Amadeo, and Mojica families for continuously uplifting me throughout this journey. I am tremendously grateful for my husband, Cesar Mojica, who has been my greatest source of support. He has provided me with meals, laughter, and breaks when they were most needed. I want to thank my mother and sister for being the role models who empowered me to define success for myself. Lastly, I want to acknowledge and honor my late father, William Jarett, who instilled in me the belief that I can do anything to which I set my mind. His words of encouragement have propelled me through my academic journey.

ABSTRACT

This dissertation explored the physiological and evolutionary implications of histone post-translational modifications (PTMs) as epigenetic marks. It began with the development of methods to reliably analyze histone PTMs in non-model organisms. These methods were applied to Mozambique tilapia (*Oreochromis mossambicus*) to uncover how salinity stress in a euryhaline fish impacts histone PTMs in the gills, kidney, and testes. Further experimentation was performed to investigate how histone PTMs in the gills are impacted through time when Mozambique tilapia are exposed to salinity challenges during specific developmental stages. Several key results emerged from this dissertation, including the following. First, the methods developed for histone PTM analysis enabled the quantification of 503 biologically relevant histone PTMs, which were shown to exhibit remarkable tissue-specificity in the gills, kidney, and testes of Mozambique tilapia. Second, salinity stress was shown to induce a histone PTM response in both the gills and testes, signifying a potential for histone PTMs to play a role in salinity acclimation and adaptation, respectively. Third, ambient salinity was shown to elicit an unexpectedly slow, widespread, and enduring response of histone PTMs in the gills. Extending beyond the context of Mozambique tilapia, this dissertation advances histone PTM research in ecological contexts. It enables a comprehensive analysis of histone PTMs in non-model organisms and reveals the timescale through which histone PTMs are likely to respond to environmental conditions.

INTRODUCTION

Histone post-translational modifications (PTMs) are epigenetic marks that can both respond to environmental stimuli and regulate heritable patterns of gene expression in an organism (Norouzitallab et al., 2019; Weishaupt et al., 2010; Zhu et al., 2013). The flexibility and functionality of histone PTMs permit them to facilitate biological resilience to an organism's changing environment; however, little is known about histone PTMs in ecological contexts, largely due to the technical barriers in studying them (Atlasi and Stunnenberg, 2017; Burggren, 2014a; Eirin-Lopez and Putnam, 2019b). This dissertation overcame such barriers in order to explore the physiological and evolutionary implications of histone PTMs in Mozambique tilapia (*Oreochromis mossambicus*). Because Mozambique tilapia are euryhaline fish that experience wide shifts in ambient salinity in nature (Stickney, 1986; Whitfield and Blaber, 1979), this dissertation sought to investigate how salinity stress impacts histone PTMs through time. Histone PTMs in the gills, kidney, and testes were analyzed in this context, as gills and kidney are both osmoregulatory organs, and testes are representative of the male germ line, where environmentally-induced histone PTMs can be transferred to future generations (Kültz, 2015; Mojica and Kültz, 2022; Sardella and Brauner, 2016).

The first chapter of this dissertation delineated a new strategy for quantifying histone PTMs in the tissues of non-model organisms. In following this strategy, tissue samples from Mozambique tilapia were dissociated into cells, samples were enriched for histone proteins, then histone proteins were digested into peptides using multiple digestion conditions. All sets of histone peptides were analyzed via liquid chromatography mass spectrometry, which yielded values of histone peptide abundance. New equations were used to quantify histone PTMs based

on values of histone peptide abundance, specifically when the histone peptides were derived through multiple protein digestions and contained multiple modification states. The average relative abundance of each histone PTM was calculated for the gills, kidney, and testes of Mozambique tilapia. These values were compared between tissues to ascertain the tissue-specificity of histone PTMs in this species.

The second chapter of this dissertation examined the influence of salinity stress on histone PTMs within Mozambique tilapia tissues. For this purpose, freshwater-adapted fish were exposed to salinity treatments that varied in intensity and duration. To investigate the histone PTM response to the strongest short-term salinity stress that Mozambique tilapia can tolerate, fish were exposed to 1) freshwater, 2) seawater for two hours, or 3) seawater for two hours followed by a recovery period in freshwater for an additional two hours (Hwang et al., 1989; Moorman et al., 2014; Moorman et al., 2015). To investigate how histone PTMs are impacted by longer-term exposure to salinity near the fish's upper tolerance limit, and whether the histone PTM response to this exposure varies depending on previous life experience, freshwater-adapted fish were exposed to 1) freshwater, 2) one "pulse" of severe salinity stress, where salinity gradually increased from freshwater to 82.5 g/kg, or 3) three pulses of severe salinity stress. Following all salinity treatments, histone PTMs in the gills, kidney, and testes were quantified and compared.

The third chapter of this dissertation sought to elucidate whether histone PTMs contribute to the extreme salinity tolerance of Mozambique tilapia by facilitating developmental plasticity (Nettle and Bateson, 2015). To test this hypothesis, Mozambique tilapia siblings were first exposed to either freshwater or hypersalinity during their early critical window of development, being gonadal sex differentiation (Anway et al., 2005; Hanson and Skinner, 2016; Nakamura and

Takahashi, 1973; Weaver et al., 2004). Following this window, fish continued their development in either freshwater or seawater, respectively, for 18 months. Another set of salinity treatments was imposed on the fish once they reached adulthood. Over the course of four weeks, fish were acclimated to either freshwater or seawater. Following salinity treatments, the gills of each fish were analyzed for their histone PTMs. Histone PTMs were compared between fish from different salinity treatment groups to investigate the potential occurrence of developmental plasticity, and to investigate how histone PTMs are impacted by environmental conditions when exposures are lifelong, long-term throughout development, or four weeks during adulthood.

Finally, this dissertation contains an appendix, which elaborates on the role of histone PTMs, among other mechanisms, in a process called stress-induced evolution. Specifically, stress-induced changes in 1) mutagenesis, 2) histone PTMs, 3) DNA methylation, 4) chromoanagenesis, and 5) transposable element activity are highlighted as mechanisms that enable organisms to accelerate evolutionary processes upon environmental stress. Once activated, each mechanism can achieve this outcome by increasing the variation of heritable phenotypes in a population, which can then be acted upon by natural selection.

AUTHOR LIST

Chapter 1: Elizabeth A. Mojica and Dietmar Kültz contributed to this work. Both EAM and DK devised the new strategy to quantify histone PTMs. EAM processed samples for histone PTM analysis, analyzed the data, and was the main contributor for writing the manuscript. DK performed LCMS of samples, contributed to data processing, and edited the manuscript.

Chapter 2: Elizabeth A. Mojica, Yuhan Fu, and Dietmar Kültz contributed to this chapter. EAM and DK designed the experiments. EAM and YF delivered all salinity treatments. EAM processed samples for histone PTM analysis, analyzed the data, and was the main contributor for writing the manuscript. DK performed LCMS of samples, contributed to data processing, and edited the manuscript. YF contributed to processing samples for histone PTM analysis.

Chapter 3: Elizabeth A. Mojica, Kathleen A. Petcu, and Dietmar Kültz contributed to this chapter. EAM and DK designed the experiments in this study. EAM delivered salinity treatments, processed samples for histone PTM analysis, analyzed the data, and was the main contributor for writing the manuscript. DK performed LCMS of samples, contributed to data processing, and edited the manuscript. KAP contributed to administering salinity treatments and processing samples for histone PTM analysis.

Appendix: Elizabeth A. Mojica and Dietmar Kültz contributed to this work, which is published in the Journal of Experimental Biology. Both EAM and DK conceptualized the focus of the review. EAM was the main contributor in writing the manuscript. DK edited the manuscript.

CHAPTER 1

A Strategy to Characterize the Global Histone PTM Landscape Within Tissues of Non-Model Organisms

Abstract

Histone post-translational modifications (PTMs) are epigenetic marks that play a critical role in the expression and maintenance of DNA, but they remain largely uninvestigated in non-model organisms due to technical challenges. To begin alleviating this issue, we developed a workflow for histone PTM analysis in the Mozambique tilapia (*Oreochromis mossambicus*), being a widespread and environmentally hardy fish, using mass spectrometry methods. By incorporating multiple protein digestion methods into the preparation of each sample, we reliably quantified 503 biologically relevant histone PTMs. All of these histone PTMs, collectively referred to as the global histone PTM landscape, were characterized in the gills, kidney, and testes of this fish. By comparing the global histone PTM landscape between the three tissues, we found that 90.46% of histone PTMs were tissue-dependent. The workflow and tools for histone PTM analysis described in this study are now publicly available and enable comprehensive investigation into the influence of environmental stress on histone PTMs in non-model organisms. Given the functionality and flexibility of histone PTMs, we anticipate that the study of histone PTMs in ecologically relevant contexts will provide ground-breaking insights into comparative physiology and evolution.

Introduction

In the nucleus of eukaryotic cells, DNA wraps around histone proteins that are each decorated with a variety of post-translational modifications (PTMs). Histone PTMs are epigenetic marks that modify the physicochemical properties of chromatin and thereby lead to alterations in the expression, replication, mutagenesis, and repair of DNA (Kouzarides, 2007; Norton et al., 1989). Due to such critical functions, histone PTMs became a focus of human disease research. Mass spectrometry emerged as a powerful tool to concurrently study hundreds of histone PTMs in cells, and this technological advance led to discoveries implicating histone PTM dysregulation in cancer and Alzheimer's Disease, among other pathologies (Audia and Campbell, 2016; Drake et al., 2004). Most knowledge of histone PTMs now comes from human disease research (Noberini et al., 2022); however, histone PTMs hold the same important functions in plants and animals, and they are influenced by many of the environmental pressures that threaten natural populations of wild species (Atlasi and Stunnenberg, 2017; Mojica and Kültz, 2022). For this reason, there is a pressing need to investigate histone PTMs in non-model organisms and in ecological contexts (Burggren, 2014a; Eirin-Lopez and Putnam, 2019b).

In this study, we first sought to optimize a workflow for histone PTM analysis in Mozambique tilapia (*Oreochromis mossambicus*) tissues. Mozambique tilapia were chosen because they are a eurytopic species of fish, capable of tolerating wide ranges of multiple environmental parameters, including salinity. This presents an opportunity to investigate how various environmental pressures mediate fish physiology through histone PTMs. Currently, there is a very limited knowledge-base of histone PTMs in fishes (Christensen et al., 1984; Ortega-Recalde et al., 2020; Østrup et al., 2014; Zhang et al., 2013), let alone Mozambique tilapia. To analyze the most inclusive list of biologically relevant histone PTMs in the most reliable manner,

we intended to tailor the mass spectrometry method of quantitative data-independent acquisition (DIA). To this extent, we aimed to create tilapia-specific DIA assay libraries to serve as lists of all modified and unmodified histone peptides targeted for quantification in every biological sample. Values of histone peptide abundance would then serve as the basis of histone PTM quantification.

Next, we sought to characterize the presence and relative abundance of all biologically relevant histone PTMs, collectively referred to as the global histone PTM landscape. We performed this task separately for the gills, kidney, and testes of Mozambique tilapia to determine how cell differentiation into specific tissues influences histone PTMs. The gills and kidney were chosen as environmentally responsive tissues where histone PTMs may play a role in their malleable physiology. The gills manage homeostasis through the transport of ions such as NaCl, acids and bases, nitrogenous waste, and dissolved gases (Sardella and Brauner, 2016). Similarly, kidneys respond to environmental changes by regulating urine production, divalent ion transport, and glomeruli function (Kültz, 2015). In this study, testes were characterized because they represent the germ line, where histone PTMs can be passed from one generation to the next (Mojica and Kültz, 2022).

The DIA assay libraries and histone PTM quantification pipeline presented here are now publicly available and can be reused for measuring how various factors, such as development and environmental stress, influence the global histone PTM landscape. Although these tools are specific to tilapia, they were designed to be easily modified for application with other non-model organisms, i.e., species for which histone PTM-specific antibodies are not available. Our study breaks new ground for comparative physiological and evolutionary investigations of how global

histone PTM landscapes depend on ecological contexts and how they differ for a given species between tissues.

Experimental Procedures

Experimental design and statistical rationale

Twenty-four Mozambique tilapia with an average weight of 60.64 ± 3.35 g were sacrificed and dissected for their gills, kidney, and if male, testes. These dissections yielded $n = 24$ samples of gills, $n = 24$ samples of kidney, and $n = 18$ samples of testes. Each tissue sample was divided into three aliquots so that they could be processed for histone PTM analysis using three different methods. Four kidney samples were excluded from statistical analyses due to inadequate recovery of tissue during dissection, which led to an insufficient protein concentration once samples were divided three ways. Therefore, $n = 20$ kidney samples were used in subsequent statistical analyses. The use of these animals was approved by the UC Davis IACUC under Protocol #21846.

Mechanical single cell suspension

Following dissection, each tissue was broken up into a suspension of single cells to increase the accessibility of the cells to reagents used in downstream protocols. The methods used for this single cell suspension were based on those reported by Leelatian et al. (2017) (Leelatian et al., 2017), with the notable exception of using a mechanical separation of tissues rather than an enzymatic separation (Kültz and Jürss, 1991). Therefore, freshly dissected tissue samples were submerged in phosphate buffered saline (PBS) without calcium and magnesium (to aid cell dissociation) in a 50 mL conical tube, then centrifuged at $100 \times g$ for 5 minutes at room

temperature. The supernatant containing dead cells was discarded, and pre-warmed (27 °C) Leibovitz's L-15 medium (Thermo Fisher Scientific, cat# 11415064) containing 5% fetal bovine serum and 1% Penicillin-Streptomycin was added to each sample to cover the remaining tissue pellet. This complete medium was chosen for its compatibility with fish cells (Gardell et al., 2014). Each sample containing tissue and medium was transferred into a 10 cm petri dish, and tissues were minced into small (1 mm³) pieces using a razor blade. Each sample was transferred back into a 50 mL conical tube and centrifuged at 100 x g for 5 minutes at room temperature. The supernatant was again discarded, and each tissue pellet was resuspended in 5 mL of warmed complete medium.

To mechanically separate tissues into single cells, each sample was pushed with a glass pestle through a cell dissociation sieve containing 40 mesh (Sigma-Aldrich, cat# S0770), which has 380 µm pores, into a new 50 mL conical tube. The resulting solution was pushed through a second cell dissociation sieve containing 200 mesh (Sigma-Aldrich, cat# S4145), which has 73.7 µm pores, into another new 50 mL conical tube. Samples were centrifuged at 100 x g for 10 minutes at room temperature. The supernatant was removed, then the pellet of cells was resuspended in 5 mL of PBS containing calcium and magnesium. Subsequently, samples were centrifuged at 300 x g for 10 minutes, then the supernatant was again discarded. Samples were flash frozen in liquid nitrogen, then stored at -80 °C until ready for processing through histone acid extraction.

Histone acid extraction

Histone acid extraction was used to isolate histone proteins from cells. Continuing from the mechanical single cell suspension, each cell pellet was directly re-suspended in 400 µL of 0.4

N H₂SO₄ and incubated with constant rotation at 4 °C for 4 hours (Govaert et al., 2016; Lin and Garcia, 2012; Shechter et al., 2007). Following acid incubation, samples were centrifuged twice at 16,000 x g for 10 minutes at 4 °C, and each time, the supernatant containing histones was transferred into a fresh 1.5 mL tube (Lin and Garcia, 2012; Shechter et al., 2007). Next, 100% trichloroacetic acid (TCA) was added to each sample in a drop-by-drop manner at a volume equal to ¼ the estimated sample volume (Shechter et al., 2007). Samples were inverted multiple times for mixing, then incubated overnight at 4 °C for the precipitation of histone proteins (Lin and Garcia, 2012). Histone proteins were collected by centrifuging samples at 3,400 x g for 5 minutes at 4 °C. The supernatant was carefully removed and discarded. The histone pellet was rinsed with ice-cold acetone with 0.1% hydrochloric acid, then centrifuged at 3,400 x g for 2 minutes at 4 °C. The supernatant was again discarded, then the remaining histone pellet was rinsed with 100% acetone. Samples were centrifuged again at 3,400 x g for 2 minutes at 4 °C, then the supernatant was discarded (Lin and Garcia, 2012). Each histone pellet was left to air dry in a fume hood for 5 minutes. Samples were then stored at -80 °C until ready for use in the in-solution digestion of histone proteins into peptides.

In-solution digestion of proteins into peptides

Histone proteins were digested into peptides for analysis via liquid chromatography mass spectrometry (LCMS). This was done according to previously described procedures (Kültz et al., 2013; Lin and Garcia, 2012; Root et al., 2021b), with some modifications. To begin the process, the histone pellet of each sample was brought to room temperature and resuspended in 8 M urea. Next, dithiothreitol (DTT) was added to equal a final concentration of 10 mM DTT. Each sample was briefly vortexed and centrifuged, then left to incubate at 37 °C for 30 minutes so that

proteins would become denatured and reduced. Following this incubation, iodoacetamide (IAA) was added to each sample to equal a final concentration of 30 mM. Samples were again briefly vortexed and centrifuged, then left to incubate in the dark for 30 minutes at room temperature so that the IAA would alkylate reduced cysteine residues and therefore prevent protein refolding. After this incubation, samples were briefly vortexed and centrifuged again to help further dissolve the proteins. A bicinchoninic acid (BCA) assay (Thermo Scientific, cat# 23250) was then performed to determine the protein concentration within each sample. Based on the results, three aliquots of 50 µg of protein were aliquoted from each sample to begin three separate digestions: once with trypsin (Promega, cat# V9013) for bottom-up proteomics, and twice with V8 (Thermo Scientific, cat# 20151) for middle-down proteomics. By employing these techniques, we anticipated that the maximal number of histone PTMs would be detected in each tissue.

The bottom-up approach to proteomics relies on creating short peptides (<3 kDa) that can be analyzed through LCMS (Önder et al., 2015). Trypsin is most commonly used as a protease for this purpose, and it typically cleaves proteins at the carboxyl end of both lysine and arginine residues. On its own, trypsin is unsuitable for histone PTM analysis because histone proteins contain a high percentage of lysine residues. The peptides generated would therefore be much too short to separate properly along an HPLC column. This is especially problematic because lysine residues are the site of many important PTMs. To correct for this, we followed a protocol to chemically derive all lysine residues so that any lysine residue that is naturally unmodified or only mono-methylated would be propionylated (Lin and Garcia, 2012). This blocks trypsin from cleaving at lysine so that it only cleaves after arginine. This process produces more appropriately

sized histone peptides and therefore enables the analysis of a higher coverage of histones, including the important PTM-containing lysine residues.

Analyzing moderately-sized peptides (5-20 kDa) through LCMS is described as the middle-down approach to proteomics (Önder et al., 2015). Each sample was digested using the protease V8 (also known as Glu-C) for this purpose. The cleavage specificity of the V8 protease depends on the buffer used. In this workflow, two V8 digestions were performed on every sample: once when V8 was in the buffer ammonium bicarbonate, and once when V8 was in the buffer sodium phosphate. V8 in ammonium bicarbonate cleaves proteins at the carboxyl end of glutamate residues. In contrast, V8 in sodium phosphate cleaves proteins at the carboxyl end of both glutamate and aspartate residues. Following the reduction and alkylation of histones as described above, samples were diluted in the chosen V8 buffer with a dilution factor of 5.6. V8 was added to samples of histone proteins at a 1:50 ratio. Samples were incubated with the protease for exactly 20 hours at 35° C on a rotator. Following the incubation, samples were centrifuged first at 500 x g for 2 minutes, then at 19,000 x g for 5 minutes. Each time, the supernatant containing peptides was transferred into a new 1.5 mL tube. Samples were concentrated using a SpeedVac (Thermo Savant, model# ISS110) until all of the buffer had just evaporated from the tube. Finally, peptides were reconstituted in LCMS-grade water containing 0.1% formic acid to equal a final peptide concentration of 333 ng/μL.

Construction of histone DIA assay libraries and DIA by LCMS

Samples were first acquired by LCMS using a conventional data-dependent acquisition (DDA) approach as previously described (Root et al., 2021a). After generating peak lists from DDA raw data (DataAnalysis 4.4, Bruker Daltonics), we used PEAKS Suite X Plus

(Bioinformatics Solutions Inc., Waterloo, Canada) and MSFragger (Kong et al., 2017) to annotate histone peptides with amino acid sequence and protein ID. The *Oreochromis niloticus* reference proteome database was used for annotation. This database contained 61,681 proteins and was downloaded from NCBI RefSeq on February 25, 2020. The same number (61,681) of randomly scrambled decoys and 282 common contaminants (e.g., human keratins, porcine trypsin) were included in this database. A first-round database search allowed for cysteine carbamidomethylation, methionine oxidation, and protein N-terminal acetylation. A second-round database search then allowed for a maximum of three PTMs per peptide including the following: acetylation, lactylation/carboxyethylation, and biotinylation on lysine residues; mono-, di-, and tri-methylation on lysine and arginine residues; oxidation and dioxidation on proline residues; ubiquitylation and ADP-ribosylation on lysine, threonine, and serine residues; citrullination on arginine residues; and phosphorylation on serine, threonine, and tyrosine residues. Mass tolerance limits were set at 10 ppm for precursors and 0.03 Da for fragment ions in PEAKS. In MSFragger, mass tolerance limits were set at 20 ppm for precursors and 0.05 Da for fragment ions.

For each of the three sets of tilapia histone peptides produced using the three different digestion methods, a spectral library was generated. Each spectral library was created using the peptide-to-spectrum matches and protein annotations generated from the PEAKS and MSFragger DDA data, which were imported into Skyline 20.0 (Pino et al., 2017) to construct a non-redundant raw library of MS2 spectra. The raw spectral libraries were then filtered with EncyclopeDIA (Searle et al., 2018; Searle et al., 2020) to remove interferences and retain only peptides and transitions that are suitable for DIA quantitation. The resulting filtered spectral libraries were imported into Skyline and used to generate three separate (protease-specific) assay

libraries of tilapia histone peptides for DIA quantitation. Transitions were excluded from the DIA assay libraries if they were ambiguous for sharing the same combination of precursor mass-to-charge ratio (m/z), product m/z , and ion type for multiple peptides. This assay represents a tier two assay (Abbatiello et al., 2017).

In addition to DDA, each sample was analyzed by a second LCMS acquisition in DIA mode. LC separation parameters and conditions were identical to those used for DDA, but only MS2 spectra were acquired. The mass range for DIA was set to 390 – 1015 m/z at 25 Hz scan rate with an isolation width of 10 m/z (0.5 m/z overlap, 2.5 sec scan interval). Quantitative analyses and visualization of DIA data were performed using Skyline 20.0. Before being filtered for ambiguity, at least four (generally six) transition peaks were detected for each peptide. Their q values were scored using the mProphet algorithm integrated into Skyline ($Q < 0.01$). The mass error threshold for all transitions was set at 20 ppm, and the resolving power was 30,000. The same number of Skyline generated decoy peptides as the number of histone target peptides in the DIA assay list were used in mProphet Q -value calculation. Abundance data for each peptide in the assay library represent the sum of peak areas of all transitions belonging to the corresponding peptide. They were normalized with Skyline against the overall median for each sample (normalized area), then exported in csv format.

Strategy for histone PTM quantification

The PTMs detected on histone peptides between the three DIA assay libraries were evaluated for their biological relevance. If a histone PTM was determined to be biologically relevant according to its Unimod accession and amino acid residue (Supplemental Table 1.1), it was quantified in every sample. For each of these histone PTMs, three values were obtained: 1)

relative abundance, 2) beta-value, and 3) M-value. These three values were all calculated using data of histone peptide abundance, called normalized area, obtained through Skyline.

The relative abundance of a histone PTM describes the percent of histones in a sample where the specific amino acid residue on a histone is occupied with the PTM. Because each tissue sample was processed using three different digestion conditions (trypsin, V8 in the buffer sodium phosphate, and V8 in the buffer ammonium bicarbonate), values of relative abundance had to be calculated in two stages, presented in Equation 1 and Equation 2. As shown in Equation 1, the relative abundance based on histone peptides from only one digestion condition (α_d), was calculated as the sum of the normalized area for all histone peptides containing the specific modification (m_x), divided by the sum of the normalized area for all histone peptides containing the specific histone amino acid residue (r_x), multiplied by 100. The value of α_d was calculated for each histone PTM three times, once for each digestion condition. However, not all digestion conditions could detect the histone amino acid residue where a PTM was reported. Therefore, whenever $r_x = 0$ using one digestion condition, the value of α_d was excluded.

$$\alpha_d = \left(\frac{\sum m_x}{\sum r_x} \right) (100) \quad (1)$$

The second stage for calculating the relative abundance of a histone PTM takes into account all digestion conditions. As shown in Equation 2, the relative abundance of a histone PTM (α) is calculated as the sum of all relative abundance values based on each individual digestion condition ($\alpha_{d,i}$), divided by the number of α_d values calculated for the given histone PTM (n).

$$\alpha = \frac{\sum_{i=0}^n \alpha_{d,i}}{n} \quad (2)$$

The beta-value of a histone PTM is similar to the relative abundance; however, it is displayed as a number between 0 and 1 rather than a percentage, and a value of 100 is added to the denominator so that the beta-values of histone PTMs located on low-intensity peptides are standardized (Chappell et al., 2021; Du et al., 2010). As with the relative abundance calculation, beta-values must be calculated in two stages, presented in Equation 3 and Equation 4, to account for multiple digestion conditions used to process each sample. Therefore, as shown in Equation 3, the beta-value based on histone peptides from only one digestion condition (β_d) is calculated as the sum of the normalized area for all histone peptides containing the specific modification (m_x), divided by the combination of 100 and the sum of the normalized area for all histone peptides containing the specific histone amino acid residue (r_x). Values of β_d were excluded whenever $r_x = 0$ using one digestion condition.

$$\beta_d = \frac{\sum m_x}{100 + \sum r_x} \quad (3)$$

The second stage for calculating the beta-value of a histone PTM, which accounts for all digestion conditions, is presented in Equation 4. The beta-value of a histone PTM (β) was calculated as the sum of beta-values based on each individual digestion condition ($\beta_{d,i}$) divided by the number of β_d values calculated for the given histone PTM (n).

$$\beta = \frac{\sum_{i=0}^n \beta_{d,i}}{n} \quad (4)$$

All statistical tests in this study were based on the M-value of histone PTMs. The M-value is a logit transformation of the beta-value (Equation 5) (Chappell et al., 2021). The reason that M-values were used for statistical purposes rather than relative abundance or beta-values is that the latter values do not conform to a normal distribution: values of relative abundance are bound by 0 and 100%, and beta-values are bound by 0 and 1. The M-value rectifies this issue, but the values themselves are unintuitive. Therefore, we calculated the relative abundance, beta-value, and M-value for each histone PTM in each sample in order to perform statistical tests properly by using the M-value and to report the relative abundance alongside statistical tests for interpretability.

$$M = \log_2 \left(\frac{\beta}{1 - \beta} \right) \quad (5)$$

The excel workbook we prepared for quickly converting values of histone peptide abundance into the relative abundance, beta-value, and M-value of each histone PTM is available in Supplemental File 1.1, along with detailed instructions for its use in Supplemental File 1.2.

Statistical analyses

The global histone PTM landscape was compared between the gills, kidney, and testes of Mozambique tilapia to elucidate the influence of tissue type on histone PTMs. First, a principal component analysis (PCA) was performed on the tissue samples using the M-values of all

histone PTMs as variables. Second, three pairwise comparisons were made between the tissues: 1) gills and kidney, 2) gills and testes, and 3) kidney and testes. For each of these tissue comparisons, t-tests were performed using the M-value of each histone PTM. The Benjamini-Hochberg correction was applied to all resulting p-values in order to account for multiple hypothesis testing (Benjamini and Hochberg, 1995). Alongside this analysis, the mean relative abundance was reported for each histone PTM in each tissue. These values were used to calculate the \log_2 fold change of histone PTMs between tissues for each pairwise comparison. In the R programming environment (version 4.2.0) (R Core Team, 2022), volcano plots were produced to visually depict these results. Additionally, histone PTM maps were constructed, containing information on the mean relative abundance of histone PTMs in each tissue. These plots were made using the R packages *ggplot2* (Wickham, 2016), *tidyverse* (Wickham et al., 2019), *ggrepel* (Slowikowski, 2021), and *cowplot* (Wilke, 2020).

Results

Reliable quantification of 503 biologically relevant histone PTMs

Histone peptides were uniformly targeted for quantification within each sample, regardless of any factor that could have affected peptide abundances (e.g., tissue type), through the application of DIA assay libraries. The three DIA assay libraries constructed for this purpose each comprised a unique set of histone peptides due to the method used to digest histone proteins. In the DIA assay library specific for histone proteins digested with V8 in ammonium bicarbonate, a total of 24 proteins, 1,434 peptides, 1,434 precursors, and 10,109 transitions were included for analysis. The DIA assay library built for the histone proteins digested with V8 in sodium phosphate consisted of 20 proteins, 1,401 peptides, 1,405 precursors, and 10,238

transitions. Lastly, the DIA assay library specific for the histone proteins digested using the modified trypsin method targeted a total of 15 proteins, 669 peptides, 672 precursors, and 5,134 transitions. Altogether, the DIA assay libraries captured 25 histone proteins based on their unique protein accession number. Due to some redundancy in the protein names associated with protein accession numbers, there were only 17 unique protein names identified in our data. We use the protein name (e.g., H1 isoform X1), rather than the protein accession number, to describe the histone PTMs in the following sections.

Using the histone peptides from all three DIA assay libraries, a list of histone PTMs was compiled according to the histone protein name, amino acid residue/position, and modification type. Once this list of histone PTMs was filtered for biological relevance, we found that 17 distinct types of modifications remained. These included the highly studied modifications of acetylation, methylation, dimethylation, trimethylation, phosphorylation, and ubiquitylation. It also included lesser studied modifications of acrolein112, oxidation, dioxidation, amidation, deamidation, formylation, biotinylation, 4-hydroxynonenalation, ADP-ribosylation, and butyrylation. Additionally, it included lactylation and/or carboxyethylation, which cannot be distinguished from each other in our dataset given their identical chemical formula and therefore mass shift (+72.021129) in mass spectrometry data.

Overall, our workflow for histone PTM analysis enabled the reliable quantification of 503 unique and biologically relevant histone PTMs in Mozambique tilapia tissues. The use of three digestion conditions in the in-solution digestion protocol was proven especially useful in increasing the number of observed histone PTMs. Individually, the amount of histone PTMs detected was 114 using the trypsin digestion method, 284 using V8 in sodium phosphate, and 265 using V8 in ammonium bicarbonate (Figure 1.1). The combination of all three digestion

conditions not only maximized the total number of histone PTMs; it also increased the diversity of modifications observed. Every digestion method detected at least one modification type exclusively. The trypsin method was the only one to detect butyrylation and acrolein112 modifications. Similarly, V8 in ammonium bicarbonate uniquely detected formylation, and V8 in sodium phosphate uniquely detected ADP-ribosylation and biotinylation.

The methods we developed for histone PTM quantification relied on the stoichiometry of modified to unmodified versions of histone peptides (Figure 1.2). Therefore, the calculations of relative abundance, beta-value, and M-value for each histone PTM depended on proportions within a given sample, rather than overall intensity. This prevented small discrepancies in the overall peptide concentration of samples from interfering in the integrity of the analysis, as all samples were internally standardized.

In the following sections, we describe histone PTMs in a slightly unconventional way so that additional information can be conveyed for previously undescribed histone PTMs. The name of each histone PTM (e.g., H2A.Z isoform X2 K4 methylation) begins with 1) the full description of the histone protein (e.g., H2A.Z isoform X2), 2) the amino acid residue and sequence position (e.g., K4), and 3) the type of modification observed (e.g., methylation). Amino acid residues are abbreviated using their one letter code; for example, lysine is K, arginine is R, serine is S, threonine is T, tyrosine is Y, and proline is P. For consistency with other studies, we removed the initial methionine (M) before determining the sequence position of subsequent amino acid residues in histone protein sequences. A complete presentation of the global histone PTM landscapes of Mozambique tilapia tissues is provided in Supplemental Table 1.2. This table includes the average relative abundance of each histone PTM in each tissue. Additionally, it provides the results of three pairwise tissue comparisons for every histone PTM in the form of

the p-value, the Benjamini-Hochberg adjusted p-value, and the \log_2 fold change of relative abundance.

Characterization of histone H1

Within each tissue sample from Mozambique tilapia, we analyzed six isoforms of histone H1 proteins, named H1, H1.0-B, H1.10, H1 isoform X1, H1-like, and protamine-like protein. Between these six proteins, 15 types of modifications were detected. This is in contrast to the 17 types of modifications detected across all histone proteins as described above. The only two types of modifications found to be absent were ADP-ribosylation and butyrylation. In total, 137 biologically relevant histone PTMs were identified and quantified on histone H1 isoforms. Those located on a representative protein, histone H1-like, are depicted as a histone PTM map (Figure 1.3A).

The PTMs on histone H1 proteins were mostly found in low abundance, which we hereby distinguish as having an average relative abundance less than 50% in each tissue. Only six histone PTMs had an average relative abundance that surpassed this amount. Five of them displayed an average relative abundance of exactly 100% in all tissues because the only peptides that contributed to their quantification contained the modification. These histone PTMs were: 1) H1-like S1 acetylation, 2) protamine-like protein S1 acetylation, 3) H1-like P9 dioxidation, 4) H1-like P11 dioxidation, and 5) H1-like S47 phosphorylation. The sixth histone PTM, H1 K267 acrolein112, was found to be highly abundant only within the testes with an average relative abundance of 52%.

The gills, kidney, and testes displayed strong differences in the abundance of PTMs on histone H1 isoforms (Figure 1.3B-D). Between the three tissues, the gills and testes were the

most dissimilar. Of the 137 histone PTMs quantified, 97 histone PTMs (70.80%) were significantly different between these tissues. Gills and kidney were the most similar; only 67 histone PTMs (48.91%) were significantly different between these two tissues. Between the kidney and testes, 95 histone PTMs (69.34%) were significantly different. When accounting for all three tissue comparisons, we determined that 123 of 137 histone PTMs (89.78%) on histone H1 isoforms were tissue-dependent.

A list of the most highly tissue-dependent PTMs on histone H1 isoforms was prepared to include the histone PTMs displaying the three lowest adjusted p-values or three highest values of \log_2 fold change when comparisons were made between the gills, kidney, and testes (Figure 1.3E). Only two distinct histone PTMs appeared on this list due to their especially low adjusted p-value and high \log_2 fold change when compared between multiple tissues. The instances where histone PTMs generated the three lowest adjusted p-values when compared between any of the tissues were the following: 1) H1-like K44 4-hydroxynonenalation (with an adjusted p-value of $7.83e-28$ when compared between the gills and testes), 2) H1-like K52 dioxidation (with an adjusted p-value of $2.99e-20$ when compared between the kidney and testes), and 3) H1-like K52 dioxidation (with an adjusted p-value of $5.58e-20$ when compared between the gills and testes). The three instances where histone PTMs had the highest values of \log_2 fold change were: 1) H1-like K52 dioxidation (with a \log_2 fold change of 8.26 between gills and testes), 2) H1-like K52 dioxidation (with a \log_2 fold change of 7.69 between kidney and testes), and 3) H1-like K44 4-hydroxynonenalation (with a \log_2 fold change of 4.74 between gills and testes).

Characterization of histone H2A

A total of 135 biologically relevant PTMs on histone H2A isoforms were targeted for quantification within our DIA assay libraries. These histone PTMs were found across five proteins: 1) H2A, 2) H2A.Z isoform X1, 3) H2A.Z isoform X2, 4) H2A, sperm-like, and 5) core histone macro-H2A.1 isoform X5. On these proteins, 14 types of modifications were observed. Compared to the complete list of 17 modification types across all histone proteins, the modification list on histone H2A isoforms excluded butyrylation, trimethylation, and formylation.

Although histone H1 proteins contained a few more biologically relevant histone PTMs than histone H2A proteins, histone H2A proteins contained nearly twice as many highly abundant PTMs. Three histone PTMs were found to have a relative abundance of 100% in every tissue, indicating that only modified versions of the amino acid residue were included in histone PTM quantification. These PTMs were H2A R35 dimethylation, H2A.Z isoform X2 K4 methylation, and H2A.Z isoform X1 K73 methylation. An additional six histone PTMs had a relative abundance between 50% and 100% in all three tissues. These histone PTMs were 1) H2A.Z isoform X1 T98 phosphorylation, 2) H2A K36 acrolein112, 3) H2A, sperm-like K120 4-hydroxynonenalation, 4) H2A S19 ubiquitylation, 5) H2A R20 methylation, and 6) H2A Y57 phosphorylation. Another histone PTM, H2A T59 phosphorylation, was found to be highly abundant only in the kidney. Many of these PTMs are portrayed in the representative histone PTM map for histone H2A (Figure 1.4A).

When the PTMs on histone H2A proteins were compared between tissues, 116 of the 135 histone PTMs (85.93%) were found to be tissue-dependent. These PTMs had an adjusted p-value less than 0.05 in at least one of the pairwise tissue comparisons. The gills and kidney were the

most similar tissues, with 56 of 135 histone PTMs (41.48%) being significantly different. The kidney and testes were the two most dissimilar tissues, with 96 of 135 histone PTMs (71.11%) being significantly different between the two tissues. Between the gills and testes, 86 of 135 histone PTMs (63.70%) were significantly different.

The most highly tissue-dependent PTMs on histone H2A proteins were identified according to their low adjusted p-value and high \log_2 fold change (Figure 1.4E). The three histone PTMs with the highest \log_2 fold change were: 1) H2A R77 deamidation (with a \log_2 fold change of 5.11 when compared between gills and kidney), 2) H2A R42 deamidation (with a \log_2 fold change of 4.02 when compared between kidney and testes), and 3) H2A K118 acetylation (with a \log_2 fold change of 3.96 when compared between gills and testes). The three histone PTMs with the lowest adjusted p-value were: 1) H2A Y50 phosphorylation (with an adjusted p-value of $4.94e-17$ when compared between gills and testes), 2) H2A K95 lactylation/carboxyethylation (with an adjusted p-value of $2.85e-14$ when compared between kidney and testes), and 3) H2A P48 dioxidation (with an adjusted p-value of $2.57e-14$ when compared between gills and testes).

Characterization of histone H2B

We identified 110 unique and biologically relevant PTMs across three isoforms of histone H2B, named H2B.L4, H2B 1/2, and H2B 1/2 isoform X. A full histone PTM map of H2B 1/2 is provided in order to exemplify these PTMs (Figure 1.5A). Between the three proteins analyzed, the following twelve types of modifications were present: 4-hydroxynonenalation, acetylation, ADP-ribosylation, biotinylation, deamidation, dimethylation, dioxidation, lactylation/carboxyethylation, methylation, oxidation, phosphorylation, and ubiquitylation.

Nearly all of the PTMs on histone H2B proteins were found at low levels. Only one histone PTM, H2B.L4 K7 oxidation, had a high average relative abundance in any of the tissues. This PTM was present at 100% in the gills, kidney, and testes because its quantification was based exclusively on histone peptides that contained the modification. A second histone PTM, H2B 1/2 P101 dioxidation was found to have a high average relative abundance exclusively in the gills (50.7%).

When the PTMs on histone H2B isoforms were compared between the gills, kidney, and testes of Mozambique tilapia, it was found that 101 of 110 histone PTMs (91.82%) were tissue-dependent. In this case, the kidney and testes were the most dissimilar in terms of their histone PTMs, and the gills and testes were most similar. Of the 110 biologically relevant histone PTMs analyzed on histone H2B isoforms, 88 (80.00%) were significantly different between the kidney and testes, 86 (78.18%) were significantly different between the gills and kidney, and 67 (60.91%) were significantly different between the gills and testes (Figure 1.5B-D).

Following the comparisons between the three tissues, the PTMs on histone H2B isoforms that displayed the three lowest adjusted p-values and the three highest values of \log_2 fold change were selected as the most highly tissue-dependent histone PTMs. The three histone PTMs with the lowest adjusted p-value in any of the three pairwise tissue comparisons were determined to be 1) H2B 1/2 K106 methylation (with an adjusted p-value of $2.00e-16$ when compared between gills and kidney), 2) H2B 1/2 S76 ubiquitylation (with an adjusted p-value of $2.51e-13$ when compared between gills and kidney), and 3) H2B 1/2 S76 ubiquitylation (with an adjusted p-value of $9.23e-13$ when compared between gills and testes). The three histone PTMs having the highest \log_2 fold change when compared between tissues were: 1) H2B.L4 T86 ubiquitylation (with a \log_2 fold change of 5.26 when compared between gills and kidney), 2) H2B.L4 T86

ubiquitylation (with a \log_2 fold change of 4.75 when compared between gills and testes), and 3) H2B.L4 K98 ubiquitylation (with a \log_2 fold change of 4.75 when compared between gills and testes). Due to overlap in these two lists, the resulting four histone PTMs exemplify tissue differences on histone H2B isoforms (Figure 1.5E).

Characterization of histone H3

Two isoforms of histone H3, namely H3 and H3.3, were analyzed in our samples of Mozambique tilapia tissues. These proteins contained the following 13 types of modifications: 4-hydroxynonenalation, acetylation, acrolein112, butyrylation, deamidation, dimethylation, dioxidation, lactylation/carboxyethylation, methylation, oxidation, phosphorylation, trimethylation, and ubiquitylation. In total, 81 unique and biologically relevant PTMs on histone H3 isoforms were identified. Four of these were found to be highly abundant. One PTM, H3 K27 dimethylation, had a relative abundance between 50% and 100% in all three tissues. Another three PTMs, being H3 K9 acrolein112, H3 K18 acrolein112, and H3 K36 ubiquitylation, had a relative abundance between 50% and 100% in the gills, but not in the kidney nor testes. All of these highly abundant PTMs are depicted in the representative histone PTM map for histone H3 (Figure 1.6A).

Histone H3 isoforms displayed the highest proportion of tissue-dependent histone PTMs. When these PTMs were compared between the gills, kidney, and testes, we found that 77 of the 81 histone PTMs (95.06%) were significantly different between at least two of the three tissues. Of the histone PTMs analyzed, 49 (60.49%) were significantly different between the kidney and testes, 61 (75.31%) were significantly different between the gills and testes, and 71 (87.65%)

were significantly different between the gills and kidney (Figure 1.6B-D). The kidney and testes were therefore the most similar, and the gills and kidney were the most dissimilar.

As before, histone PTMs were selected as being most highly tissue-dependent based on their low adjusted p-value or high \log_2 fold change (Figure 1.6E). The following three histone PTMs were selected for their lowest adjusted p-values: 1) H3 K23 acetylation (with an adjusted p-value of $7.23e-18$ when compared between gills and kidney), 2) H3 S86 phosphorylation (with an adjusted p-value of $1.62e-17$ when compared between gills and testes), and 3) H3 R83 methylation (with an adjusted p-value of $1.78e-12$ when compared between gills and testes). For their highest values of \log_2 fold change between tissues, these additional three histone PTMs were selected: 1) H3 R40 dimethylation (with a \log_2 fold change of -5.90 when compared between gills and kidney), 2) H3 K64 ubiquitylation (with a \log_2 fold change of 5.79 when compared between gills and kidney), and 3) H3 K64 acetylation (with a \log_2 fold change of 4.19 when compared between gills and kidney).

Characterization of histone H4

One histone H4 isoform was included in our DIA assay libraries for histone PTM analysis. This protein was named H4-like, and it displayed modifications of acetylation, deamidation, dimethylation, dioxidation, lactylation/carboxyethylation, methylation, oxidation, phosphorylation, and ubiquitylation. We identified and quantified 40 biologically relevant histone PTMs on this protein (Figure 1.7A). The only one found to be highly abundant was H4-like K79 dioxidation. Its average relative abundance was between 50% and 100% in the gills, kidney, and testes.

Of the 40 histone PTMs analyzed on the histone H4 isoform, 38 (95.00%) were found to be tissue-dependent. This group of histone PTMs followed a pattern similar to PTMs on histone H2A and opposite to PTMs on histone H3: here, the kidney and testes were the most dissimilar, and the gills and kidney were the most similar. Between the kidney and testes, 36 histone PTMs (90.00%) were found to be significantly different. Comparisons between the gills and kidney revealed that 21 of the 40 histone PTMs (52.50%) were significantly different. Between the gills and testes, 32 of the 40 histone PTMs (80.00%) were found to be significantly different (Figure 1.7B-D).

To further characterize tissue differences in the global histone PTM landscape, we depicted the PTMs on histone H4 isoforms that displayed the three lowest adjusted p-values and the three highest values of \log_2 fold change when comparisons were made between the gills, kidney, and testes (Figure 1.7E). The three histone PTMs with the lowest adjusted p-value when compared between any two of the three tissues were: 1) H4-like K61 acetylation (with an adjusted p-value of $1.82e-18$ when compared between kidney and testes), 2) H4-like T84 phosphorylation (with an adjusted p-value of $6.59e-18$ when compared between gills and testes), and 3) H4-like R80 dioxidation (with an adjusted p-value of $9.30e-18$ when compared between gills and testes). The histone PTMs selected for their high \log_2 fold change when compared between any two of the three tissues were: 1) H4-like R42 dimethylation (with a \log_2 fold change of 3.52 when compared between gills and kidney), 2) H4-like K61 dioxidation (with a \log_2 fold change of -2.62 when compared between kidney and testes), and 3) H4-like T84 phosphorylation (with a \log_2 fold change of -2.23 when compared between gills and testes). Because the histone PTM of H4-like T84 phosphorylation was selected for both its low adjusted p-value and high

\log_2 fold change, a total of five histone PTMs were selected as the most highly tissue-dependent PTMs on histone H4 isoforms.

Tissue-specific variation in the global histone PTM landscape

Across all histone proteins analyzed in this study, 455 of 503 histone PTMs (90.46%) were found to be tissue-dependent through the pairwise comparisons of the gills, kidney, and testes. Accordingly, a PCA performed on all samples revealed clear distinctions based on tissue type when the 503 histone PTMs were used as variables (Figure 1.8). In this analysis, PC1 accounted for 25.1% of variation, and PC2 accounted for 20.4% variation in the global histone PTM landscape of samples. The top contributors to this variance were 1) H2B 1/2 T94 acetylation, 2) H2B 1/2 S110 phosphorylation, 3) H3 R83 dimethylation, 4) H3 K64 acetylation, and 5) H2B 1/2 R97 oxidation.

To further characterize tissue differences in the global histone PTM landscape, we investigated whether specific types of modification (e.g., acetylation, methylation) were consistently more abundant in certain tissues. For each type of modification, we recorded the number of instances that tissue-dependent histone PTMs had an increased relative abundance in a given tissue when compared to the other two tissues (Supplemental Table 1.3). Here we highlight the cases where a tissue displayed an increased relative abundance for at least 67% of the histone PTMs from a given modification type when compared to each of the other tissues.

Overall, gills were found to have the highest levels of histone acetylation, acrolein112, amidation, and formylation. Of the tissue-dependent histone PTMs containing acetyl groups, 73% had a higher relative abundance in the gills than in the kidney, and 67% had a higher relative abundance in the gills than in the testes. Histone modifications with acrolein112 showed

a similar pattern. When compared to the kidney, gills displayed an increase in 67% of the tissue-dependent histone PTMs containing acrolein112 modifications. The gills displayed an increase in 80% of the tissue-dependent histone PTMs containing acrolein112 modifications when compared to the testes. Of the tissue-dependent instances of histone amidation, 67% had a higher relative abundance in the gills when compared to the kidney, and 75% had a higher relative abundance in the gills when compared to the testes. For histone formylation, 100% of the tissue-dependent histone PTMs had a higher relative abundance in the gills than in the kidney or testes.

Testes were found to have the highest levels of histone biotinylation and trimethylation between the three tissues analyzed in this study. Of the tissue-dependent histone PTMs containing biotin modifications, 100% were higher in relative abundance in the testes than in the kidney or gills. Of the tissue-dependent histone PTMs containing trimethyl modifications, 100% were higher in the testes when compared to the gills, and 80% were higher in the testes when compared to the kidney. The kidneys were found to display the highest levels of histone butyrylation, with 100% of tissue-dependent histone PTMs containing butyryl groups having a higher relative abundance in the kidney when compared to the gills or testes.

To determine whether specific types of modification were consistently less abundant in certain tissues, we recorded the number of instances that tissue-dependent histone PTMs from each modification type displayed a decreased relative abundance in a given tissue when compared to the other two tissues (Supplemental Table 1.3). Through this analysis, gills were found to display the lowest levels of histone butyrylation and trimethylation. Of the tissue-dependent butyryl modifications, 100% had a lower relative abundance in the gills when compared to either the kidney or testes. In terms of histone trimethylation, 67% of significantly different histone PTMs were less abundant in the gills than the kidney, and 100% were less

abundant in the gills than the testes. The kidney was found to have the lowest levels of histone ADP-ribosylation and acrolein112. Of the tissue-dependent ADP-ribosylation modifications, 100% were lower in abundance in the kidney when compared to the gills, and 67% were lower in abundance in the kidney than in the testes. Of the tissue-dependent histone PTMs containing an acrolein112 modification, 67% were lower in abundance in the kidney than in the gills, and 75% were lower in abundance in the kidney than in the testes.

Discussion

The use of multiple digestion methods maximizes histone PTM coverage

To date, approximately 700 biologically relevant histone PTMs have been identified in the scientific literature (Millán-Zambrano et al., 2022; Zhang et al., 2019; Zhao and Garcia, 2015). This number, however, far exceeds the amount that have been quantified in individual biological samples. Recent studies have managed to capture up to 200 histone PTMs in samples by using DIA methods (Daled et al., 2021; de Lima et al., 2020). Here, we demonstrate that histone PTM coverage can be dramatically improved by processing samples through multiple digestion methods. By incorporating three parallel digestions methods into our workflow for histone PTM analysis, we quantified 503 biologically relevant histone PTMs in every sample of Mozambique tilapia tissue. The digestion method using V8 in sodium phosphate was most successful for detecting the highest number of histone PTMs at 284; however, V8 in ammonium bicarbonate detected almost as many histone PTMs at 265, and there was a large overlap of 142 histone PTMs that could be detected using either of these two digestion methods. Although the trypsin digestion method captured the fewest number of histone PTMs at only 114, 103 of these histone PTMs could not be detected using the other digestion methods. This study, therefore,

confirms that both bottom-up (e.g., trypsin) and middle-down (e.g., V8) approaches to proteomics add value to histone PTM analysis (Janssen et al., 2019; Lothrop et al., 2013; Önder et al., 2015). Furthermore, it offers a framework for integrating the histone peptides from multiple digestions into histone PTM quantification.

Although the analysis of histone PTMs has been generally limited to model organisms and biomedical research, we show here that hundreds of histone PTMs can be simultaneously quantified in a non-model organism. Continuing such investigations into the histone PTMs of non-model organisms is critical. These epigenetic marks have been shown to drive evolutionary processes when organisms experience environmental stress (Mojica and Kültz, 2022). However, histone PTM landscapes do not appear to be conserved across species. For example, a study that used consistent methods for histone PTM analysis found 49 unique histone PTMs in human cells, but only 33 histone PTMs in calf thymus (Kalli et al., 2013). Another study found that the conservation of histone PTMs between species even varies depending on histone protein. When histone PTMs were compared between the sperm of mice and humans, the percent of histone PTMs conserved between the two species was 85% for the PTMs on histone H3, but 0% for the PTMs on histone H1 (Luense et al., 2016).

The workflow and tools established through this project for histone PTM analysis are now publicly available and can be adopted and/or modified to serve the needs of the research community. Not all digestion methods need to be completed for a comprehensive analysis of the global histone PTM landscape using our approach; instead, any combination of digestion methods can be chosen, including ones not attempted in this study. Additional proteases that have shown promise for histone PTM analysis include ProAlanase, pepsin, and Asp-N (Kalli et al., 2013; Samodova et al., 2020; Zhang et al., 2003). ProAlanase, for example, has been shown

to increase sequence coverage of histone isoforms beyond what could be achieved through the use of either V8 or trypsin (Samodova et al., 2020). In Supplemental Table 1.2, we specified which histone PTMs were detected using each digestion condition in our study. We encourage others to use this table to select the most informative digestion method for their goals. Regardless of any modifications made to this workflow, the process for calculating the relative abundance, beta-value, and M-value for each histone PTM using histone peptide abundance will remain reliable and unchanged.

The global histone PTM landscape distinctly varies by tissue in Mozambique tilapia

By characterizing the global histone PTM landscape of the gills, kidney, and testes of Mozambique tilapia, we found that the abundances of most histone PTMs are highly dependent on tissue type. Between the three tissues, 90.46% of all quantified histone PTMs were significantly different based on their M-values. This finding supports the notion that histone PTMs uphold patterns of gene expression determined during cellular differentiation and tissue formation (Atlasi and Stunnenberg, 2017; Garcia et al., 2008; Ikeuchi et al., 2015; Rugg-Gunn et al., 2010; Yaschenko et al., 2022). Overall, the kidney and testes were the most dissimilar two tissues, as they differed in 72.37% of their histone PTMs. The two most similar tissues were the gills and kidney, where 59.84% of histone PTMs were significantly different. Between the gills and testes, 68.19% of histone PTMs were significantly different. Notably, the differences in histone PTMs were so pronounced between Mozambique tilapia tissues that they were detected at a global level, independent of the genomic distribution of histone PTMs.

We expect that histone PTMs vary even more dramatically between tissues at the local level, as histone PTMs frequently mediate transcriptional regulation of associated genes. For

example, histone H3 lysine 27 acetylation (H3K27ac) is known to cluster around active gene enhancers and promote transcription (Creyghton et al., 2010; Heintzman et al., 2009; Raisner et al., 2018). Its prevalence across the genome has even been used to predict enhancer sequences (He et al., 2017). In this study, we found that the global relative abundance of H3K27ac was significantly higher in the gills (9.7%) than either the kidney (5.0%) or testes (5.4%). This histone PTM was not significantly different between the kidney and testes. We hypothesize that all of these tissues differ in their genomic distribution of H3K27ac because the activity of enhancers varies between tissues (Visel et al., 2009). Tools including ChIP-seq and reverse ChIP can be used to answer questions concerning histone PTM distribution, but such analyses are currently constricted to either a limited set of pre-determined histone PTMs or a limited set of pre-determined genes (Rusk, 2009; Tsui et al., 2018). Still, these tools can be very useful in ascertaining the function of histone PTMs. For example, a recent study used ChIP-seq to demonstrate that the genomic distribution of histone H3 lysine 27 trimethylation (H3K27me3) and histone H3 lysine 4 trimethylation (H3K4me3) enforces the cellular identity of stomatal guard cells in *Arabidopsis* (Lee et al., 2019).

Even at a global level, several histone PTMs associated with transcriptional upregulation were observed to be highly tissue-dependent in this study. Histone H3 lysine 64 acetylation (H3K64ac), for example, is known to increase transcription of associated genes by facilitating nucleosome eviction (Di Cerbo et al., 2014), and this PTM was found to be significantly more abundant in the gills (1.5%) than in either the kidney (0.1%) or testes (0.2%) of Mozambique tilapia. In a similar example, we found the average relative abundance of histone H3 lysine 23 acetylation (H3K23ac) to be significantly higher in the gills (33.9%) when compared to the kidney (16.6%) or testes (13.1%). H3K23ac has been associated with highly expressed genes;

however, evidence suggests that the role of this PTM may itself be tissue-specific (Lu et al., 2015; Zhao and Garcia, 2015). Pathological implications for this PTM include the activation of breast and prostate cancers in humans (Groner et al., 2016; Klein et al., 2019; Ma et al., 2016).

Histone PTMs associated with transcriptional downregulation were also observed to be tissue-dependent in this study. For example, histone H3 lysine 36 methylation (H3K36me) has been shown to maintain transcriptional fidelity by limiting the initiation of transcription from within gene bodies (DiFiore et al., 2020), and we found the abundance of this PTM to increase by 3.4-fold in the kidney (0.28%) when compared to the testes (0.08%). In another example, we found histone H3 lysine 27 dimethylation (H3K27me₂) to be significantly more abundant in the gills than either the kidney or testes. This PTM is typically enriched over exons across the genome and associated with transcriptional downregulation (Zhou et al., 2014). The abundance of this PTM appears to vary dramatically between species. In the filamentous fungus *Neurospora crassa*, it was estimated that H3K27me₂ covers 7% of the genome (Jamieson et al., 2013). However, studies on mouse embryonic stem cells estimated that 70% of histone H3 proteins contain this PTM (Ferrari et al., 2014). The latter is more consistent with our results. We found the average relative abundance of H3K27me₂ to be 70.4% in the gills, 63.0% in the kidney, and 54.6% in the testes of Mozambique tilapia.

Metabolite concentrations in tissues may uphold global levels of histone modifications

Histone PTMs are written and erased by histone modifying enzymes (HMEs), which require substrates for catalysis. Depending on the type of modification being added to a histone, the required substrate could be acetyl-CoA (acetylation), S-adenosylmethionine (methylation), NAD⁺ (ADP-ribosylation), lactate (lactylation), or biotin (biotinylation), to name a few (Fan et

al., 2015a; Hottiger, 2011; Zempleni et al., 2009; Zhang et al., 2019). The available concentration of these substrates in the nucleus influences the rate of HME activity (Wapenaar and Dekker, 2016). In this study, we evaluated whether specific types of modifications, such as acetylation, were consistently more abundant or less abundant in certain tissues. We anticipated that such trends would exist because tissues balance metabolites in different manners (Carrer et al., 2017; Wu et al., 2022). Our results provide evidence in support of this hypothesis. Of the 17 types of modifications analyzed in this study, six were found to be differentially abundant in the gills. Histone acetylation, acrolein112, amidation, and formylation tended to be more abundant, while histone butyrylation and trimethylation tended to be less abundant in the gills when compared to the kidney or testes. The kidney tended to have higher levels of histone butyrylation, but it also displayed lower levels of histone ADP-ribosylation and acrolein112 than either the gills or testes. In the testes, levels of histone biotinylation and trimethylation tended to be higher than those in the gills or kidney.

Based on these results, it is likely that differences between each tissue's global histone PTM landscape depends, in part, on the tissue's balance of key metabolites. However, the trends described above were not absolute. The gills, for example, displayed the highest relative abundance for acetylation on histone H3 lysine 23, but they also displayed the lowest relative abundance for acetylation on histone H3 lysine 56 when compared between the three tissues. Additionally, the gills exhibited the lowest levels of histone trimethylation, but maintained moderate levels of histone dimethylation. These results seem counterintuitive because both types of modifications are balanced by the concentrations of S-adenosylmethionine, α -ketoglutarate, FADH₂, and oxygen (Fan et al., 2015a). A possible explanation is that the concentration of these metabolites in the gills are limited and preferentially utilized for dimethylation rather than

trimethylation. Clearly, the concentration of metabolites in a tissue cannot alone predict the relative abundance of all histone PTMs, or even of certain modification types. These observations underscore the importance of quantifying specific histone PTMs (e.g., H3K23ac), instead of relying solely on the overall patterns of abundance for each modification type (e.g., acetylation) when conducting experiments on histone PTMs in non-model organisms.

Acknowledgements

We would like to thank Yuhua Fu for her assistance dissecting the fish used in this experiment. This work was supported by the National Science Foundation Grant IOS-2209383 and BARD grant IS-4800-15 to D.K.

Data Availability

All DDA and DIA raw data are available at Panorama Public (<https://panoramaweb.org/eam01kl.url>, doi: [10.6069/585h-8612](https://doi.org/10.6069/585h-8612)) and ProteomeXchange (PXD040536). The three complete DIA assay libraries including all relevant metadata and corresponding DIA data are available at Panorama Public (<https://panoramaweb.org/eam01kl.url>, doi: [10.6069/585h-8612](https://doi.org/10.6069/585h-8612)). The statistical analyses performed in this study are publicly available at https://github.com/emojica2/Histone_PTMs_Quantification_Pipeline.

Supplemental Data

This article contains supplemental data.

Abbreviations

BCA (bicinchoninic acid), DDA (data-dependent acquisition), DIA (data-independent acquisition), HME (histone modifying enzyme), IAA (iodoacetamide), K (lysine), M (methionine), m/z (mass-to-charge ratio), me (methylation), me2 (dimethylation), me3 (trimethylation), P (proline), PCA (principal component analysis), PTM (post-translational modification), R (arginine), S (serine), T (threonine), TCA (trichloroacetic acid), Y (tyrosine)

Figure Legends

Figure 1.1: Histone PTMs Detected Using Each Digestion Condition. Samples of histone proteins were digested into peptides using three methods in parallel. Each digestion method produced a distinct set of histone peptides that, when analyzed through LCMS, captured different histone PTMs for quantification. Shown are the number of unique histone PTMs, from each modification type, that can be detected using the three digestion conditions.

Figure 1.2: Strategy for Histone PTM Quantification. To calculate the relative abundance of H1.0-B R91 methylation in each sample, the normalized area of the modified peptide was divided by the sum of the normalized area from all peptides containing the residue of the PTM site, then multiplied by 100, as described in Equation 1. A mass shift of +14 on a peptide represents methylation. Panels A-C describe the modified peptide, $\text{HTK}^{+56}\text{GIGASGS}^{-18}\text{FR}^{+14}$, and panels D-F describe an example unmodified peptide, $\text{H}^{+57}\text{T}^{-18}\text{K}^{+56}\text{TKGIGASGSFR}$. Depicted in this figure are the library spectra for each peptide (**A**, **D**), the transitions of the most abundant MSMS ions in the library spectrum at distinctive retention times (**B**, **E**), and the normalized area for each sample (**C**, **F**).

Figure 1.3: Characterization of the Histone PTMs on Histone H1. **A)** All histone PTMs were mapped on a representative protein, histone H1-like (XP_003459589.1). Each panel represents a different amino acid position where at least one histone PTM was detected on this protein. The x-axis displays the three tissues characterized in this study: gills (G), kidney (K), and testes (T). **B-D)** Volcano plots depict the differences in PTMs on histone H1 proteins between tissues. These histone PTMs were plotted based on their adjusted p-value and fold change when comparisons were made between gill and kidney samples (B), gill and testes samples (C), and kidney and testes samples (D). Histone PTMs were colored according to their significance in terms of adjusted p-value (blue), fold change (green), both adjusted p-value and fold change (red), or neither (gray). **E)** The most highly tissue-dependent PTMs on histone H1 proteins were determined for either their low adjusted p-value or high fold change in the pairwise tissue comparisons. Error bars represent the mean \pm the standard error of the mean.

Figure 1.4: Characterization of the Histone PTMs on Histone H2A. **A)** All histone PTMs were mapped on a representative protein, histone H2A (XP_003448939.1). Each panel represents a different amino acid position where at least one histone PTM was detected on this protein. The x-axis displays the three tissues characterized in this study: gills (G), kidney (K), and testes (T). **B-D)** Volcano plots depict the differences in PTMs on histone H2A proteins between tissues. These histone PTMs were plotted based on their adjusted p-value and fold change when comparisons were made between gill and kidney samples (B), gill and testes samples (C), and kidney and testes samples (D). Histone PTMs were colored according to their significance in terms of adjusted p-value (blue), fold change (green), both adjusted p-value and fold change

(red), or neither (gray). **E**) The most highly tissue-dependent PTMs on histone H2A proteins were determined for either their low adjusted p-value or high fold change in the pairwise tissue comparisons. Error bars represent the mean \pm the standard error of the mean.

Figure 1.5: Characterization of the Histone PTMs on Histone H2B. **A**) All histone PTMs were mapped on a representative protein, histone H2B 1/2 (XP_003451196.1). Each panel represents a different amino acid position where at least one histone PTM was detected on this protein. The x-axis displays the three tissues characterized in this study: gills (G), kidney (K), and testes (T). **B-D**) Volcano plots depict the differences in PTMs on histone H2B proteins between tissues. These histone PTMs were plotted based on their adjusted p-value and fold change when comparisons were made between gill and kidney samples (B), gill and testes samples (C), and kidney and testes samples (D). Histone PTMs were colored according to their significance in terms of adjusted p-value (blue), fold change (green), both adjusted p-value and fold change (red), or neither (gray). **E**) The most highly tissue-dependent PTMs on histone H2B proteins were determined for either their low adjusted p-value or high fold change in the pairwise tissue comparisons. Error bars represent the mean \pm the standard error of the mean.

Figure 1.6: Characterization of the Histone PTMs on Histone H3. **A**) All histone PTMs were mapped on a representative protein, histone H3 (XP_005463512.2). Each panel represents a different amino acid position where at least one histone PTM was detected on this protein. The x-axis displays the three tissues characterized in this study: gills (G), kidney (K), and testes (T). **B-D**) Volcano plots depict the differences in PTMs on histone H3 proteins between tissues. These histone PTMs were plotted based on their adjusted p-value and fold change when

comparisons were made between gill and kidney samples (B), gill and testes samples (C), and kidney and testes samples (D). Histone PTMs were colored according to their significance in terms of adjusted p-value (blue), fold change (green), both adjusted p-value and fold change (red), or neither (gray). **E**) The most highly tissue-dependent PTMs on histone H3 proteins were determined for either their low adjusted p-value or high fold change in the pairwise tissue comparisons. Error bars represent the mean \pm the standard error of the mean.

Figure 1.7: Characterization of the Histone PTMs on Histone H4. **A**) All histone PTMs were mapped on a representative protein, histone H4-like (XP_025766521.1). Each panel represents a different amino acid position where at least one histone PTM was detected on this protein. The x-axis displays the three tissues characterized in this study: gills (G), kidney (K), and testes (T). **B-D**) Volcano plots depict the differences in PTMs on histone H4 proteins between tissues. These histone PTMs were plotted based on their adjusted p-value and fold change when comparisons were made between gill and kidney samples (B), gill and testes samples (C), and kidney and testes samples (D). Histone PTMs were colored according to their significance in terms of adjusted p-value (blue), fold change (green), both adjusted p-value and fold change (red), or neither (gray). **E**) The most highly tissue-dependent PTMs on histone H4 proteins were determined for either their low adjusted p-value or high fold change in the pairwise tissue comparisons. Error bars represent the mean \pm the standard error of the mean.

Figure 1.8: PCA Plot of Tissue Samples. The M-values of all 503 histone PTMs were used as variables to construct the PCA plot of tissue samples. Samples of gills (green), kidney (blue), and

testes (purple) are plotted according to PC1 and PC2. A 95% confidence ellipse surrounds the cluster of each tissue type.

Figures

Figure 1.1

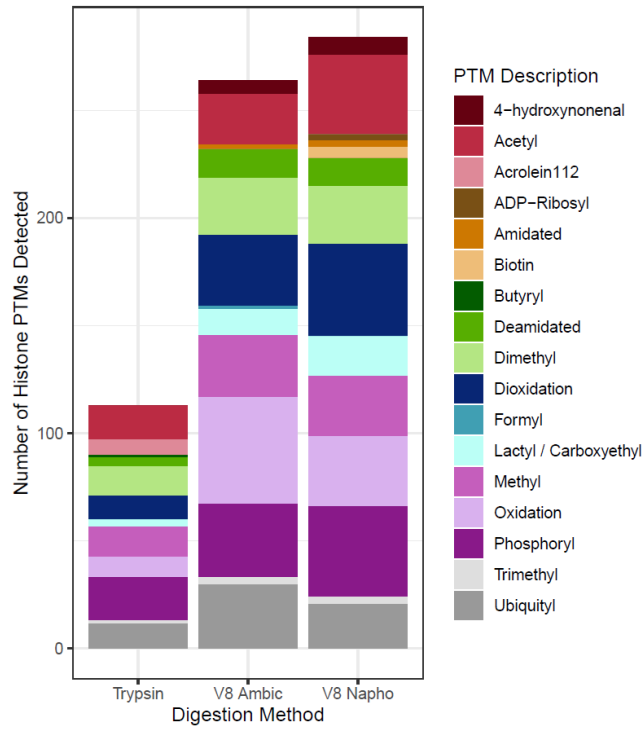


Figure 1.2

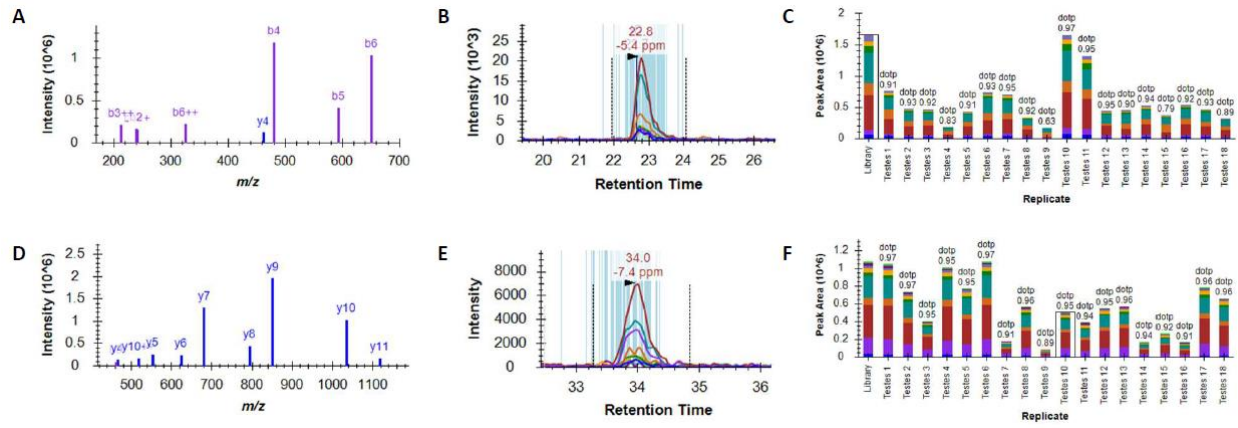


Figure 1.3

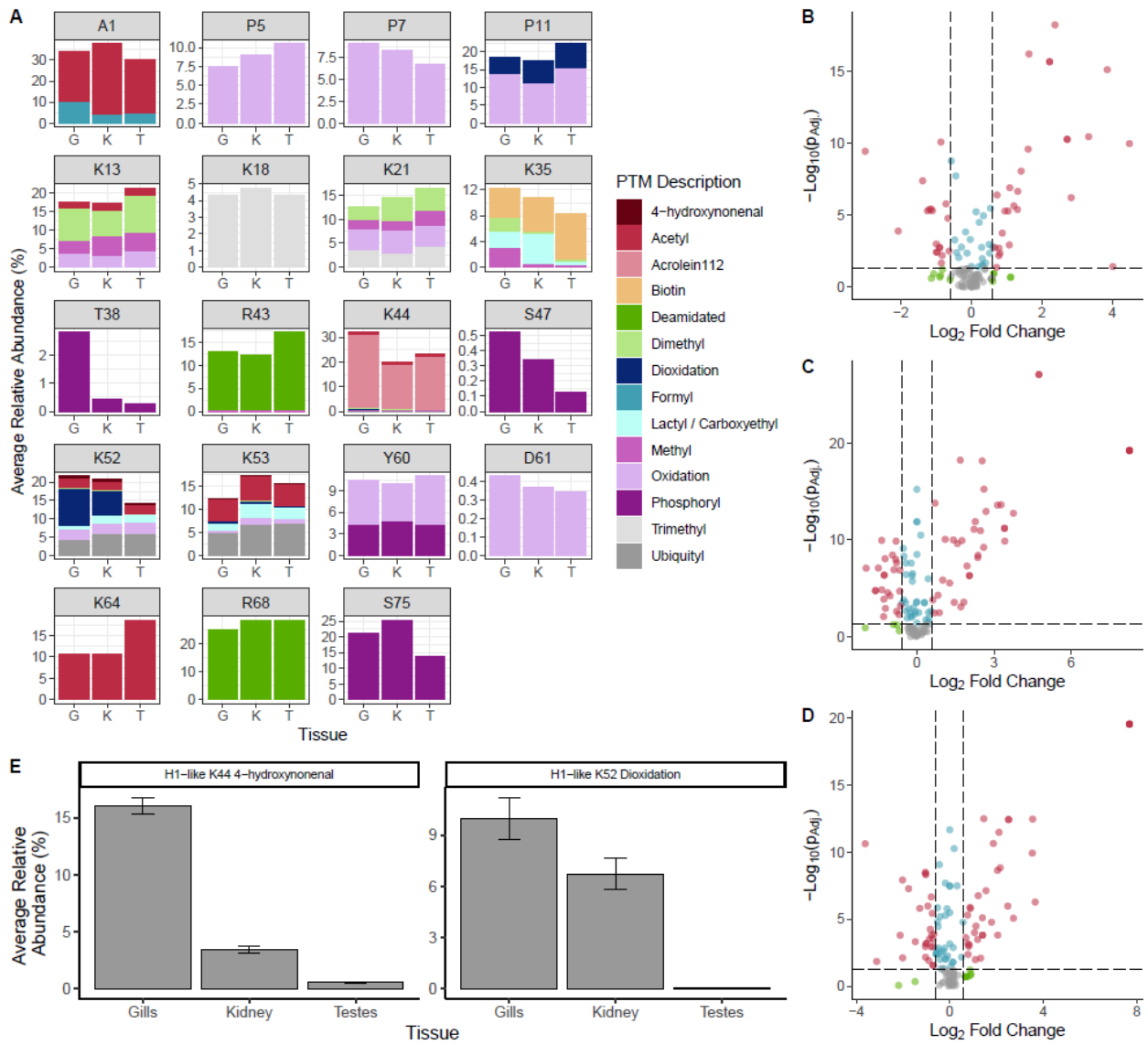


Figure 1.4

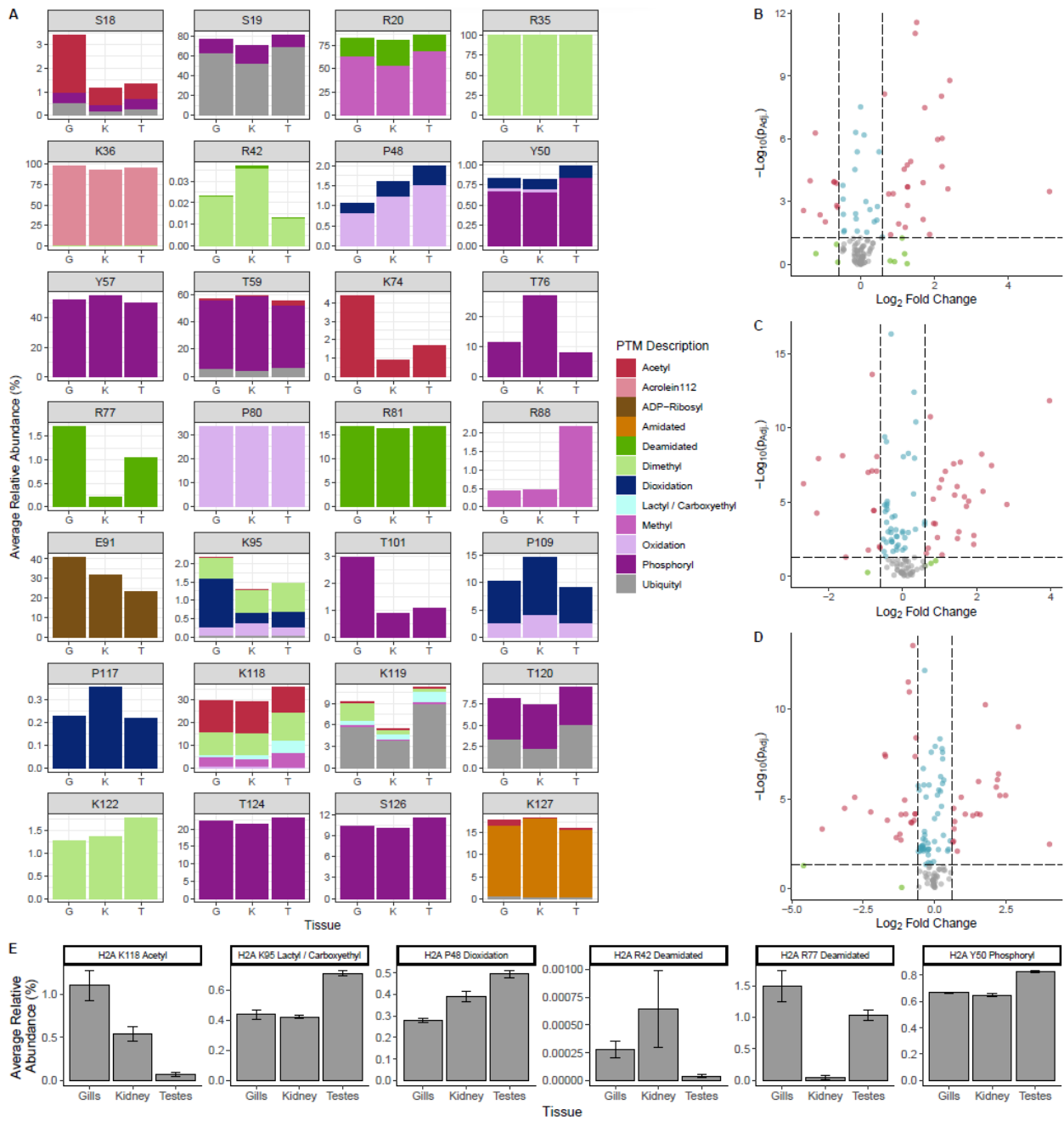


Figure 1.5

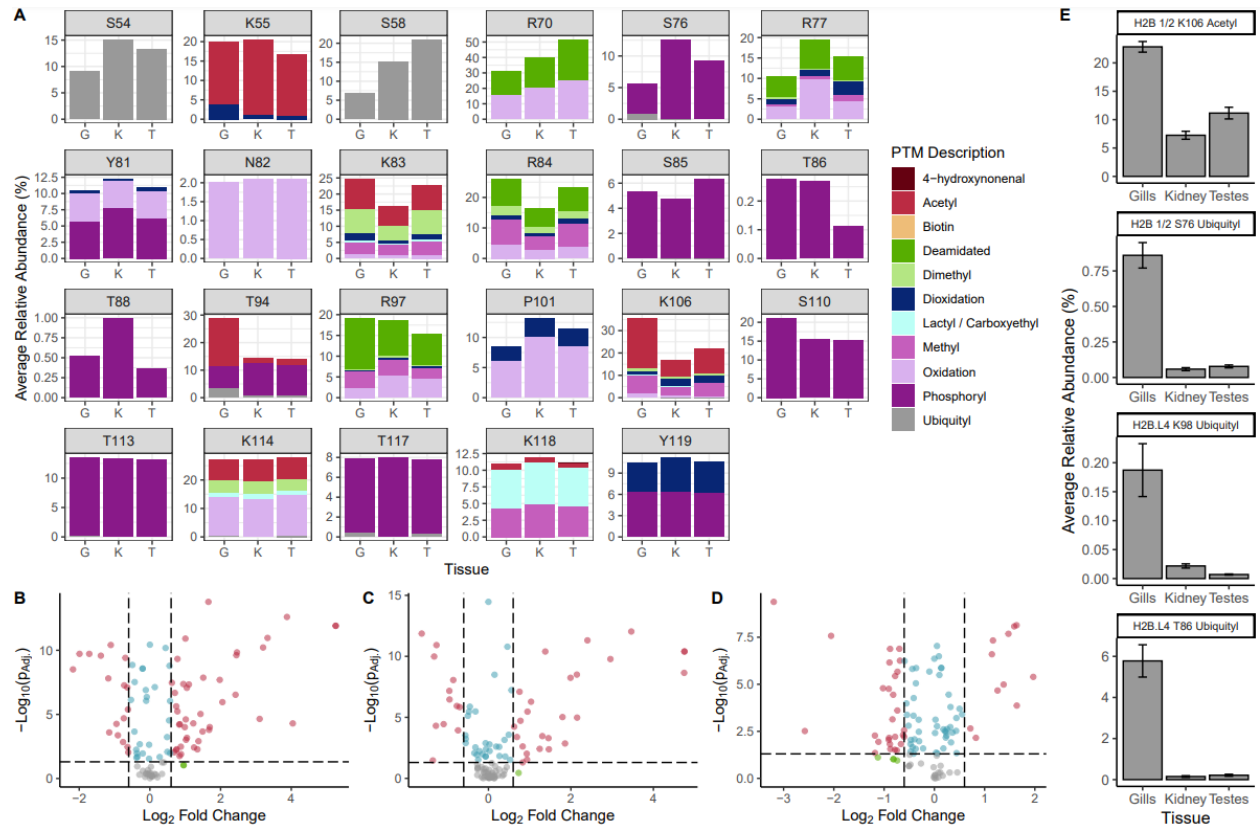


Figure 1.6

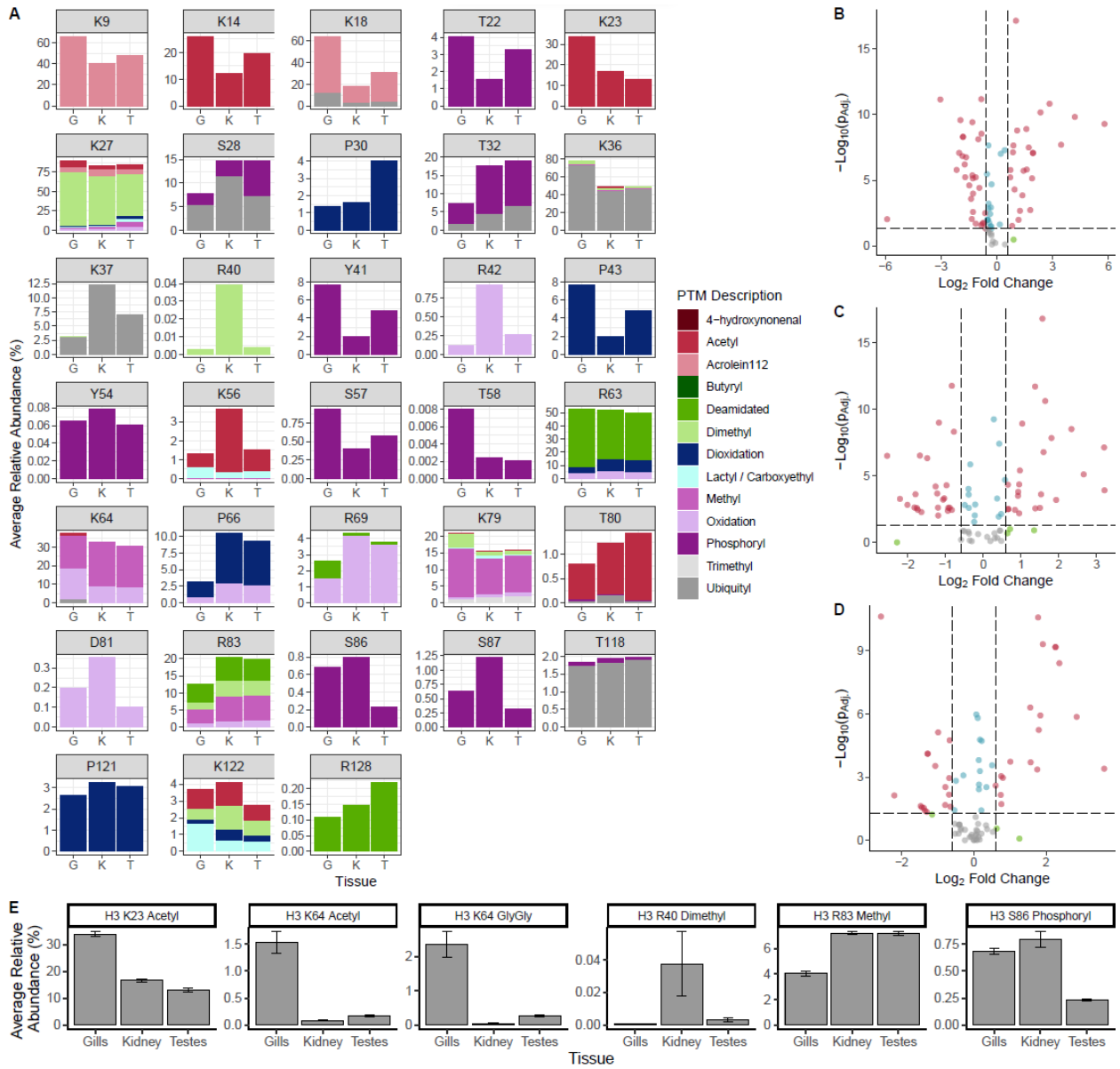


Figure 1.7

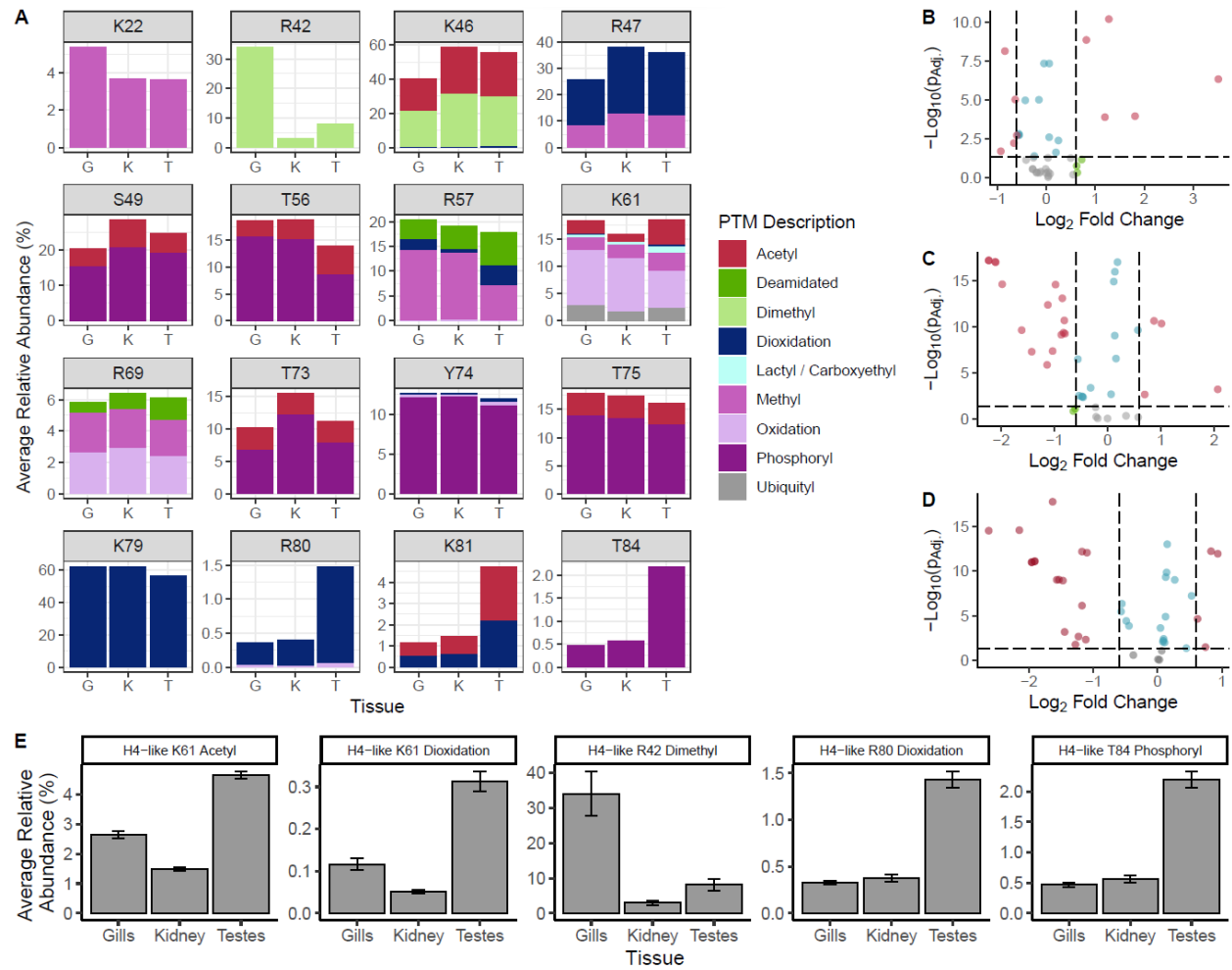
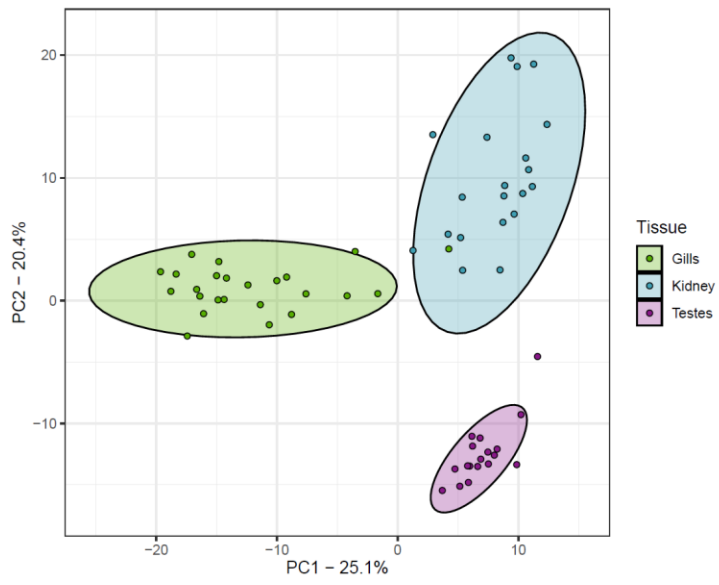


Figure 1.8



CHAPTER 2:

H3K14ac, H3K18ub, and H1K16ub Identified as Salinity-Responsive Histone PTMs in Mozambique Tilapia (*Oreochromis mossambicus*)

Abstract

Background: Histone post-translational modifications (PTMs) are epigenetic marks that can be induced by environmental stress and elicit heritable patterns of gene expression. To investigate this process in an ecological context, we characterized the influence of salinity stress on histone PTMs within the gills, kidney, and testes of Mozambique tilapia (*Oreochromis mossambicus*). A total of 503 histone PTMs were quantified in each tissue sample and compared between freshwater-adapted fish exposed to salinity treatments that varied in intensity and duration.

Results: Three salinity-responsive histone PTMs were identified in this study. When freshwater-adapted fish were exposed to seawater for two hours, the relative abundance of H1K16ub significantly increased in the gills. Long-term salinity stress elicited changes in H3K14ac and H3K18ub in the testes. When freshwater-adapted fish were exposed to a pulse of severe salinity stress, where salinity gradually increased from freshwater to a maximum of 82.5 g/kg, the relative abundance of both H3K14ac and H3K18ub decreased significantly in the testes.

Conclusions: This study demonstrates that salinity stress can alter histone PTMs in Mozambique tilapia, both in an osmoregulatory organ and in the germ line. These results signify a potential for histone PTMs to be involved in salinity acclimation and adaptation in euryhaline fishes, thereby

adding to a growing body of evidence that epigenetic mechanisms are involved in such processes.

Background

Epigenetic marks contribute to the regulation of gene expression patterns in the cells of eukaryotic organisms. Histone post-translational modifications (PTMs) and DNA methylation represent two classes of epigenetic marks, and they each can be influenced by numerous factors, including cell type, the organism's developmental stage, and environmental conditions (Atlasi and Stunnenberg, 2017; Creyghton et al., 2010; Maegawa et al., 2010; Mojica and Kültz, 2022; Østrup et al., 2014). Under ideal circumstances, environmentally-induced epigenetic marks enable organisms to alter their gene expression in a way that better prepares them to survive and thrive within their environments. The evidence of this phenomenon occurring in nature is rapidly growing, particularly with the epigenetic mark of DNA methylation (Norouzitallab et al., 2014; Ryu et al., 2018; Strader et al., 2019). However, there is still a paucity of epigenetic research in fishes, especially in response to globally changing environmental factors, such as salinity (Eirin-Lopez and Putnam, 2019a).

The few studies conducted in this research area point to the involvement of DNA methylation in the acclimation and adaptation of fishes to salinity stress. The brown trout (*Salmo trutta*) presents an interesting example within this context (Morán et al., 2013). Juveniles of this species can develop into either freshwater trout or migratory sea trout, which are genetically indistinguishable. Yet, the priority for conservation efforts has been to specifically enrich populations of the migratory morphotype, rather than the freshwater one. Following challenges in establishing the desired morphotype from hatchery-raised fish, it was found that feeding fish a

high-salt diet altered the DNA methylation at key osmoregulatory genes, which led to an increased proportion of hatchery-raised fish that developed into migratory sea trout (Morán et al., 2013). Examples of the putative involvement of epigenetic mechanisms in salinity adaptation come from studies on the three-spined stickleback (*Gasterosteus aculeatus*), which consist of several discrete populations locally adapted to different salinities. When compared between populations of sticklebacks adapted to different salinities, DNA methylation was found to vary at genes associated with osmoregulation (Artemov et al., 2017; Hu et al., 2021). Moreover, once sticklebacks from a low salinity environment were acclimated to high salinity, they acquired intergenerationally stable patterns of DNA methylation that were similar to those found in the populations of sticklebacks locally adapted to high salinity (Heckwolf et al., 2020).

Unlike DNA methylation, histone PTMs as an epigenetic mark have not yet been investigated in fishes experiencing salinity stress. Therefore, the purpose of this study was to characterize how histone PTMs respond to salinity stress in Mozambique tilapia (*Oreochromis mossambicus*). This species is strongly euryhaline, capable of tolerating salinities from freshwater (0 g/kg) to about four-times the salinity of seawater (120 g/kg), as long as fish have sufficient time to gradually acclimate to higher salinities (Root and Kültz, 2022; Stickney, 1986). Time is needed during these acclimations so that the fish's osmoregulatory organs (e.g., gills and kidney) can adjust their morphology and physiology in a way that switches their strategies for osmoregulation depending on environmental salinity (Kültz, 2015). To determine whether histone PTMs could be involved in this adjustment, and therefore salinity acclimation, we characterized the impact of salinity stress on histone PTMs in the gills and kidney. Furthermore, we tested whether salinity stress could impact histone PTMs in the testes, being representative of

the male germ line, where epigenetic changes could be passed onto future generations. Such a process could facilitate salinity adaptation.

In this study, we imposed a variety of salinity treatments on Mozambique tilapia in order to test whether the intensity and duration of salinity stress differentially impacts histone PTMs in the gills, kidney, and testes. The first set of salinity treatments that we imposed on fish represented the strongest short-term salinity stress that Mozambique tilapia could tolerate. Due to their temporal limitations in salinity tolerance, Mozambique tilapia adapted to freshwater can only survive an immediate change in salinity up to 25 g/kg. However, they can temporarily tolerate an immediate change in salinity from freshwater to seawater (30 g/kg), as long as salinity decreases within six hours (Hwang et al., 1989; Moorman et al., 2015). Frequent changes between freshwater and seawater are regularly experienced in Mozambique tilapia when they inhabit tidal estuaries (Moorman et al., 2014). To mimic these large salinity changes, we exposed freshwater-adapted Mozambique tilapia to 1) freshwater, 2) seawater for two hours, or 3) seawater for two hours followed by a recovery in freshwater for two hours. The second set of salinity treatments was designed to reveal how long-term exposure to salinities near the upper tolerance limit of Mozambique tilapia influenced histone PTMs in different tissues. Additionally, it was designed to uncover whether the histone PTM response to severe salinity stress differed depending on the fish's previous experience with salinity stress. Therefore, we exposed freshwater-adapted fish to 1) freshwater, 2) one "pulse" of severe salinity stress, where salinity gradually increased from freshwater to 82.5 g/kg, or 3) three pulses of severe salinity stress.

Results

Standards established for determining whether histone PTMs are salinity-responsive

For every sample of tissue collected from Mozambique tilapia following salinity treatments, a total of 3,504 peptides located on 25 different histone proteins were quantified. Values of histone peptide abundance were used to calculate the relative abundance, beta-value, and M-value of 503 biologically relevant histone PTMs, as we have described in detail in a previous publication (Mojica and Kültz, 2023a). To determine whether histone PTMs were salinity-responsive, we compared the M-values for all 503 histone PTMs between the fish from different salinity treatments using t-tests. Because the salinity treatments were conducted as two experiments, we made comparisons between the fish from all short-term salinity treatments (Figure 2.1), and we separately made comparisons between the fish from all long-term salinity treatments (Figure 2.2). These comparisons were performed independently for each tissue.

Several histone PTMs were found to have a raw p-value < 0.05 when compared between fish from different salinity treatments; however, a correction was needed for determining the significance of these histone PTMs because multiple hypotheses (503) were tested within each comparison. We used Boca and Leek's FDR regression method for multiple hypothesis testing correction because it provides high power by accounting for covariates (Korthauer et al., 2019; Leek et al., 2022). The covariate we chose for this correction was the type of modification (e.g., acetylation, methylation) of each histone PTM, as indicated by the Unimod accession number. A conditioned q-value is the output of each test correction, and this value represents the proportion of false discoveries in the list of significant results. We determined histone PTMs to be salinity-responsive if they had a conditioned q-value of less than 0.1 when compared between fish exposed to different salinity treatments. This value would indicate that less than 10% of the

histone PTMs deemed significant are false discoveries. In this study, three histone PTMs met this criterion and were determined to be salinity-responsive in Mozambique tilapia. One histone PTM was found to differ in the gills of fish exposed to short-term salinity stress, and two histone PTMs were found to differ in the testes of fish exposed to long-term salinity stress. A complete account of how histone PTMs respond to salinity stress in the gills, kidney, and testes is presented in Supplemental Table 2.1.

Short-term salinity stress altered one histone PTM in the gills

Freshwater-adapted Mozambique tilapia were given one of three salinity treatments. Fish in the first treatment group were directly transferred from freshwater to seawater, then kept at seawater for exactly two hours before euthanization. The fish from the second treatment group were directly transferred from freshwater to seawater, kept at seawater for exactly two hours, then directly transferred back to freshwater. These fish were maintained in freshwater for an additional two hours as a recovery period before euthanization. Fish in the control group were transferred from freshwater to another tank containing freshwater. When histone PTMs in the gills, kidney, and testes were compared between the fish from the three different short-term salinity treatments, one histone PTM met the criterion above as being salinity-responsive (Figure 2.1A). This histone PTM was histone H1 isoform X1 lysine 16 ubiquitylation (H1K16ub), and it was found to be significantly different between the gills of fish exposed only to freshwater and the gills of fish exposed to seawater for two hours (p -value = $3.48e-04$; conditioned q -value = 0.09).

The influence of salinity stress on the global relative abundance of H1K16ub is displayed in Figure 2.3. Exposure to seawater increased relative abundance when compared to fish only

exposed to freshwater. Fish exposed to freshwater had an average relative abundance of H1K16ub of 2.03%. Exposure to seawater for two hours led to the significant increase in this histone PTM to a relative abundance of 3.78%. The relative abundance of H1K16ub in fish from the final treatment group, having been transferred from freshwater to seawater and back to freshwater, was not significantly different from either of the other treatment groups, as there was a higher variance in this histone PTM's abundance. The mean relative abundance, however, remained high like it was in the fish exposed to seawater for two hours. In this case, the mean relative abundance of H1K16ub was 3.33%.

While H1K16ub was the only histone PTM to meet our criterion as a salinity-responsive histone PTM under short-term salinity stress, the volcano plots in Figure 2.1 reveal further insight into how salinity stress influences histone PTMs in the gills, kidney, and testes. For example, salinity was shown to have a particularly low impact on histone PTMs in the kidneys (Figure 2.1D-F). Some histone PTMs in the testes stood out from the rest for responding to salinity stress (Figure 2.1G-H). These included histone H1-like proline 5 dioxidation (p-value = 9.55×10^{-4} ; conditioned q-value = 0.15), histone H1-like K13 lactylation/carboxyethylation (p-value = 6.58×10^{-4} ; conditioned q-value = 0.16), and histone H1-like P11 dioxidation (p-value = 1.54×10^{-3} , conditioned q-value = 0.16) when comparisons were made between the testes of fish exposed to seawater for two hours and the testes of fish exposed only to freshwater (Figure 2.1G). In the gills, the histone PTM of H1K16ub was found to be significantly different between fish exposed to seawater for two hours and fish exposed only to freshwater, but it is worth noting that several additional histone PTMs approached significance in this comparison (Figure 2.1A). These histone PTMs included histone H1-like lysine 13 dimethylation (p-value = 1.12×10^{-3} ; conditioned q-value = 0.11), histone H1 isoform X1 lysine 13 methylation (p-value = 6.78×10^{-4} ;

conditioned q-value = 0.12), histone H1-like K16 lactylation/carboxyethylation (p-value = 9.42e-04; conditioned q-value = 0.13), and histone H2A threonine 101 ubiquitylation (p-value = 3.40e-03; conditioned q-value = 0.18).

Long-term salinity stress altered two histone PTMs in the testes

Examinations into the effect of long-term salinity stress on histone PTMs in Mozambique tilapia consisted of three treatment groups. Fish in the first treatment group (S1) were exposed to one pulse of severe salinity stress, where salinity was gradually increased from 0 g/kg (freshwater) to 82.5 g/kg (nearly three times the salinity of seawater). The second group of fish (S3) experienced the same “pulse” of severe salinity stress as the first treatment group, but instead of one pulse, they experienced three pulses of salinity stress over the course of 62 days. Fish in the final treatment group (S0) were handled as a control group and only ever experienced freshwater. The 503 histone PTMs quantified in this study were compared between fish from each group of long-term salinity treatments. These comparisons were performed separately for the gills, kidney, and testes (Figure 2.2). In the testes, two histone PTMs were found to change significantly with salinity stress. Between the fish exposed only to freshwater and the fish exposed to one pulse of salinity stress, the PTMs of histone H3 lysine 18 ubiquitylation (H3K18ub; p-value = 2.68e-04; conditioned q-value = 0.09) and histone H3 lysine 14 acetylation (H3K14ac; p-value = 3.87e-04; conditioned q-value = 0.09) were significantly different (Figure 2.2G).

The manner in which salinity influenced the global relative abundance of these histone PTMs in the testes is depicted in Figures 2.4 and 2.5. In the case of H3K14ac (Figure 2.4), relative abundance was highest at 27.5% when fish were only ever exposed to freshwater. Once

the fish were exposed to one pulse of severe salinity stress, the relative abundance decreased significantly to 15.3%. Similarly, fish exposed to three pulses of severe salinity stress exhibited a relative abundance of 16.0%; however, this value was not significantly different when compared to either of the other long-term salinity treatments. The case of H3K18ub (Figure 2.5) is similar to that of H3K14ac. Relative abundance of H3K18ub was highest at 5.0% in the fish only ever exposed to freshwater. Upon exposure to one pulse of severe salinity stress, relative abundance decreased significantly to 2.2%. The relative abundance of H3K18ub remained low at 2.6% when fish were exposed to three pulses of salinity stress, but again this value was not significantly different from the other two long-term salinity treatments.

Long-term salinity stress led to the most pronounced histone PTM differences in testes, rather than the gills or kidney (Figure 2.2). As with short-term salinity stress, histone PTMs in the kidneys of Mozambique tilapia were largely unaffected by long-term salinity stress (Figure 2.2D-F). Although no histone PTMs met the criterion for being salinity-responsive in the gills under long-term salinity stress, volcano plots depict widespread but subtle changes in histone PTMs in the gills of fish exposed to either one or three pulses of severe stress when compared to the gills of fish in freshwater (Figure 2.2A-B). The histone PTMs that stood out from the rest in the gills of fish experiencing one pulse of severe salinity when compared to fish in freshwater included histone H2B.L4 arginine 89 dioxidation (p-value = 3.23e-03; conditioned q-value = 0.23), core histone macro-H2A.1 isoform X5 threonine phosphorylation (p-value = 1.07e-03; conditioned q-value = 0.23), histone H1-like serine 1 acetylation (p-value = 5.23e-04; conditioned q-value = 0.24), and histone H2B 1/2 arginine 97 dimethylation (p-value = 1.95e-05; conditioned q-value = 0.24).

Human analogs of the salinity-responsive histone PTMs

To determine whether the salinity-responsive histone PTMs identified in this study are analogous to human histone PTMs, we performed sequence alignments between the primary protein structures of tilapia histone proteins and the corresponding human histone proteins (Supplemental Figures 2.1-2.2) using Clustal Omega (Sievers and Higgins, 2018). One sequence alignment was made between the tilapia histone H1 isoform X1 (accession number XP_019210164.1) and the human histone H1 protein (accession number AAA63187.1). This alignment demonstrated that tilapia histone H1 isoform X1 lysine 16, on which we identified the salinity-responsive histone PTM of H1K16ub, aligned to human histone H1 arginine 24. Because ubiquitylation does not occur as a post-translational modification on arginine residues, we determined that there is no human analog of the salinity-responsive histone PTM of H1K16ub. A second sequence alignment was made between the histone H3 proteins in tilapia (accession number XP_005463512.2) and in humans (accession number AAN39284.1). The two salinity-responsive histone PTMs detected in tilapia, being H3K14ac and H3K18ub, aligned exactly to those in humans. Furthermore, these two histone PTMs have been previously detected and characterized across several species, including humans (Table 2.1).

Discussion

Three histone PTMs responded to salinity stress in Mozambique tilapia tissues

The goal of this study was to characterize the influence of salinity stress on histone PTMs in Mozambique tilapia. By measuring the histone PTM response to salinity of varying intensities and duration in the gills, kidney, and testes, we sought to determine whether histone PTMs could be involved in salinity acclimation and adaptation. This hypothesis was supported by the

alteration of H1K16ub in the gills, being an osmoregulatory organ, and by the alteration of H3K14ac and H3K18ub in the testes, being representative of the male germ line. To our knowledge, the investigation of salinity-responsive histone PTMs has only previously been conducted in plants (Bilichak et al., 2012; Li et al., 2014; Paul et al., 2017; Rashid et al., 2022; Sokol et al., 2007; Wu et al., 2011; Zheng et al., 2019). Yet, despite the large taxonomic differences between fishes and plants, H3K14ac has now been shown to respond to salinity in tilapia in addition to soybean, tobacco, rice, and Arabidopsis (Paul et al., 2017; Sokol et al., 2007; Wu et al., 2011; Zheng et al., 2019). In plants, salinity stress influenced H3K14ac by causing its relative abundance to increase. The opposite effect was observed in tilapia. In this experiment, the fish only exposed to freshwater had the highest average relative abundance of H3K14ac in their testes at 27.5%. This value decreased significantly to 15.3% in fish exposed to one pulse of severe salinity stress, and it remained low at 16.0%, although nonsignificantly different, in the testes of fish exposed to three pulses of severe salinity stress.

H3K14ac is a highly studied histone PTM often associated with transcriptional activation (Kuo et al., 1996; Schiltz et al., 1999; Zhao and Garcia, 2015), and it seems to exhibit dynamic regulation in response to stress, such that its abundance can decrease with stress (Mahalingaiah et al., 2016), increase with stress (Porter et al., 2019), or decrease immediately after stress but later increase (Covington et al., 2009; Karen and Rajan, 2019). This feature may explain why H3K14ac responded in opposite directions to salinity stress between our study in tilapia and studies conducted in plants. Moreover, a global significant increase in overall histone PTM abundance across the entire chromatin does not exclude the possibility of a significant reduction at specific genomic loci. Nonetheless, the decreased global relative abundance of H3K14ac observed in the testes of Mozambique tilapia is consistent with a recent study conducted on Nile

tilapia (*Oreochromis niloticus*) (Cruz Vieira et al., 2019). When Nile tilapia were exposed to salinities near their upper tolerance limit, they experienced only subtle changes in spermatogenesis, but exhibited protein-level changes in the heat shock protein 70 (HSP70) and proliferating cell nuclear antigen (PCNA) in their testes (Cruz Vieira et al., 2019). As salinity increased, the abundance of HSP70 decreased, and the abundance of PCNA increased (Cruz Vieira et al., 2019). The abundance of HSP70 has previously been found to exhibit a positive correlation with H3K14ac (Belova et al., 2008; Kugler et al., 2012). Therefore, a decrease in HSP70 would likely correspond to a decrease in the relative abundance of H3K14ac. Less expected was the trend observed for PCNA in the testes of Nile tilapia (Cruz Vieira et al., 2019). PCNA is used as a biomarker of cell proliferation and spermatogenesis (Tousson et al., 2011), and its abundance has been positively correlated to that of H3K18ub, which we identified as another salinity-responsive histone PTM in Mozambique tilapia.

H3K18ub plays a critical role in maintaining patterns of DNA methylation after DNA replication (Harrison et al.; Qin et al., 2015). Like histone PTMs, DNA methylation can be impacted by an organism's environment and contributes to upholding patterns of gene expression. Patterns of DNA methylation can endure across cycles of DNA replication, but due to the semi-conserved manner in which DNA replicates, DNA replication leaves DNA as hemi-methylated, such that the template strands of DNA are methylated in their "proper" pattern and the newly synthesized strands of DNA are unmethylated. Hemi-methylated DNA recruits the protein UHRF1 to begin the process of restoring proper DNA methylation patterns to newly synthesized DNA. UHRF1 ubiquitylates histone H3, with a preference for ubiquitylating H3K18 (Harrison et al.). Following histone ubiquitylation, the DNA methylation enzyme DNMT1 is recruited to the genomic loci so that it can copy the DNA methylation pattern of the template

strand onto the newly synthesized strand (Qin et al., 2015). PCNA mediates the recruitment of DNMT1 to enhance the efficiency of DNA methylation restoration onto the newly synthesized strand of DNA (Bostick et al., 2007; Schermelleh et al., 2007). In this experiment, one pulse of severe salinity stress reduced the prevalence of H3K18ub in the testes of Mozambique tilapia. Although these results seem counterintuitive based on the previous study in Nile tilapia that found salinity stress to increase the abundance of PCNA in the testes (Cruz Vieira et al., 2019), they are consistent with other findings that salinity stress can cause cell cycle arrest, including in *O. mossambicus* (Kammerer et al., 2009; Kültz et al., 1998).

The salinity-responsive histone PTM identified in the gills of Mozambique tilapia experiencing short-term salinity stress, H1K16ub, does not have a human analog and has not been previously described. Ubiquitylation on histone H1 isoforms, however, has been associated with gene expression and the DNA damage response (Hölmüller et al., 2021; Pham and Sauer, 2000; Thorslund et al., 2015). Because the relative abundance of H1K16ub increased in the gills upon short-term exposure to seawater, but histone PTMs associated with gene expression and cellular proliferation (H3K14ac and H3K18ub) decreased in the testes upon long-term exposure to hypersalinity, the salinity-responsive histone PTMs may be reflective of a shift in energy away from the testes and towards the gills during certain types of salinity stress.

The intensity and duration of the salinity challenge differentially impacted histone PTMs

The concept of salinity stress in fishes is highly complex. Even in the context of euryhaline fishes like Mozambique tilapia, which can tolerate a wide range of salinity, there are numerous caveats to this tolerance. How “stressful” a salinity challenge is to a euryhaline fish depends on several factors, including those specific to the environment, such as the starting

salinity, the rate of salinity change, and the duration of altered salinity (Hwang et al., 1989; Root and Kültz, 2022). Additionally, it includes factors specific to the fish, such as age and developmental stage, overall nourishment, and prior exposure to salinity stress (Hwang et al., 1999; Schreck and Tort, 2016; Stickney, 1986; Whitfield, 2015). The histone PTM response to salinity in Mozambique tilapia tissues reflects the complex notion of salinity stress. In this study, short-term salinity stress influenced one histone PTM in the gills, but long-term salinity stress did not. In the testes, long-term salinity stress influenced two histone PTMs, but short-term salinity stress did not.

We hypothesize that the histone PTM response in the gills relates to the extensive remodeling that gills undergo to adjust the flux of salts in and out of a fish during critical salinity changes (Kültz, 2015). Because the time needed for gills to make these physiological and morphological adjustments exceeds two hours, it is likely that only the fish exposed to long-term salinity stress in this study experienced gill remodeling relative to fish in freshwater. The relative abundance of H1K16ub significantly increased in the gills of fish when fish were transferred directly from freshwater to seawater and kept there for two hours, but it was not significantly different between the gills of fish exposed to different long-term salinity treatments. Therefore, it is possible that H1K16ub aids in the tolerance to salinity stress in fish prior to gill remodeling. As for the testes, it is likely that short-term exposure to seawater was not extensive enough to elicit any changes to reproductive strategies, but that long-term exposure to hypersalinity (82.5 g/kg) was severe enough to alter patterns of energy expenditure in the fish and thereby lead to decreased relative abundances of H3K14ac and H3K18ub.

The salinity treatments imposed on fish in this study were designed to investigate two additional features of the epigenetic response to salinity stress: 1) whether stress-induced histone

PTMs persist after exposure to stress subsides, and 2) whether the histone PTM response to salinity stress depends on previous life experience. Investigating these features is especially relevant in Mozambique tilapia because many populations of this species inhabit hypersaline lakes, which regularly fluctuate in salinity depending on precipitation and evaporation (Kienel et al., 2013; Whitfield and Blaber, 1979). We therefore questioned whether the histone PTM response to salinity stress in fish would depend on the frequency of precipitation/evaporation cycles. Our hypothesis that stress-induced histone PTMs can persist after stress would have been supported if H1K16ub remained significantly higher in the gills of fish after fish were transferred back to freshwater from a two-hour exposure to seawater. We did not find sufficient evidence to support this hypothesis; however, as shown in Figure 2.3, the average relative abundance of H1K16ub remained relatively high in the group of fish recovering from short-term exposure to seawater. Nonetheless, this value was not significantly different from either of the other salinity treatments groups due to increased variance in H1K16ub relative abundance. Our hypothesis that the histone PTM response to salinity stress depends on previous life experience would have been supported either if the salinity-responsive histone PTMs that changed with one pulse of severe salinity stress responded in opposite directions to fish experiencing three pulses of severe salinity stress, or if entirely different histone PTMs were affected by severe salinity stress when fish were exposed to either one pulse or three pulses of the stress. This hypothesis was not supported in this study. Although the histone PTMs of H3K14ac and H3K18ub were only found to be significantly different between the testes of fish exposed to one pulse of severe salinity stress and the testes of fish exposed to freshwater, fish exposed to three pulses of severe salinity stress exhibited a similar, though nonsignificant, response with these histone PTMs in the testes (Figures 2.4 and 2.5).

Limitations and Recommendations for Future Studies

Implicit to the experimental design used for this study was the considerable limitation that salinity-responsive histone PTMs could only be detected if they changed on a global, cellular level. Our study could not have captured how histone PTMs changed with salinity stress on a local, genomic loci-specific level. Given the functional role of histone PTMs in gene expression and maintenance, the genomic distribution of histone PTMs is likely to be of high importance. We anticipate that future studies would benefit from investigating the genomic distribution of the salinity-responsive histone PTMs identified here across various contexts of salinity exposures and time. Chromatin immunoprecipitation followed by sequencing (ChIP-seq) could be used for this purpose if appropriate antibodies for the identified histone PTMs are available (Park, 2009). Additionally, the histones surrounding genes of interest can be targeted for histone PTM analysis through methods of reverse-chromatin immunoprecipitation (R-ChIP), including Cas9 Locus-Associated Proteome (CLASP), Isolation of DNA Associated Proteins (IDAP), and Chromatin-of-Interest Fragment Isolation (CoIFI) (Isogawa et al., 2020; Tsui et al., 2018). By targeting the histone PTMs associated with osmotically regulated genes, a more refined view of the histone PTM response to salinity could be obtained. Because three histone PTMs were detected for being salinity-responsive on a global level, their response across the genome must have been quite dramatic and consistent.

Conclusions

In this study, Mozambique tilapia were exposed to salinity treatments that varied in intensity and duration before their gills, kidney, and testes were processed for histone PTM

analysis. Of the 503 histone PTMs quantified and compared between tissues from fish in each salinity treatment, three were found to be salinity-responsive. Short-term salinity stress led to a significant increase in the relative abundance of H1K16ub in the gills, and long-term salinity stress led to the significant decrease in the relative abundances of both H3K14ac and H3K18ub in the testes. Notably, H3K14ac and H3K18ub have been well-documented in the scientific literature, and H3K14ac has been previously found to respond to salinity stress in plants. The results presented here complement a growing body of evidence that epigenetic mechanisms are involved in the acclimation and adaptation of euryhaline fishes to salinity stress. We demonstrate that specific types of salinity stress can alter histone PTMs in an osmoregulatory organ, where stress-induced histone PTMs could contribute to salinity acclimation, and in the testes, where stress-induced histone PTMs could be meiotically inherited and thereby contribute to salinity adaptation. Future work will be needed to sufficiently characterize the nature of this histone PTM response to salinity stress and confirm any physiological or evolutionary function.

Methods

Salinity Treatments and Tissue Collection

In this study, a set of short-term salinity treatments and a set of long-term salinity treatments were delivered to a total of 42 adult Mozambique tilapia. The short-term and long-term salinity treatments were conducted as separate experiments, where 18 fish were used for the short-term salinity treatments, and 24 fish were used for the long-term salinity treatments. For all treatments, salinity was adjusted using Instant Ocean (Instant Ocean, Cincinnati, OH, USA) and confirmed using a refractometer on a daily basis. Fish were maintained on a 12 hour light to 12 hour dark schedule, and they were fed ad libitum daily.

For the short-term salinity treatments (Supplemental Figure 2.3), each treatment group was composed of six fish as biological replicates, and fish were individually housed in 20 gallon tanks during their salinity exposures. Fish in the treatment group FW were only ever exposed to freshwater (0 g/kg). In treatment group SW, fish were transferred directly from freshwater to seawater (30 g/kg) and kept there for exactly two hours. Finally, the fish in the treatment group SW/FW were transferred directly from freshwater to seawater, kept there for exactly two hours, then transferred directly back to freshwater and kept there for an additional two hours. Following exposures, all fish were euthanized and dissected for their gills, kidney, and in males, testes. Due to the sexes of the fish randomly selected for this experiment, dissections yielded $n = 6$ gill samples, $n = 6$ kidney samples, and $n = 3$ testes samples per treatment group. Tissue samples were immediately placed in room temperature phosphate buffered saline (PBS) in preparation for histone PTM analysis, described below.

For the long-term salinity treatments (Supplemental Figure 2.4), each treatment group was composed of eight fish, and fish were housed in 55 gallon tanks according to their treatment group. Fish in treatment group S0 acted as a control group and were only ever exposed to freshwater. Fish in treatment group S1 experienced a gradual shift in salinity from freshwater to a salinity of 82.5 g/kg, being nearly three times the salinity of seawater. For this treatment, salinity increased at a rate of 7.5 g/kg per day, then salinity was maintained at 82.5 g/kg for two days. Fish in treatment group S3 were exposed to the same “pulse” of salinity stress as in treatment group S1, but instead of one pulse, they experienced three pulses of salinity stress. Therefore, salinity shifted from freshwater to 82.5 g/kg at a rate of 7.5 g/kg per day, then it decreased back to freshwater. The fish were maintained in freshwater for seven days before salinity was again increased to 82.5 g/kg. This pattern continued until three pulses of salinity

stress were achieved after 62 days. For all long-term salinity treatments, salinity was increased by replacing 20% of the tank's water volume with water containing a higher salinity. To control for the handling stress associated with water changes, 20% of the water volume was replaced in all of the tanks housing experimental fish whenever one treatment group experienced an increase in salinity. To decrease salinity following a pulse of salinity stress, 30% of the total volume of water was replaced with freshwater for four consecutive days. On the fifth day, 50% of the total water volume was replaced with freshwater, and on the sixth day, 100% of the water volume was replaced with freshwater. In order to change 100% of the water from each tank, fish were temporarily moved to a holding tank as water changes were made. As before, water changes were performed on all tanks housing experimental fish in order to control for handling stress. Following salinity treatments, all fish were euthanized, and their gills, kidney, and testes (if male) were collected for histone PTM analysis. These dissections yielded $n = 8$ gill samples, $n = 6$ kidney samples, and $n = 6$ testes samples per treatment group. The tissue samples were immediately placed in room temperature PBS following dissection to begin histone PTM analysis as described below. Notably, the resulting histone PTM data from these 24 fish were previously published without analyzing any effects of salinity when we thoroughly documented our methods for histone PTM analysis (Mojica and Kültz, 2023a).

Processing samples for histone PTM analysis

The workflow for histone PTM analysis was conducted as we have previously described (Mojica and Kültz, 2023a). As such, dissected tissues entered the workflow by being broken down into detached cells through a protocol of mechanical single cell suspension. Next, samples were enriched for histone proteins through histone acid extraction. Histone proteins were

digested into peptides through the use of three parallel digestion methods: 1) using the protease trypsin (Promega Corporation, Madison, WI, USA) after chemically deriving proteins through propionylation (Lin and Garcia, 2012), 2) using the protease V8 (Thermo Scientific, Thermo Fisher Scientific, Inc., Rockford, IL, USA) in the buffer ammonium bicarbonate, and 3) using the protease V8 in the buffer sodium phosphate. Each digestion method produced a distinct set of histone peptides. Samples of histone peptides were then analyzed using liquid chromatography mass spectrometry using previously described parameters (Root et al., 2021a). All DIA raw files were internally mass calibrated using DataAnalysis 4.1 (Bruker Daltonics) to yield a mean mass error of 0 ppm across all transitions. The absolute mass error allowed for any transition was 20 ppm, but the great majority had mass errors much smaller than 10 ppm (Supplemental Figure 2.5). Previously constructed DIA assay libraries were used to quantify all tilapia-specific histone peptides, and these values were used to calculate the relative abundance, beta-value, and M-value of each histone PTM as done before (Mojica and Kültz, 2023a). The relative abundance of each histone PTM was reported as an intuitive value that represents the percent of histones in a sample where a specific amino acid residue is occupied by the PTM of interest. Similarly, the beta-value represents the proportion of histones in a sample that contain the PTM of interest. A logit-transformation of the beta-value is called the M-value. The M-value of each histone PTM was calculated so that statistical analyses could be performed using values that follow a normal distribution. In total, 503 biologically relevant histone PTMs were quantified in each sample using these methods.

Statistical analyses

To test the effect of each salinity treatment on histone PTMs in Mozambique tilapia tissues, t-tests were performed on the M-values of all 503 quantified histone PTMs. Pairwise comparisons were made between fish exposed to each of the short-term salinity treatments, and these comparisons were made separately for the gills, kidney, and testes. Similarly, pairwise comparisons were made for each tissue between fish exposed to each of the long-term salinity treatments. The raw p-values resulting from each treatment comparison were corrected for multiple hypothesis testing. Boca and Leek's FDR regression method was used for this purpose, as it provides a higher power than that of the commonly used Benjamini-Hochberg method by accounting for covariates (Korthauer et al., 2019; Leek et al., 2022). The covariate chosen for these tests was the type of modification (e.g., acetylation, methylation) of each histone PTM, and this was specified using the Unimod accession number. Statistical analyses were completed in the R programming environment (version 4.2.0) (R Core Team, 2022) using the R package *swfdr* (Leek et al., 2022). Following analyses, multiple sequence alignments were performed using the program Clustal Omega (Sievers and Higgins, 2018) in order to determine the human analog of all salinity-responsive histone PTMs. Plots were prepared using the R packages *ggplot2* (Wickham, 2016), *ggrepel* (Slowikowski, 2021) and *tidyverse* (Wickham et al., 2019) to visualize key results.

List of Abbreviations

ac: Acetylation; ChIP-seq: Chromatin immunoprecipitation sequencing; CLASP: Cas9 Locus-Associated Proteome; CoIFI: Chromatin-of-Interest Fragment Isolation; FW: Freshwater; H1K16ub: Histone H1 isoform X1 lysine 16 ubiquitylation; H3K14ac: Histone H3 lysine 14

acetylation; H3K18ub: Histone H3 lysine 18 ubiquitylation; HSP70: Heat shock protein 70; IDAP: Isolation of DNA Associated Proteins; K: Lysine; PBS: Phosphate buffered saline; PCNA: Proliferating cell nuclear antigen; PTM: Post-translational modification; R-ChIP: Reverse-chromatin immunoprecipitation; SW: Seawater; ub: Ubiquitylation.

Declarations

Ethic approval and consent to participate

The use of all 42 fish in this study was approved by the UC Davis IACUC under Protocol #21846.

Consent for publication

Not applicable

Availability of data and materials

All datasets generated and analyzed in this study are available at Panorama Public (<https://panoramaweb.org/eam02kl.url>, doi: [10.6069/xdtd-4b83](https://doi.org/10.6069/xdtd-4b83)) and ProteomeXchange (PXD040557).

Competing interests

The authors declare that they have no competing interests

Funding

This work was supported by the National Science Foundation Grant IOS- 2209383 and BARD grant IS-4800-15 to DK.

Authors' contributions

EAM and DK designed the experiments for this study. EAM and YF delivered all salinity treatments. EAM processed all samples for histone PTM analysis, analyzed the data, and was the main contributor for writing the manuscript. DK performed LCMS of all samples, contributed to data processing, and edited the manuscript. YF contributed to processing samples for histone PTM analysis. All authors read and approved the final manuscript.

Acknowledgments

We would like to thank Lorna Haworth, Tracy Le, Chanhee Kim, and Meranda Corona for their help with dissecting the fish used for this study.

Figure Legends

Supplemental Table 2.1: Complete characterization of the histone PTM response to salinity stress in Mozambique tilapia. For each combination of salinity treatment and tissue, the mean relative abundance of every histone PTM is presented. Furthermore, for every comparison of a histone PTM between salinity treatments, the \log_2 fold change, raw p-value, and conditioned q-value are provided.

Table 2.1: Salinity-responsive histone PTMs. For each salinity-responsive histone PTM, the full name, abbreviated name, and human analog are listed.

Figure 2.1: Impact of short-term salinity treatments on histone PTMs. Volcano plots depict the differences in histone PTMs between short-term salinity treatments. All histone PTMs were plotted based on their conditioned q-value and fold change. Panels A-C depict histone PTMs in the gills when comparisons were made between the fish exposed to SW and FW treatments (A), SW/FW and FW treatments (B), and SW and SW/FW treatments (C). Panels D-F depict histone PTMs in the kidney when comparisons were made between the fish exposed to SW and FW treatments (D), SW/FW and FW treatments (E), and SW and SW/FW treatments (F). Finally, panels G-I depict histone PTMs in the testes when comparisons were made between the fish exposed to SW and FW treatments (G), SW/FW and FW treatments (H), and SW and SW/FW treatments (I). Histone PTMs were colored according to their significance in terms of conditioned q-value (blue), fold change (green), both conditioned q-value and fold change (red), or neither (gray). The salinity-responsive histone PTM H1K16ub is labeled accordingly.

Figure 2.2: Impact of long-term salinity treatments on histone PTMs. Volcano plots depict the differences in histone PTMs between long-term salinity treatments. All histone PTMs were plotted based on their conditioned q-value and fold change. Panels A-C depict histone PTMs in the gills when comparisons were made between the fish exposed to S1 and S0 treatments (A), S3 and S0 treatments (B), and S3 and S1 treatments (C). Panels D-F depict histone PTMs in the kidney when comparisons were made between the fish exposed to S1 and S0 treatments (D), S3 and S0 treatments (E), and S3 and S1 treatments (F). Finally, panels G-I depict histone PTMs in

the testes when comparisons were made between the fish exposed to S1 and S0 treatments (G), S3 and S0 treatments (H), and S3 and S1 treatments (I). Histone PTMs were colored according to their significance in terms of conditioned q-value (blue), fold change (green), both conditioned q-value and fold change (red), or neither (gray). Salinity-responsive histone PTMs are labeled according to their abbreviated names.

Figure 2.3: The influence of short-term salinity stress on H1K16ub. The mean relative abundance of H1K16ub in the gills is displayed for fish exposed to each of the short-term salinity treatments (A). Error bars represent the mean \pm the standard error of the mean. The quantification of H1K16ub was based on the abundance of six modified versions of peptides and 39 unmodified versions of peptides. Panels B-C correspond to one of the modified peptides, SEEAPAPAPAKAAK[+114]KKTTASKPKKVGPSVGE, that contributed to H1K16ub quantification. The library spectrum (B) and an example peak (C) of this modified peptide are presented. Panels D-E depict a distinctive library spectrum (D) and example peak (E) from one of the unmodified peptides, S[+42]EEAPAPAPAK[+57]AAKKKTTASKPKKVGPSVGE.

Figure 2.4: The influence of long-term salinity stress on H3K14ac. The mean relative abundance of H3K14ac in the testes is displayed for fish exposed to each of the long-term salinity treatments (A). Error bars represent the mean \pm the standard error of the mean. The quantification of H3K14ac was based on the abundance of three modified versions of peptides and seven unmodified versions of peptides. Panels B-C represent one of the modified peptides that contributed to H3K14ac quantification, being K[+112]STGGK[+42]APR. For this modified peptide, the library spectrum (B) and an example peak (C) from the program Skyline are shown.

Panels D-E correspond to one of the unmodified peptides, K[+112]STGGK[+56]APR, which has a distinctive library spectrum (D) and example peak (E).

Figure 2.5: The influence of long-term salinity stress on H3K18ub. The mean relative abundance of H3K18ub in the testes is displayed for fish exposed to each of the long-term salinity treatments (A). Error bars represent the mean \pm the standard error of the mean. The quantification of H3K18ub was based on the abundance of two modified versions of peptides and 13 unmodified versions of peptides. Panels B-C represent one of the modified peptides, **K[+114]QLATK[+42]AAR**, that contributed to H3K18ub quantification. The library spectrum (B) and an example peak (C) from the program Skyline are shown for this modified peptide. Panels D-E depict a distinctive library spectrum (D) and example peak (E) from one of the unmodified peptides, K[+56]QLATK[+42]AAR.

Supplemental Figure 2.1: Sequence alignment of tilapia and human histone H1 proteins.

Clustal Omega was used to align the amino acid sequence of tilapia histone H1 isoform X1 (accession number XP_019210164.1) and human histone H1 (accession number AAA63187.1).

Supplemental Figure 2.2: Sequence alignment of tilapia and human histone H3 proteins.

Clustal Omega was used to align the amino acid sequence of tilapia histone H3 (accession number XP_005463512.2) and human histone H3 (accession number AAN39284.1).

Supplemental Figure 2.3: Experimental design for testing effects of short-term salinity stress. Three groups of six fish received a different salinity treatment designed to elicit large

differences in plasma osmolality. The fish in treatment group FW acted as a control and were only ever exposed to freshwater. The fish in treatment group SW experienced a direct transfer from freshwater to seawater and were kept there for two hours before dissection. Finally, the fish in treatment group SW/FW experienced a direct transfer from freshwater to seawater, were kept in seawater for two hours, then were transferred back to freshwater and kept there an additional two hours before being dissected. Red points indicate the time at which fish were dissected.

Supplemental Figure 2.4: Experimental design for testing effects of long-term salinity stress. Three groups of eight fish were exposed to a different salinity treatment over the course of 62 days. Fish in treatment group S0 were only ever exposed to freshwater. Fish in treatment group S1 were maintained in freshwater before experience one “pulse” of severe salinity stress delivered gradually up to a final salinity of 82.5 g/kg. Fish in treatment group S3 experienced three pulses of severe salinity stress before their dissection. Red points indicate time of dissection, and blue dashed boxes indicate each pulse of severe salinity stress.

Supplemental Figure 2.5: Mass Error Histogram. The mass error histogram is presented for each Skyline file individually processed in this study. Panels A-C correspond to the files containing gill samples from fish exposed to short-term salinity treatments, where tissues were processed using V8 in ammonium bicarbonate (A), V8 in sodium phosphate (B), and trypsin (C). Panels D-F correspond to the files containing gill samples from fish exposed to long-term salinity treatments, where tissues were processed using V8 in ammonium bicarbonate (D), V8 in sodium phosphate (E), and trypsin (F). Panels G-I correspond to the files containing kidney samples from fish exposed to short-term salinity treatments, where tissues were processed using

V8 in ammonium bicarbonate (G), V8 in sodium phosphate (H), and trypsin (I). Panels J-L correspond to the files containing kidney samples from fish exposed to long-term salinity treatments, where tissues were processed using V8 in ammonium bicarbonate (J), V8 in sodium phosphate (K), and trypsin (L). Panels M-O correspond to the files containing testes samples from fish exposed to short-term salinity treatments, where tissues were processed using V8 in ammonium bicarbonate (M), V8 in sodium phosphate (N), and trypsin (O). Panels P-R correspond to the files containing testes samples from fish exposed to long-term salinity treatments, where tissues were processed using V8 in ammonium bicarbonate (P), V8 in sodium phosphate (Q), and trypsin (R).

Figures

Figure 2.1

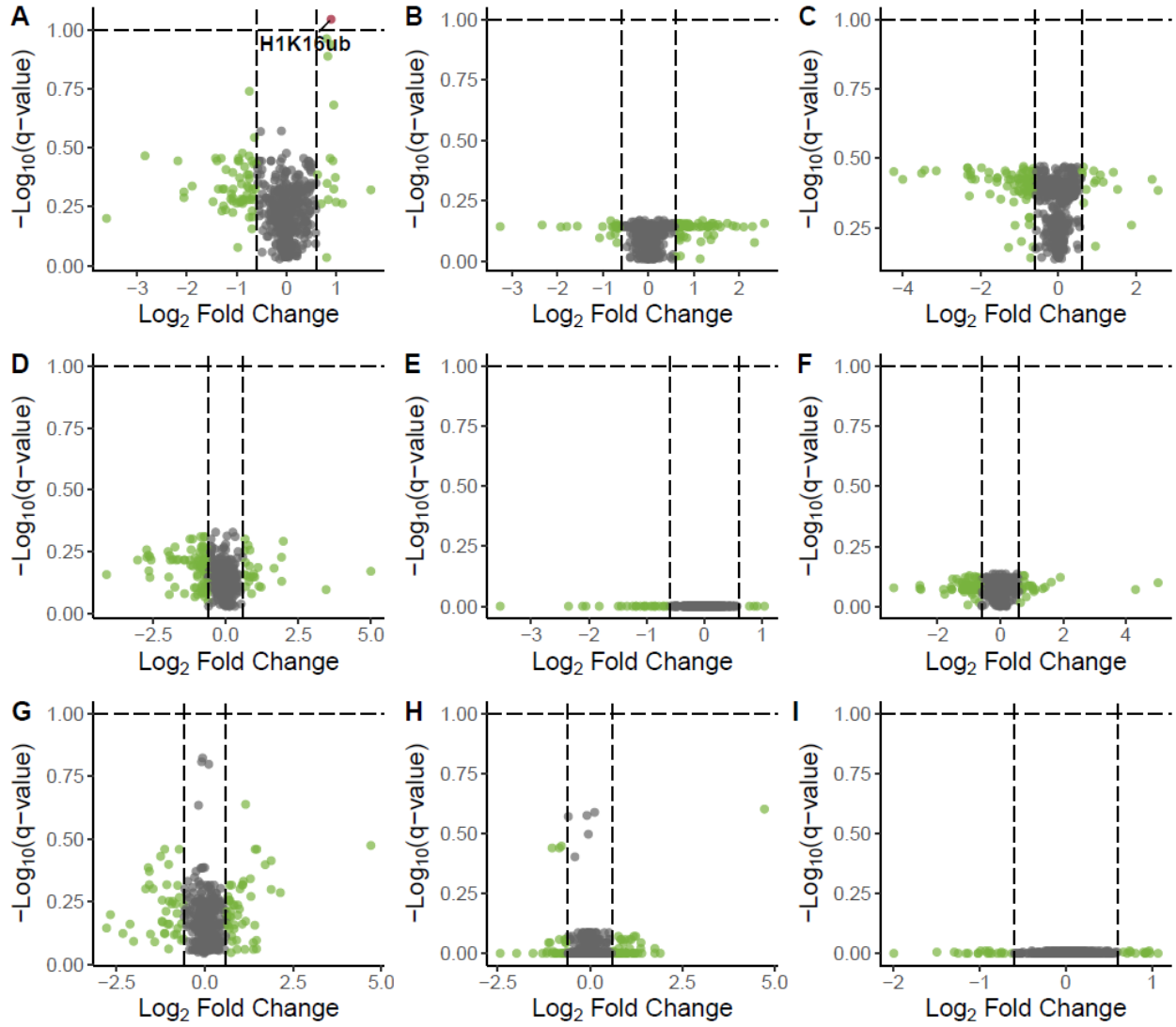


Figure 2.2

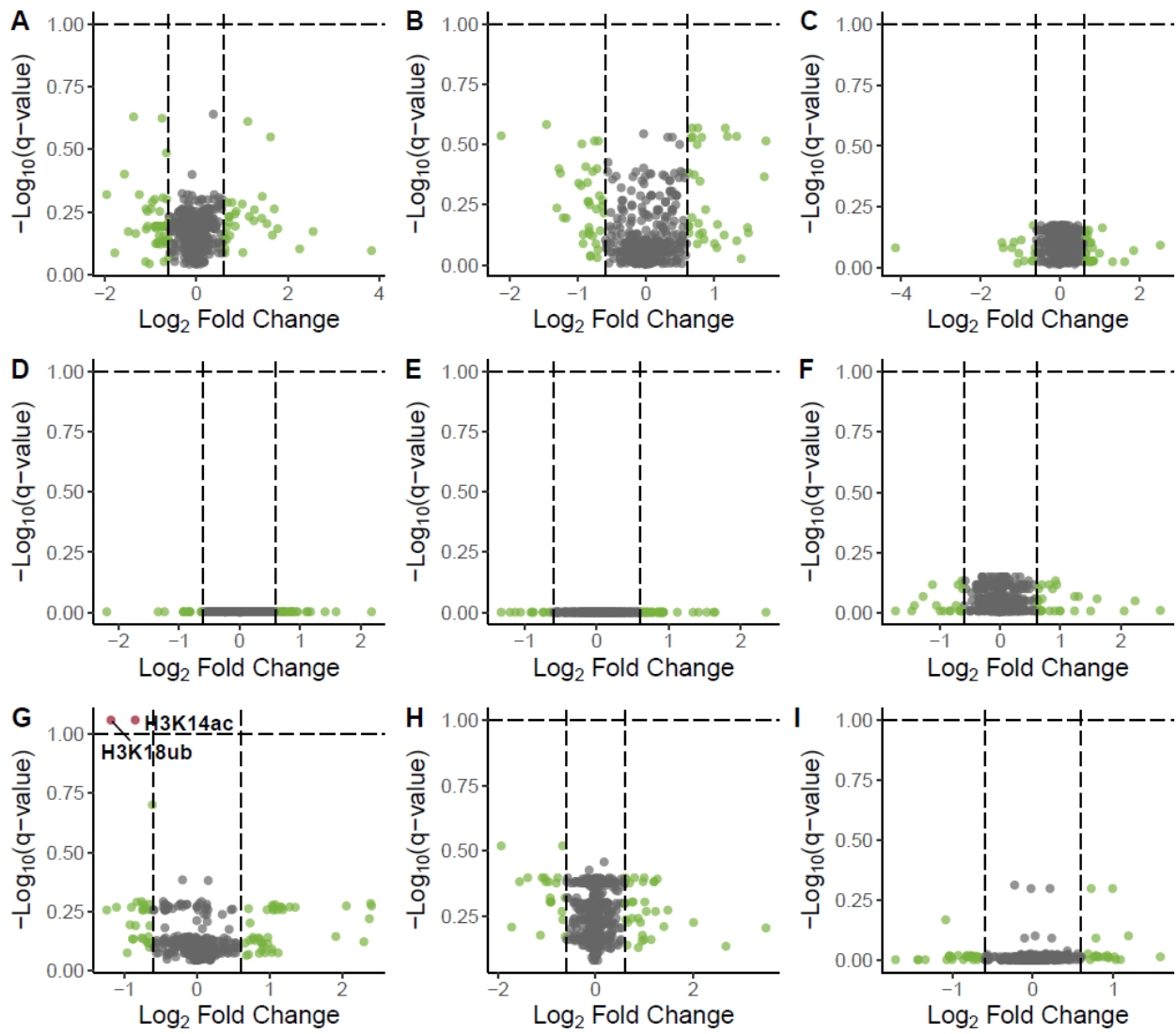


Figure 2.3

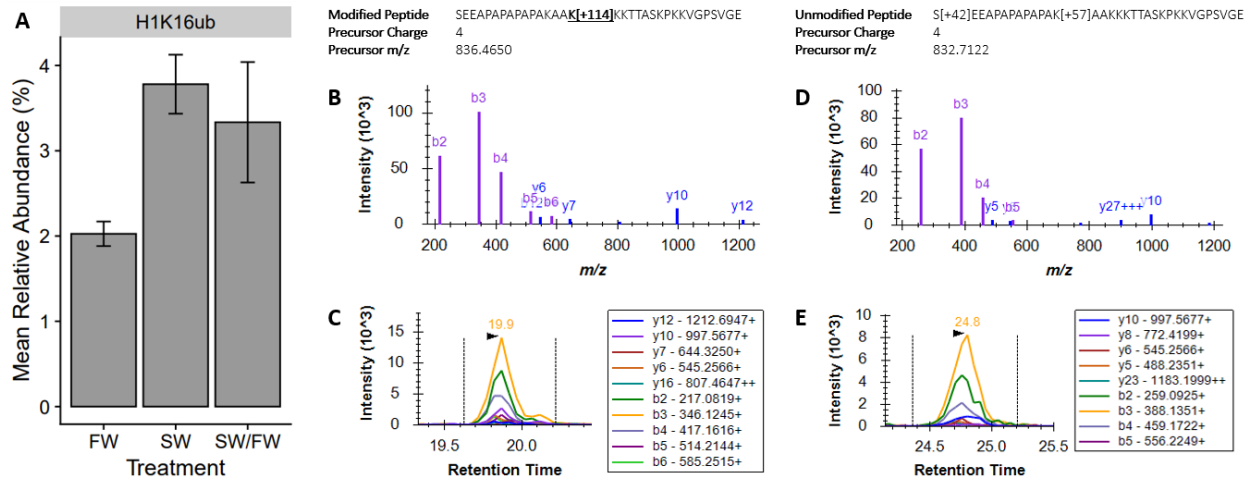


Figure 2.4

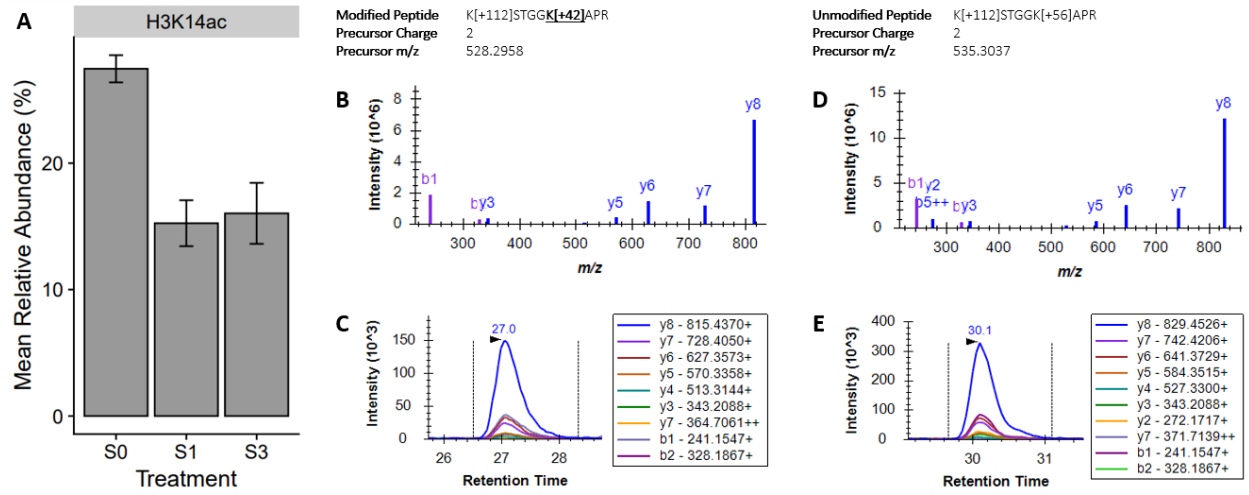
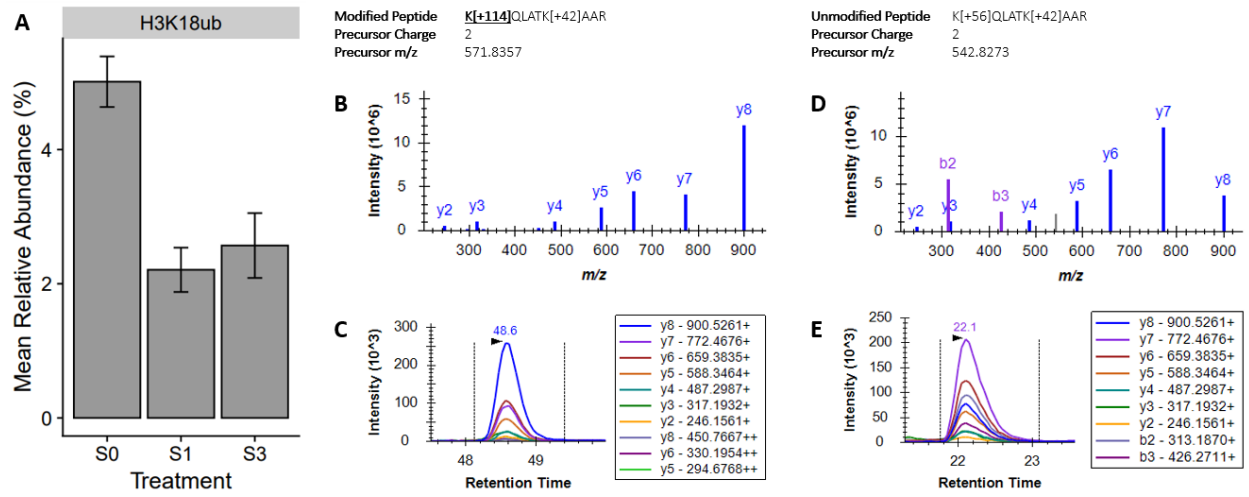


Figure 2.5



Tables

Table 2.1

| Salinity-Responsive Histone PTM | Abbreviated Name of Histone PTM | Human Analog |
|----------------------------------|---------------------------------|--------------|
| H1 isoform X1 K16 ubiquitylation | H1K16ub | NA |
| H3 K14 acetylation | H3K14ac | H3K14ac* |
| H3 K18 ubiquitylation | H3K18ub | H3K18ub* |

* Previously detected in humans

Supplemental Figures

Supplemental Figure 2.1

CLUSTAL O(1.2.4) multiple sequence alignment

```
XP_019210164.1    MSEEAPAPAPAPAK-----AAKKTTASKPKKVGPSVGE LIVKAVAASKERSGVSAA    52
AAA63187.1        MSETAPAAPAAPAPAEKTPVKKKARKSAGAAKRKASGPPVSELITKAVAASKERSGVSLA    60
                  *** **      ***          *.: * * * * * .***.***** *
XP_019210164.1    ALKKALAAGGYDVKNKARVKTAIKSLVAKGTLVQTKGTGASGSFKMNKKATESKAKKPA    112
AAA63187.1        ALKKALAAAGYDVEKNNSRIKLGKSLVSKGTLVQTKGTGASGSFKLNKKAASGEAKPKA    120
                  ***** .***.***.:*.:* * .:****:*****:*****:****:..:* *
XP_019210164.1    KKAAPKAKKPAAAKAKKPAAAKKSPKKAAAANKPAAAKKSPKKAKKPAAAKK-VTKSP    171
AAA63187.1        K-----KAGAAKAKKPAGAAKKPKKATGAATPKKSAKKTPKKAKKPAAAGAKKAKSP    173
                  *      * .*****.*** * :.*. :***.***** :***
XP_019210164.1    K-----KAAKSPKKVLKAPAAKSPAKKAAKPKVKAAT-AAKKKCLRFI    216
AAA63187.1        KKAKAAKPKKAPKSPAKAKAVKPKAAK---PKTAKPKAAKPKKAAAKK-----    219
                  *      ** ** * . * * * * :****. * . *****
```

Supplemental Figure 2.2

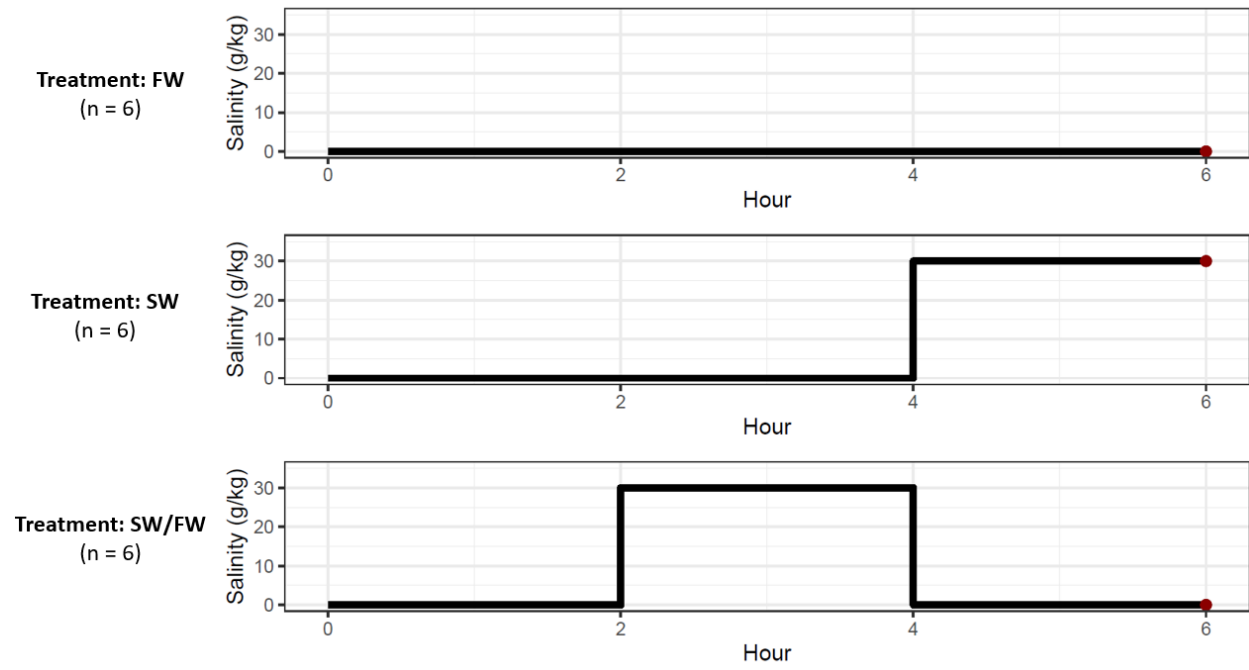
CLUSTAL O(1.2.4) multiple sequence alignment

```
XP_005463512.2    MARTKQTARKSTGGKAPRKQLATKAARKSAPATGGVKKPHRYRPGTVALREIRRYQKSTE    60
AAN39284.1        MARTKQTARKSTGGKAPRKQLATKVARKSAPATGGVKKPHRYRPGTVALREIRRYQKSTE    60
*****.*****.*****.*****.*****.*****.*****.*****

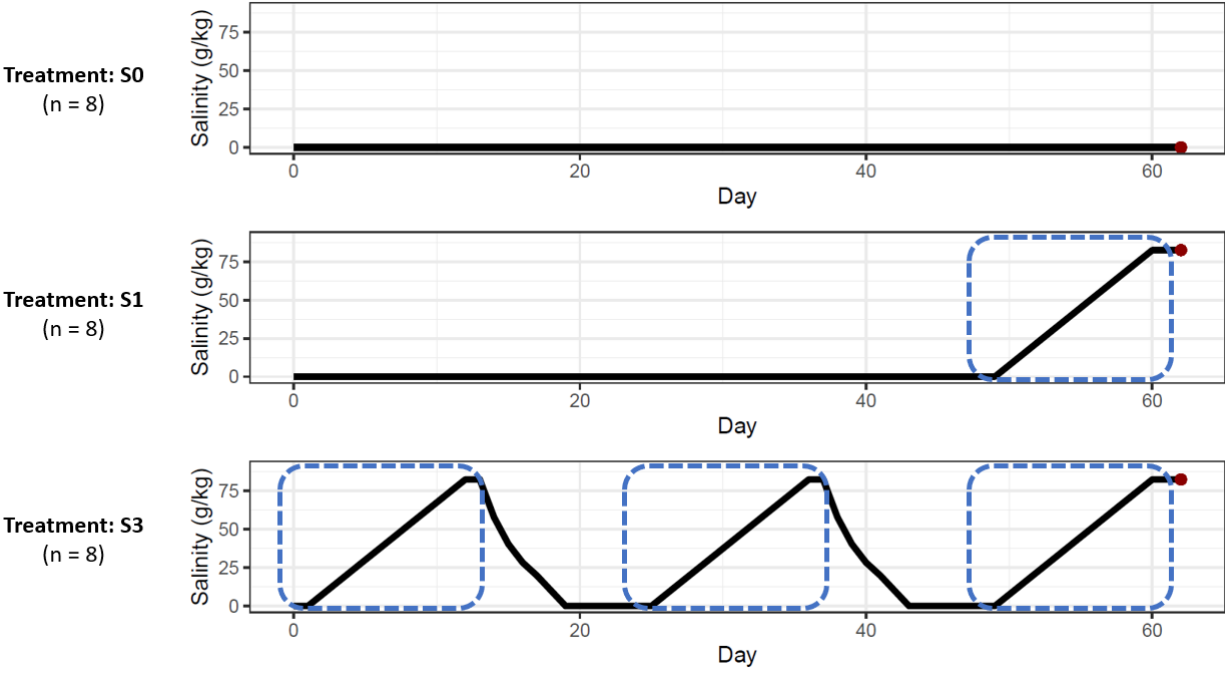
XP_005463512.2    LLIRKLPFQRLVREIAQDFKTDLRFQSSAVMALQEASEAYLVGLFEDTNLCAIHAKRVTI    120
AAN39284.1        LLIRKLPFQRLMREIAQDFKTDLRFQSSAVMALQEACESYLVGLFEDTNLCVIHAKRVTI    120
*****.*****.*****.*****.*****.*****.*****.*****

XP_005463512.2    MPKDIQLARRIRGRGLKI 139
AAN39284.1        MPKDIQLARRIRGERA--- 136
*****.
```

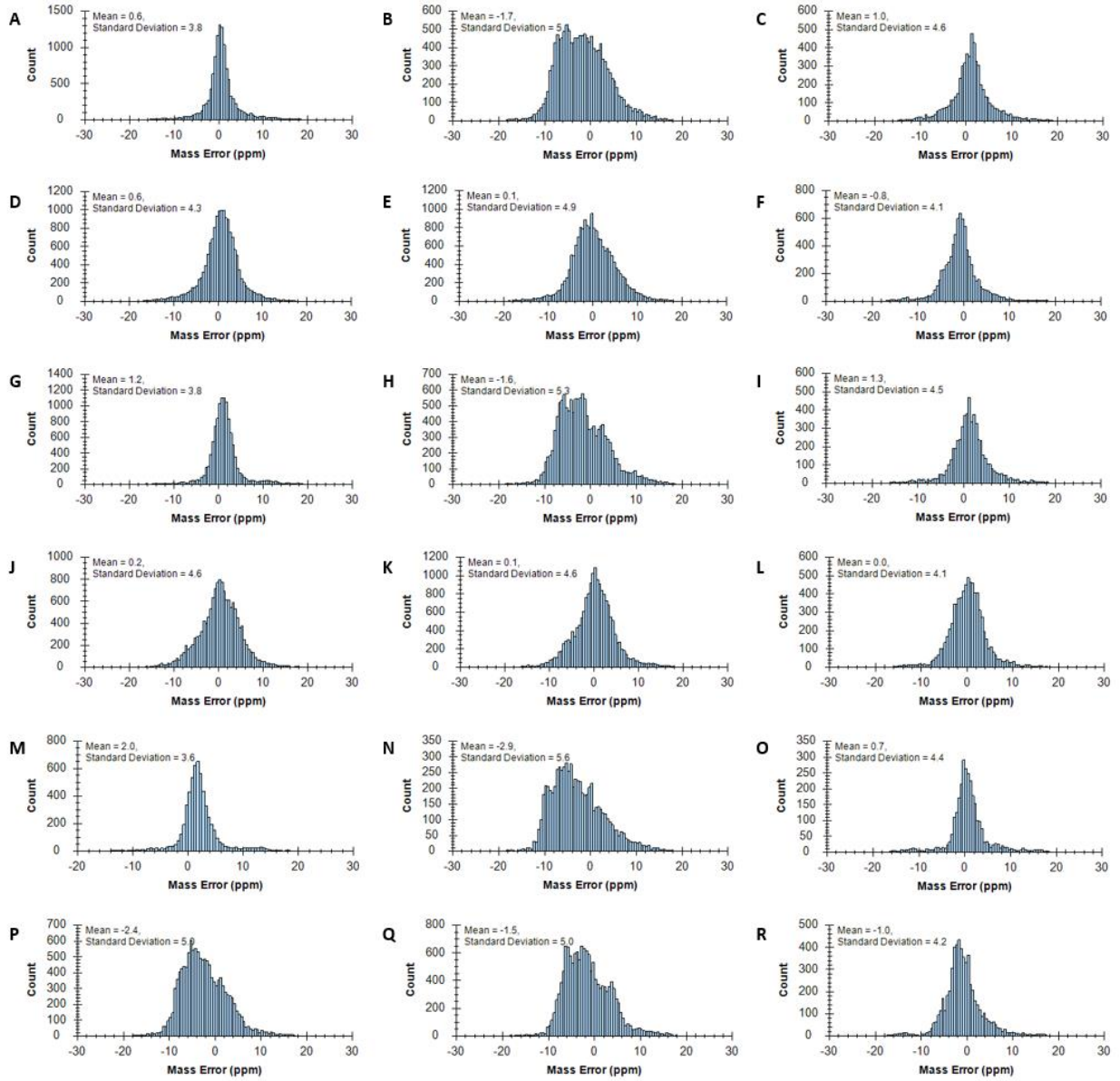
Supplemental Figure 2.3



Supplemental Figure 2.4



Supplemental Figure 2.5



CHAPTER 3

Environmental Conditions Elicit a Slow but Enduring Response of Histone Post-Translational Modifications in Mozambique Tilapia

Abstract

Histone post-translational modifications (PTMs) are epigenetic marks that operate within the central dogma of molecular biology: upon an environmental stimulus, the histone PTMs surrounding DNA can be changed in a way that modifies gene expression, and, therefore, the abundance and composition of RNA and proteins within cells (Schneider-Poetsch and Yoshida, 2018). Once a change is induced, histone PTMs can offer organisms resilience to their environments through processes such as developmental plasticity (Nettle and Bateson, 2015; Norouzitallab et al., 2019). The purpose of this study was to investigate whether histone PTMs mediate developmental plasticity in Mozambique tilapia facing salinity challenges. To this aim, we exposed fish to either freshwater or hypersalinity during their early critical window of development, then continued to raise the fish in either freshwater or seawater, respectively, for 18 months. Once the fish reached adulthood, we acclimated them to either freshwater or seawater. Following salinity treatments, we quantified 343 histone PTMs in the gills of each fish. We show here that histone PTMs differed dramatically between fish exposed to distinct environmental conditions for 18 months, and that the majority of histone PTM alterations persist for at least four weeks. However, histone PTMs responded minimally to salinity acclimation during adulthood. These results challenge our prior assumptions regarding the timescale of the histone PTM response, indicating that it does not necessarily precede the proteomic response or

acclimation. Although this finding complicates our interpretation of developmental plasticity, it signifies that histone PTMs reflect prolonged exposure to environmental conditions.

Significance statement

Histone PTMs are epigenetic marks that can regulate patterns of gene expression depending on an organism's environment. In this study, we demonstrate that the histone PTM response to environmental conditions can be pervasive and persistent, but that it does not necessarily precede acclimation. Histone PTMs were quantified in the gills of Mozambique tilapia following salinity treatments over the course of their lifetimes. We show here that fish fully acclimated to distinct salinities during adulthood display minimal differences in their histone PTMs; however, histone PTMs differ dramatically between fish exposed to distinct salinities throughout their lives. The majority of these histone PTM alterations persist even after fish are acclimated to new salinities.

Introduction

Phenotypes arise from the collective action of numerous cellular components, including histone post-translational modifications (PTMs). Histone PTMs are epigenetic marks that regulate heritable patterns of gene expression, and they too exhibit complex regulation. For example, histone PTMs can be influenced by cell type, an organism's developmental stage and environmental conditions, and the life experiences of ancestors (Norouzitallab et al., 2019; Weishaupt et al., 2010; Zhu et al., 2013). As such, histone PTMs are challenging to study, but they are emerging as an ecologically important mediator of physiological and evolutionary processes (Mojica and Kültz, 2022; Weaver et al., 2004; Xie et al., 2013). They can offer

organisms, and their descendants, biological resilience to changing environments (Holt and Comizzoli, 2022; Miller et al., 2012; Salinas and Munch, 2012). Developmental plasticity is one strategy by which histone PTMs can facilitate resilience within an organism's lifetime. In this process, an organism's environmental condition during specific developmental stages influences its phenotype during adulthood, theoretically in a manner that maximizes fitness (Nettle and Bateson, 2015).

In this study, we sought to determine whether histone PTMs facilitate developmental plasticity in Mozambique tilapia (*Oreochromis mossambicus*) amid salinity challenges. Mozambique tilapia inhabit a wide range of salinities in nature, from freshwater to four times the salinity of seawater (Stickney, 1986; Whitfield and Blaber, 1979). Their exceptional tolerance to salinity, however, is restrained by both prior life experience and the rate of acclimation to new salinities (Hwang et al., 1989; Root and Kültz, 2022; Schreck and Tort, 2016; Stickney, 1986). To test whether histone PTMs contribute to salinity tolerance through developmental plasticity, we exposed Mozambique tilapia to two sets of salinity treatments. The first set of salinity treatments was administered throughout fish development. We exposed Mozambique tilapia to either freshwater or hypersalinity during their early critical window of development, being gonadal sex differentiation (Anway et al., 2005; Hanson and Skinner, 2016; Nakamura and Takahashi, 1973; Weaver et al., 2004), then we continued to raise the fish in either freshwater or seawater, respectively, for 18 months. Therefore, fish were raised either in freshwater or under salinity stress. Once the fish reached adulthood, we began the second set of salinity treatments. Fish were acclimated to either freshwater or seawater for four weeks because, within that timeframe, Mozambique tilapia reach complete acclimation to either of the environmental conditions by altering their gill morphology and physiology (Febry and Lutz, 1987; Kültz, 2015;

Morgan et al., 1997; Sardella and Brauner, 2008). To maximize the power for detecting environmentally-induced changes in histone PTMs, we used siblings of Mozambique tilapia, collected as larvae, for this study. The siblings belonged to the same clutch and therefore shared the epigenetic history of their ancestors (Ho and Burggren, 2010; Jablonka, 2004).

In total, four distinct salinity treatments were administered to fish over the course of their lifetimes: 1) salinity stress during development and seawater during adulthood (HS*/S), 2) salinity stress during development and freshwater during adulthood (HS*/F), 3) freshwater during development and seawater during adulthood (FF*/S), and 4) freshwater during both development and adulthood (FF*/F). Following all salinity treatments, we quantified 343 biologically relevant histone PTMs, collectively referred to as the global histone PTM landscape, in the gills of each fish. By comparing the global histone PTM landscape between fish given different salinity treatments, we investigated not only developmental plasticity, but also whether histone PTMs are impacted by environmental conditions when exposures are lifelong, long-term throughout development, or four weeks during adulthood.

The results of this study challenge our previous perceptions of how histone PTMs fit into the central dogma of molecular biology. As a consequence, we are left with a nondefinitive conclusion as to whether histone PTMs facilitate developmental plasticity in the context of Mozambique tilapia facing salinity challenges. However, we gain insight into the timescale at which histone PTMs change and persist, and thereby break new ground for epigenetics research in the context of ecology.

Results

The 343 histone PTMs, collectively referred to as the global histone PTM landscape, were quantified within the gills of each fish, then subjected to five pairwise comparisons. To determine whether lifelong exposure to two distinct environmental conditions impacts histone PTMs, we first compared the global histone PTM landscape between fish exposed exclusively to freshwater and fish exposed exclusively to increased salinity for 18 months (treatments FF*/F and HS*/S). Two comparisons were made to evaluate the influence of long-term environmental exposures during development. First, we compared histone PTMs between the fish that experienced freshwater or salinity stress during development when, as adults, the fish were acclimated to freshwater (treatments FF*/F and HS*/F). Second, we compared histone PTMs between the fish raised in freshwater or under salinity stress when the fish were acclimated to seawater as adults (treatments FF*/S and HS*/S). Another two comparisons were made to determine whether salinity acclimation during adulthood alters the global histone PTM landscape. In one instance, histone PTMs were compared between fish acclimated to either freshwater or seawater during adulthood when the fish were raised in freshwater (treatments FF*/F and FF*/S). Similarly, histone PTMs were compared between fish acclimated to either freshwater or seawater when the fish were raised under salinity stress (treatments HS*/F and HS*/S). A complete account of the results from this study is displayed in Supplemental Table 3.1, which includes, for each salinity treatment group, the mean relative abundance and M-value of all 343 histone PTMs, and for each salinity treatment comparison, values of \log_2 fold change, p-value, and conditioned q-value. In the following sections, we highlight the major findings.

Lifetime exposure to environmental conditions

When the 343 histone PTMs were compared between fish exposed to distinct environmental conditions throughout their lives (treatments FF*/F and HS*/S), results revealed 34 histone PTMs (9.9%) to be significantly different (Figure 3.1). The histone PTMs detected to change included modifications of methylation, dimethylation, trimethylation, and biotinylation, for which fish in freshwater displayed low relative abundance of the modifications on a genome-wide level when compared to the fish exposed to increased salinity. The modification of lactylation and/or carboxyethylation also followed this pattern. It should be noted that lactylation and carboxyethylation cannot be distinguished from each other using our method of histone PTM analysis because these two chemical groups have the same molecular formula. We hereby refer to modifications of lactylation and/or carboxyethylation simply as lactylation, because lactylation is more likely to appear as a histone PTM than carboxyethylation (Zhang et al., 2022). The environmentally-responsive histone PTMs containing modifications of 4-hydroxynonelation and amidation displayed the highest relative abundance in the gills of fish exposed only to freshwater and the lowest relative abundance in the gills of fish exposed to increased salinity. Mixed patterns of change were observed for histone PTMs containing modifications of acetylation, phosphorylation, oxidation, dioxidation, and deamidation; in some instances, these histone PTMs had the lowest relative abundance in fish exposed to freshwater and the highest relative abundance in fish exposed to increased salinity, but in other instances, the opposite pattern was observed.

Long-term exposure to environmental conditions during development

To determine whether histone PTMs induced by long-term environmental exposures during development persist within the gills of fish after their environmental conditions change in adulthood, we performed two sets of comparisons. First, we compared histone PTMs between fish raised either in freshwater or under salinity stress when the fish were acclimated to freshwater as adults (treatments FF*/F and HS*/F). Between these fish, 27 of 343 histone PTMs (7.9%) were found to be significantly different (Figure 3.2). The 27 histone PTMs detected in this treatment comparison included modifications of acetylation, methylation, oxidation, dimethylation, 4-hydroxynonelation, lactylation, dioxidation, phosphorylation, and deamidation. A few patterns emerged from this comparison. First, the modification of 4-hydroxynonelation had the highest relative abundance when the fish were raised in freshwater and a significantly lower relative abundance when fish were raised under salinity stress. Yet, several types of modifications exhibited the opposite pattern. Specifically, the histone PTMs containing methylation, dimethylation, and lactylation had low relative abundances when fish were raised in freshwater and significantly higher relative abundances when fish were raised under salinity stress. A mixed pattern of change was observed for histone PTMs containing modifications of acetylation, oxidation, dioxidation, deamidation, and phosphorylation. Of the 27 histone PTMs found to be significantly different between fish in the FF*/F and HS*/F treatment groups, only eight were not also significantly different between fish in the FF*/F and HS*/S treatment groups. The histone PTMs that did not overlap in their significance are histone H2A lysine 122 dimethylation, histone H2A proline 48 dioxidation, histone H2A lysine 122 methylation, histone H3 arginine 83 deamidation, histone H2A.Z isoform X1 lysine 156 methylation, histone H1.10

lysine 116 acetylation, histone H4-like threonine 73 acetylation, and H4-like threonine 75 acetylation.

To further evaluate the influence of long-term environmental exposures during development, we compared histone PTMs between the fish raised either in freshwater or under salinity stress when the fish were acclimated to seawater as adults (treatments FF*/S and HS*/S; Figure 3.3). This comparison revealed nine of 343 histone PTMs (2.6%) to be significantly different. The nine histone PTMs that significantly differed between the fish in these salinity treatment groups were composed of acetylation, phosphorylation, oxidation, and 4-hydroxynonelation. In the cases of histone phosphorylation, oxidation, and 4-hydroxynonenation, all environmentally-responsive histone PTMs in the gills had a higher relative abundance in fish raised in freshwater than in fish raised under salinity stress. Only one of the histone acetylation modifications was shown to have a higher relative abundance in the gills of fish raised under salinity stress when compared to fish raised in freshwater.

Acclimation to environmental conditions during adulthood

To determine the influence of salinity acclimation on histone PTMs, we compared the global histone PTM landscape of the gills between fish acclimated to either freshwater or seawater during adulthood. This comparison was made twice: once when fish were raised in freshwater, and once when fish were raised under salinity stress (Figure 3.4). Among the fish raised in freshwater, only one of the 343 histone PTMs (0.3%) exhibited a significant difference when fish were acclimated to either freshwater or seawater as adults. This histone PTM was histone H3 lysine 79 dioxidation (p-value: 1.81e-05; conditioned q-value: 0.0057), and its relative abundance was highest in fish acclimated to freshwater (0.044%) and lowest in fish

acclimated to seawater (0.017%). Among the fish raised under salinity stress, none of the 343 quantified histone PTMs in the gills were found to be significantly different between fish acclimated to either freshwater or seawater as adults.

Discussion

Three key results shape our overarching conclusion that environmental conditions elicit a slow but enduring response of histone PTMs in the gills of Mozambique tilapia. First, histone PTMs vary dramatically between fish exposed to distinct environmental conditions throughout their entire lives. Second, the majority of the environmentally-induced changes in histone PTMs persist after fish acclimate to new salinities during adulthood. Third, the acclimation of fish to different salinities during adulthood lead to minimal changes in histone PTMs.

To begin interpreting these results, we will first consider what happens to fish when they acclimate to either freshwater or seawater during adulthood. Four weeks is the time attributed to full acclimation of Mozambique tilapia to these salinities, as the necessary morphological and physiological changes in the gills take place within that timeframe (Febry and Lutz, 1987; Morgan et al., 1997; Sardella and Brauner, 2008). In this study, we investigated the impact of salinity acclimation during adulthood on histone PTMs across two scenarios: once when fish were raised in freshwater, and once when fish were raised under salinity stress. Between these two scenarios, only one histone PTM was found to change significantly between fish acclimated to either freshwater or seawater during adulthood. This histone PTM was histone H3 lysine 79 dioxidation, and it changed significantly between these salinities when the fish were raised in freshwater. The extent of this histone PTM response is consistent with a previous study we

conducted on acute salinity stress in Mozambique tilapia, where only one histone PTM significantly responded to salinity stress in the gills (Mojica and Kültz, 2023b).

What we did not anticipate was the extent to which histone PTMs vary in the gills of fish following a lifetime of exposure to distinct environmental conditions. When the 343 histone PTMs that we quantified were compared between fish exposed exclusively to freshwater and fish exposed exclusively to increased salinity, 34 histone PTMs (9.9%) were found to be significantly different at a genome-wide level. This result was particularly surprising because the histone PTM response to environmental stimuli is presumed to occur within a matter of minutes (Meagher, 2014; Norouzitallab et al., 2019). A quick response like this is intuitive given the central dogma of molecular biology, where DNA is transcribed into RNA, and RNA is translated into protein (Schneider-Poetsch and Yoshida, 2018). If histone PTMs mediate the transcription of DNA into RNA, and if proteins are responsive to environmental stimuli, it would follow that the histone PTM response to environmental stimuli precedes the proteomic response (Schneider-Poetsch and Yoshida, 2018). Because Mozambique tilapia experiencing an ambient salinity change compensate for osmoregulation by altering gill proteome networks well within four weeks of exposure (Kültz et al., 2013), we assumed that histone PTMs would respond fully to ambient salinity change during adulthood within that timeframe as well. This assumption was invalidated upon our finding that histone PTMs are impacted minimally by a four-week acclimation, but dramatically by lifelong exposure to different salinities.

Because our experimental design was founded on the invalid assumption that the histone PTM response to environmental stimuli precedes the proteomic response, we were unable to detangle the influence of exposure to hypersalinity during gonadal sex differentiation (i.e., an early critical window of development) from the influence of long-term exposure to seawater on

histone PTMs in this study. Therefore, as early life history impacts the histone PTM response to ambient salinity during adulthood (Figures 3.2 and 3.3), we perceive two explanations for this change. The first explanation is that histone PTMs facilitate developmental plasticity in the gills. Developmental plasticity is a common event that is often attributed to epigenetic marks established during early critical windows of development (Burdge and Lillycrop, 2010; Champagne, 2013; Moczek, 2015). Even within humans, early life experiences impact the progression of non-communicable diseases in adulthood through epigenetic processes (Godfrey et al., 2016). The second explanation of our results, however, is that enduring levels of histone PTMs result from the gradual accumulation of life experiences over a very long time.

Based on the patterns of change exhibited by the environmentally-responsive histone PTMs identified in this study (Figures 3.1-3.4), we find stronger support for the second explanation that unexpectedly large amounts of time are needed to establish global histone PTM landscapes representative of an organism's life experience. The fish that were exposed to distinct environmental conditions throughout their lifetimes tended to display the extreme values of relative abundance for these histone PTMs (Figure 3.1). In other words, the highest and lowest values of relative abundance for the environmentally-responsive histone PTMs were typically found in fish that were exposed exclusively to freshwater (treatment FF*/F) or increased salinity (treatment HS*/S), while intermediate values of relative abundance were exhibited by the fish acclimated to new salinities for four weeks during adulthood (treatments FF*/S and HS*/F). This pattern suggests that, given more time, the relative abundance of histone PTMs in fish exposed to new salinities during adulthood would have resembled the relative abundance of histone PTMs in fish exposed to those salinities throughout their lives. This, however, does not preclude the possibility that both developmental plasticity and long-term exposure meaningfully contributed,

perhaps at disproportionate degrees, to the global histone PTM landscape (Gluckman et al., 2009; Schaefer and Ryan, 2006).

Regardless of the mechanism by which histone PTMs were influenced, the majority of induced changes persisted within the gills of Mozambique tilapia, even four weeks after fish were transferred to new environmental conditions. This is evident in the number of histone PTMs that, within fish acclimated to the same salinity during adulthood, differed significantly depending on the environmental conditions in which the fish were raised. In this context, fish acclimated to freshwater differed in 27 histone PTMs, of which 19 were also different between fish exposed to distinct environmental conditions throughout their lives (Figure 3.2). Fish acclimated to seawater displayed nine significantly different histone PTMs, of which six also differed between fish that experienced lifelong exposure to distinct environmental conditions (Figure 3.3). Due to the difference in the extent to which histone PTMs are retained when fish are acclimated to seawater or freshwater, we speculate that seawater elicits a stronger histone PTM response than freshwater. The influence of salinity on histone H3 lysine 79 dioxidation further reinforces this speculation, as fish exposed to seawater for any duration and at any developmental stage in this study displayed a significantly lower relative abundance of this histone PTM in their gills compared to fish only exposed to freshwater (Figure 3.4). All of these persistent histone PTMs signify epigenetic memory of environmental conditions, and their four-week retention is striking, especially given the rapid turnover of histone proteins (Zee et al., 2010). Such retention of histone PTMs can nonetheless be explained by processes such as genomic bookmarking and the faithful transmission of PTMs on parent histones to newly synthesized histones (Alabert et al., 2015; Michieletto et al., 2018). Altogether, our results reveal that environmental conditions elicit global changes in histone PTMs on a scale much slower than

previously thought, but that alterations in histone PTMs are highly persistent. This finding sheds light on the variability of histone PTM responses and epigenetic memory previously reported across taxa, as experimental treatments have ranged in duration from hours to lifetimes (Kwon et al., 2009; Mojica and Kültz, 2023b; Norouzitallab et al., 2014; Sani et al., 2013; Whittle et al., 2009; Zheng et al., 2021). We therefore anticipate that histone PTM responses to environmental stimuli would prove much more pervasive if investigated in ecological contexts, where organisms experience prolonged exposure to environmental parameters of interest.

Based on the results of this study, several open questions remain, including the following. To what extent did developmental plasticity versus long-term exposure contribute to environmentally-induced changes in histone PTMs? Where along the genome do these histone PTMs accumulate? How long could each of the histone PTM alterations have persisted within organisms and their descendants? Do the histone PTM alterations impart a beneficial phenotype? Further investigation into questions such as these, which address the physiological and evolutionary role of environmentally-induced changes in histone PTMs, represents a critical next step in epigenetic research that we anticipate will unlock the potential to use histone PTMs as tools to predict an organism's environmental past and phenotypic future.

Materials and Methods

Salinity Treatments

The salinity treatments imposed on Mozambique tilapia in this study were conducted in two phases. The first phase of salinity treatments was designed to extend throughout fish development, and the second phase of salinity treatments was designed to represent a period of salinity acclimation of fish during adulthood. For this purpose, Mozambique tilapia larvae from a

single clutch were collected at an estimated age of seven days post-hatch (dph). Upon collection, fish were separated randomly into one of two primary treatment groups: the freshwater primary treatment group (FF*) or the salinity stressed primary treatment group (HS*). Fish assigned to the freshwater primary treatment group were exposed only to freshwater throughout development. For fish in the salinity stressed primary treatment group, salinity was increased from freshwater at a rate of 7.5 g/kg each day, beginning on day nine post-hatch. This rate of salinity increase continued until salinity reached a maximum of 85 g/kg on day 20 post-hatch. Salinity was maintained at 85 g/kg until day 25 post-hatch. The period of exposure to these hypersaline conditions corresponded to a critical early window of development in Mozambique tilapia, being gonadal sex differentiation (Nakamura and Takahashi, 1973). Starting on day 26 post-hatch, salinity was decreased at a rate of 10 g/kg per day, until a final salinity of 30 g/kg (i.e., seawater) was reached on day 31 post-hatch.

Fish were maintained in the designated salinity of their primary treatment groups until reaching 1.5 years of age. At that point, the fish in each primary exposure condition were further divided into two secondary treatment groups: the freshwater secondary treatment group (F) and the seawater secondary treatment group (S). Each secondary treatment represented a four-week exposure to either freshwater or seawater. In order to transition fish from freshwater to seawater, or vice versa, for their secondary salinity treatment, salinity was increased or decreased at a rate of 5 g/kg per day. Once the desired salinity was reached, the four-week period of exposure began.

In summary, fish were exposed to four distinct salinity treatments in this study: 1) salinity stress during development and seawater during adulthood (HS*/S), 2) salinity stress during development and freshwater during adulthood (HS*/F), 3) freshwater during development and

seawater during adulthood (FF*/S), and 4) freshwater during both development and adulthood (FF*/F). Upon the completion of these salinity treatments, all fish were euthanized, and the gill epithelial tissue from each fish was collected. The use of the 40 fish used in this experiment was approved by the UC Davis IACUC under protocol number 21846.

Processing samples for histone PTM analysis

Samples of gill epithelial tissue were processed through our previously described workflow for histone PTM analysis, where tissues are dissociated into cells through a protocol of mechanical single cell suspension, cells are enriched for histone proteins through histone acid extraction, and histone proteins are digested into peptides using multiple digestion methods in parallel (Mojica and Kültz, 2023a). The digestion methods chosen for this study were 1) the protease V8 in the buffer ammonium bicarbonate, which cleaves proteins at the carboxyl end of glutamate, and 2) the protease V8 in the buffer sodium phosphate, which cleaves proteins at the carboxyl end of both glutamate and aspartate (Thermo Scientific, cat# 20151). Liquid chromatography mass spectrometry was employed to obtain values of histone peptide abundance, which were then converted to values of histone PTM abundance (Mojica and Kültz, 2023a). Using these methods, we quantified the relative abundance and M-value of 343 biologically relevant histone PTMs in each sample of gill epithelial tissue.

Statistical analyses

To elucidate how histone PTMs in the gills of Mozambique tilapia respond to environmental conditions through time, we compared all 343 quantified histone PTMs, collectively referred to as the global histone PTM landscape, between fish exposed to specific

salinity treatments using t-tests. To determine how lifelong exposure to distinct environmental conditions impacts histone PTMs, the global histone PTM landscape was compared between fish in the FF*/F and HS*/S treatment groups. Two sets of comparisons were made to determine the impact of long-term environmental conditions during development on histone PTMs. First, the global histone PTM landscape was compared between fish in the FF*/S and HS*/S treatment groups. Second, the global histone PTM landscape was compared between fish in the FF*/F and HS*/F treatment groups. Another two sets of comparisons were made to determine the impact of salinity acclimation during adulthood on histone PTMs in the gills. First, the global histone PTM landscape was compared between fish in the FF*/F and FF*/S treatment groups. Second, the global histone PTM landscape was compared between fish in the HS*/F and HS*/S treatment groups. To correct for the multiple hypothesis testing within each salinity treatment comparison, we applied Boca and Leek's FDR regression method (Korthauer et al., 2019; Leek et al., 2022). Because this method of multiple hypothesis testing correction increases power in statistical analyses by accounting for covariates, we designated the modification type (e.g., acetylation, phosphorylation) of each histone PTM as the covariate in our analyses. Using the R programming environment (version 4.2.0) (R Core Team, 2022), we prepared volcano plots and bar graphs with the R packages *ggplot2* (Wickham, 2016) and *tidyverse* (Wickham et al., 2019) to depict major results.

Acknowledgments and funding sources

We would like to thank Sophie Scott, Selina Zhang, and Shae Hill for their assistance in dissecting the fish used in this experiment. This work was supported by the National Science Foundation Grant IOS-2209383 and BARD grant IS-4800-15 to D.K.

Figure Legends

Supplemental Table 3.1: Complete account of the histone PTM response to environmental conditions. For each of the 343 histone PTMs quantified, the mean relative abundance and M-value is displayed for fish in all salinity treatment groups. Additionally, the log₂ fold change, p-value, and conditioned q-value of every histone PTM is presented for each of the five pairwise comparisons between salinity treatments.

Figure 3.1: Impact of lifelong environmental exposures on histone PTMs. **A)** The global histone PTM landscape of the gills was compared between fish exposed exclusively to freshwater (treatment FF*/F) and fish exposed exclusively to increased salinity (treatment HS*/S). **B)** A volcano plot depicts the pattern of change for all 343 histone PTMs between the fish in these treatment groups, where colored points represent histone PTMs found to have a high fold change (green), low conditioned q-value (blue), both a high fold change and low conditioned q-value (red), or no substantial difference (gray). **C)** For each of the histone PTMs found to have both a high fold change and low conditioned q-value when compared between fish in the FF*/F and HS*/S treatment groups (blue), the mean relative abundance is displayed for each salinity treatment group. Error bars represent the mean relative abundance \pm the standard error of the mean.

Figure 3.2: Impact of long-term environmental exposures on histone PTMs in fish acclimated to freshwater. **A)** The global histone PTM landscape of the gills was compared

between fish exposed exclusively to freshwater (treatment FF*/F) and fish that were raised under salinity stress but acclimated to freshwater during adulthood (treatment HS*/F). **B)** The pattern of change for all 343 histone PTMs is depicted in a volcano plot. Colored points represent the histone PTMs found to have a high fold change (green), low conditioned q-value (blue), both a high fold change and low conditioned q-value (red), or no substantial difference (gray). **C)** The histone PTMs found to have both a high fold change and low conditioned q-value when compared between the gills of fish in the FF*/F and HS*/F treatment groups (blue) are further depicted in bar graphs, which display the mean relative abundance of the histone PTMs in each salinity treatment group. Error bars represent the mean relative abundance \pm the standard error of the mean.

Figure 3.3: Impact of long-term environmental exposures on histone PTMs in fish

acclimated to seawater. A) The global histone PTM landscape of the gills was compared between fish exposed exclusively to increased salinity (treatment HS*/S) and fish that were raised in freshwater then acclimated to seawater during adulthood (treatment FF*/S). **B)** A volcano plot portrays the influence of salinity treatment on all 343 histone PTMs. The colored points represent histone PTMs found to have a high fold change (green), low conditioned q-value (blue), both a high fold change and low conditioned q-value (red), or no substantial difference (gray). **C)** For the histone PTMs found to have both a high fold change and low conditioned q-value when compared between fish in the HS*/S and FF*/S treatment groups (blue), the mean relative abundance in each salinity treatment group is displayed. Error bars represent the mean relative abundance \pm the standard error of the mean.

Figure 3.4: Impact of salinity acclimation during adulthood on histone PTMs. **A)** First, the global histone PTM landscape of the gills was compared between fish acclimated to either freshwater or seawater during adulthood, specifically when the fish were raised in freshwater (treatments FF*/F and FF*/S, respectively). **B)** A volcano plot depicts the pattern of change for all 343 histone PTMs between the fish in these treatment groups. **C)** For the one histone PTM found to have both a high fold change and low conditioned q-value when compared between fish in the FF*/F and FF*/S treatment groups (blue), the mean relative abundance in each salinity treatment group is displayed, with error bars representing the mean \pm the standard error of the mean. **D)** Second, the global histone PTM landscape of the gills was compared between fish acclimated to either freshwater or seawater during adulthood, specifically when the fish were raised under salinity stress (treatments HS*/F and HS*/S, respectively). **E)** The pattern of change for all quantified histone PTMs is depicted in a volcano plot. In both volcano plots shown here (B and E), colored points represent histone PTMs found to have a high fold change (green), both a high fold change and low conditioned q-value (red), or no substantial difference (gray).

Figures

Figure 3.1

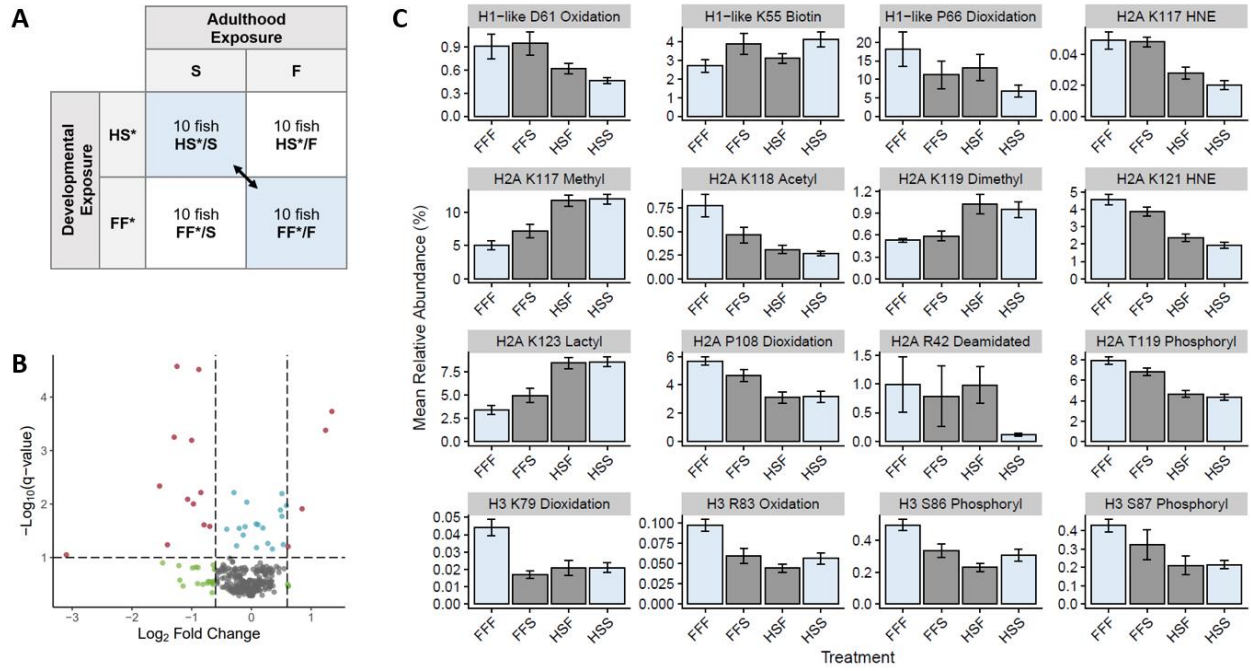


Figure 3.2

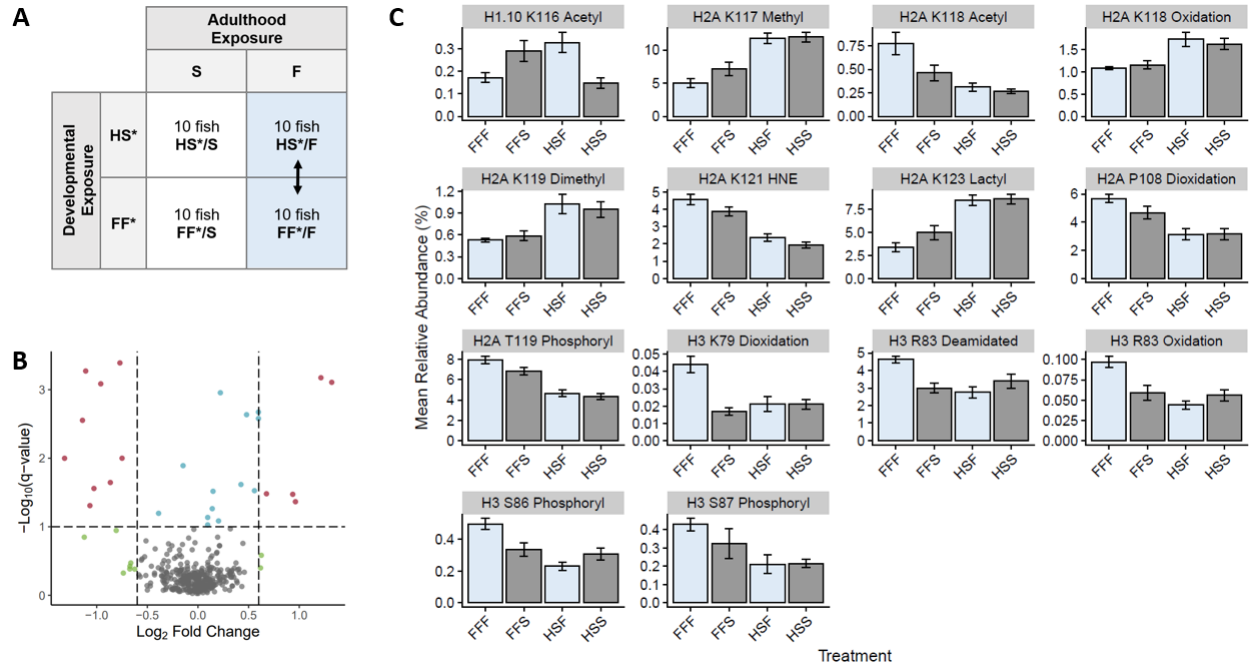


Figure 3.3

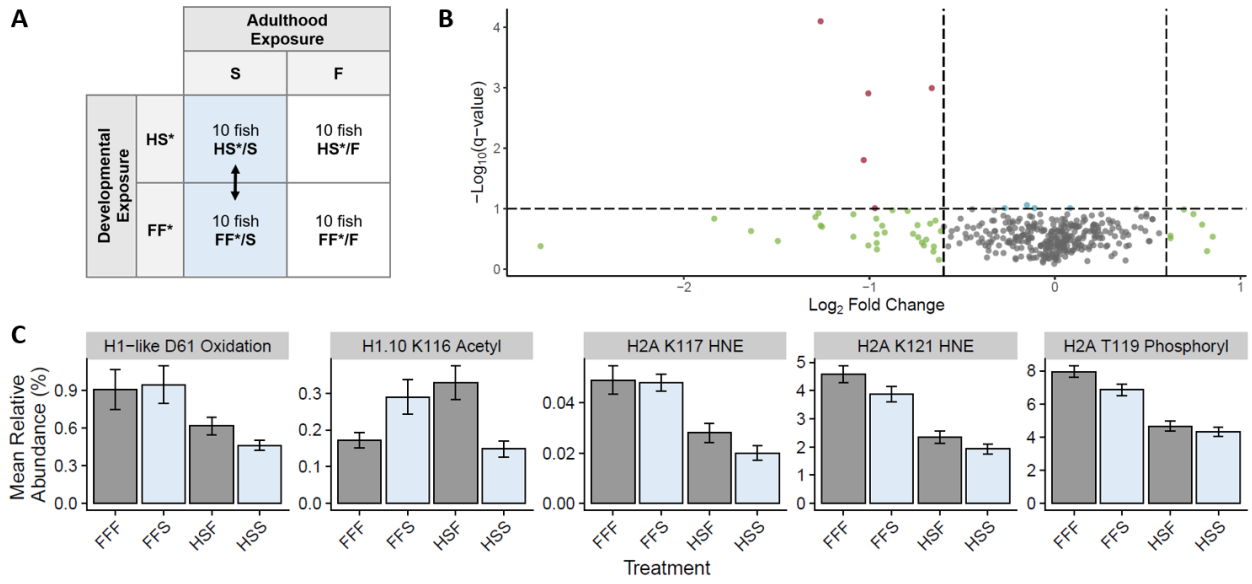
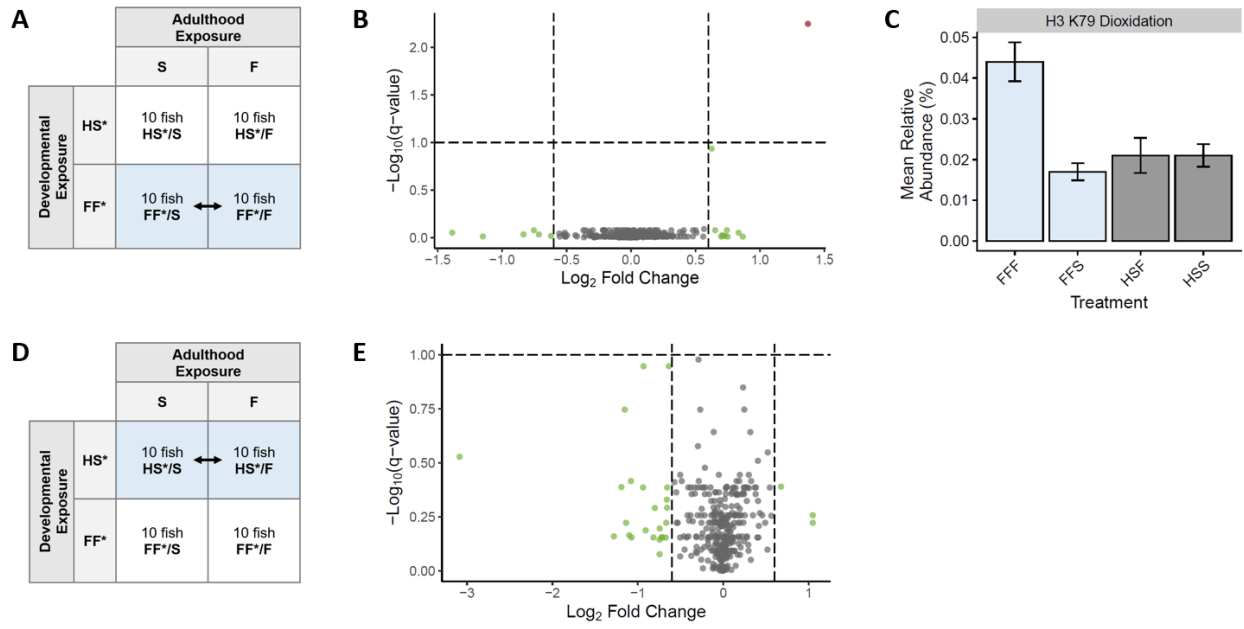


Figure 3.4



APPENDIX

Physiological Mechanisms of Stress-Induced Evolution

Summary statement

This article presents five mechanisms that eukaryotes can employ when experiencing stress to accelerate the process of adaptation. These mechanisms are outlined with emphasis on examples in animals.

Abstract

Organisms mount the cellular stress response (CSR) whenever environmental parameters exceed the range that is conducive to maintaining homeostasis. This response is critical for survival in emergency situations because it protects macromolecular integrity and, therefore, cell/organismal function. From an evolutionary perspective, the cellular stress response counteracts severe stress by accelerating adaptation via a process called stress-induced evolution (SIE). In this review, we summarize five key physiological mechanisms of stress-induced evolution. Namely, these are stress-induced changes in 1) mutation rates, 2) histone post-translational modifications, 3) DNA methylation, 4) chromoanagenesis, and 5) transposable element activity. Through each of these mechanisms, organisms rapidly generate heritable phenotypes that may be adaptive, maladaptive, or neutral in specific contexts. Regardless of their consequences to individual fitness, these mechanisms produce phenotypic variation at the population level. Because variation fuels natural selection, the physiological mechanisms of stress-induced evolution increase the likelihood that populations can avoid extirpation and instead adapt under the stress of new environmental conditions.

Introduction

All living organisms exist under the stress of their environment. Stress, in this sense, refers to any environmental parameter exerting strain on biological systems (Kültz, 2020a). When organisms are well-adapted to their environments, they harbor mechanisms that counteract imposed strain and therefore maintain homeostasis. Whenever environmental parameters change, organisms must adjust these mechanisms to uphold the balance between stress and the forces that oppose it. If the change in stress is minor enough, only the cellular homeostasis response (CHR) is needed for this adjustment. However, the capacity of the CHR may be exceeded depending on the magnitude of stress and how rapidly it arises. This threshold for stress tolerance is termed the “elastic limit,” and once it is surpassed, organisms must activate the cellular stress response (CSR) in order to survive (Kültz, 2020a; Call et al., 2017; Tian et al., 2012). Stress of this degree is becoming increasingly relevant and concerning to life on Earth amid climate change. As the atmosphere continues to collect greenhouse gases, numerous environmental factors, including the temperature, salinity, and acidity of water, change globally and much more rapidly than during previous geological periods (Cheng et al., 2020; Hoegh-Guldberg et al., 2007; Karger et al., 2020). When populations are limited in their ability to migrate to more suitable environments, they must somehow adapt in order to remain viable.

Under these circumstances, the CSR can employ physiological mechanisms of stress-induced evolution (SIE). These are strategies by which individuals rapidly generate new heritable phenotypes. At the population level, SIE produces widespread phenotypic variation and therefore accelerates evolutionary processes. In one mechanism, stress triggers mutagenesis by causing both increased DNA damage and decreased DNA repair fidelity (Chatterjee and Walker,

2017). In a more flexible response, stress induces the alteration of epigenetic marks, including histone post-translational modifications (PTMs) and DNA methylation. These epigenetic marks modify the expression patterns of DNA. Therefore, even if an individual's sequence of DNA remains unchanged, expression patterns (and corresponding phenotypes) can be passed through generations. In a more radical response, stress can prompt the formation of structural genomic variants through either chromoanagenesis or transposable element (TE) activity. These processes can produce especially distinctive phenotypes by reorganizing gene regulatory networks, e.g., via activation or inhibition of *cis*-regulatory elements (CREs), modifying gene products, and creating and deleting genes (Lanciano and Mirouze, 2018; Mérot et al., 2020; Pellestor and Gatinois, 2020; Ye et al., 2018).

In this review, we will summarize key physiological mechanisms of SIE in eukaryotes. An emphasis will be placed on animals for supporting examples. Throughout the article, we will demonstrate on a molecular level how life experience can alter the phenotype of an individual and its progeny. Notably, these mechanisms may or may not increase an individual's fitness; oftentimes, they result in disease or sterility. Nonetheless, they facilitate the generation of phenotypic variation within populations, where individuals may develop novel solutions to compensate for stress. In doing so, these mechanisms increase the likelihood that populations will adapt under stress.

Stress triggers mutagenesis through increased DNA damage and decreased DNA repair fidelity

DNA damage is an unavoidable part of life. Even under ideal environmental conditions, DNA is continuously damaged by spontaneous alkylation, strand breaks, hydrolytic loss of

nitrogenous bases, and base conversion (Chakarov et al., 2014). In humans, it is estimated that 2×10^4 events of DNA damage take place every day in each cell (Barzilai and Yamamoto, 2004). Damage, however, is not always detrimental, as the DNA damage response network has evolved to either repair DNA damage or tolerate it (Pilzecker et al., 2019). Only a fraction of DNA damage events lead to mutations that are retained and potentially inherited. In humans, despite the high frequency of DNA damage, rates of retained mutation are about 2.8×10^{-7} per base pair in somatic cells and 1.2×10^{-8} per base pair in the germline (Milholland et al., 2017).

Stress increases the rate of DNA damage, and therefore the rate of mutation, beyond what happens spontaneously. Diverse cellular stresses achieve this either directly or by secondarily stimulating the production of reactive oxygen species (ROS) in cells (Chakarov et al., 2014; Cheng et al., 2018; Kültz, 2005; Kültz, 2020b). ROS can damage DNA by causing strand breaks or oxidizing nucleotides into a plethora of compounds, including thymine glycol and 8-oxo-deoxyguanosine (Grollman and Moriya, 1993; Honda et al., 2001; Sallmyr et al., 2008). Through alternative routes, stress can damage DNA by producing single-strand breaks (SSBs), double-strand breaks (DSBs), apurinic (AP) sites, deaminated cytosine, cyclobutane pyrimidine dimers (CPD), and pyrimidine-pyrimidone photoproducts (6-4PP). In Table 4.1, we outline specific stresses that can produce these DNA lesions.

Cells attempt to repair all types of stress-induced DNA lesions. The strategy to repair DNA strand breaks depends on whether they are SSBs or DSBs. DSBs are especially mutagenic. When cells attempt to repair them, they can use the high-fidelity process of homologous recombination (HR), but most often they use the error-prone process of non-homologous end joining (NHEJ) (Chang et al., 2017). To address oxidized nucleotides, cells initiate base excision repair (BER) (Chatterjee and Walker, 2017). Nonetheless, approximately 2-5% of these lesions

escape repair, and when they do, they often cause mutations from G:C to A:T (Chatterjee and Walker, 2017; Grollman and Moriya, 1993; Moriya, 1993). The remaining stress-induced lesions are often repaired through a combination of BER and nucleotide excision repair (NER). However, if the cell cycle progresses into S phase before the lesions can be repaired, DNA damage tolerance pathways are activated instead (Chatterjee and Walker, 2017; Duncan and Miller, 1980; Pilzecker and Jacobs, 2019). Translesion DNA synthesis (TLS) is a prominent mechanism of the DNA damage tolerance pathway, and it functions to ensure that DNA replication can proceed even when DNA lesions are present. TLS promotes mutagenesis by using low-fidelity DNA polymerases that lack corrective exonuclease activity (Gerlach et al., 1999; Masuda et al., 2016).

While DNA repair is naturally fallible, stress can further reduce its fidelity and thereby increase the retention of mutations. Heat stress, for example, can inhibit both the BER and NER systems (Kantidze et al., 2016). This inhibition compromises the repair of DNA damage inflicted by stress. Similarly, proteins required for mismatch repair are downregulated under the stresses of both hypoxia and toxins (Chatterjee and Walker, 2017; Mihaylova et al., 2003). The mechanism of DSB repair can also be altered by stress, ensuring that low-fidelity NHEJ is used for repair, e.g., during hypoxia and heat stresses (Galhardo et al., 2007; Kantidze et al., 2016).

Through these and many other mechanisms, stress increases the incidence and retention of mutations. Stress-induced mutagenesis is likely an adaptive strategy as it provides an avenue for a maladapted population to accumulate genetic diversity in response to environmental change. Selection can act on the resulting genetic variation, enabling the population to become better suited for stressful environments. These mutations are not entirely random. Stress-induced mutations accumulate at different rates in transcriptionally active versus silent genes since the

susceptibility to DNA damage differs between corresponding eu- and hetero-chromatin (Makova and Hardison, 2015). This effect can accelerate evolution in genes that are actively involved in defining the phenotype of a specific cell type in a specific context. Altered cellular phenotypes, in turn, influence phenotypes at higher levels of organization, including the whole organism level.

Stress causes heritable (epigenetic) changes in histone post-translational modifications

In the nucleus of eukaryotic organisms, DNA wraps around an octamer of the four core histones: H2A, H2B, H3, and H4 (Luger et al., 1997). These proteins are subject to a wide variety of post-translational modifications (PTMs) (Zhao and Garcia, 2015). Histone PTMs are epigenetic marks that can modify the state of chromatin and influence gene expression. They can do this by altering the manner in which DNA is packaged, thus changing the accessibility of the DNA for proteins involved in transcription and repair (Norton et al., 1989). Histone PTMs also modulate the recruitment of histone reader proteins to specific genetic loci to carry out physiological functions, such as DNA repair, replication, transcription, and chromosome condensation (Kouzarides, 2007).

Stress can alter the histone PTM landscape, which is the relative abundance and genomic distribution of all histone PTMs in a cell (Table 4.2). Histone PTMs are “written” and “erased” by histone modifying enzymes, but the catalytic activity of these enzymes can be modified under stress, e.g., through chemical inhibition or alteration of cosubstrate availability (Fan et al., 2015b). Both of these strategies apply to the histone demethylase enzyme JmjC. Oxidative stress causes the iron in its catalytic center to be oxidized from Fe(II) to Fe(III), which inhibits its function and leads to histone hypermethylation (García-Giménez et al., 2021). Interestingly,

hypoxia also represses the activity of this demethylase because JmjC requires oxygen as a cosubstrate (Hsu et al., 2021). At the same time, however, hypoxia-inducible factors transcriptionally upregulate JmjC to fine-tune the overall histone demethylation activity (Hsu et al., 2021). This example illustrates that the effects of stress on the regulation of histone PTMs are pervasive and highly complex.

By modifying the histone PTM landscape, stress can facilitate an appropriate physiological response, e.g., during temperature and salinity stresses. Heat stress increases the relative abundance of H3K27me3 in the adrenal gland of chickens (*Gallus gallus domesticus*) (Zheng et al., 2021). This epigenetic response is associated with increased glucocorticoid production, which assists in heat dissipation (Zheng et al., 2021). During cold stress, the relative abundance of H3K27me3 decreases in thale cress (*Arabidopsis thaliana*), and it does so specifically at the loci of two cold stress genes, leading to their activation (Yuan et al., 2013). On the contrary, stress-induced histone PTMs can be associated with maladaptive phenotypes. For example, people working in steel plants breathe in toxic particulate matter. As their time of employment increases, their levels of H3K4me2 and H3K9ac also increase. In this case, the histone PTM landscape is associated with an increased risk for lung cancer (Cantone et al., 2011).

Even once the stress has subsided, induced histone PTMs can be retained within individuals, via “intragenerational” inheritance by mitosis (Alabert and Groth, 2012). When stress causes changes to histone PTMs in the germline, the epigenetic marks can be retained across generations (Figure 4.1). This retention can occur through different processes. In one process sometimes called “intergenerational” inheritance, stress directly induces histone PTMs in the gametes of exposed parents. Upon fertilization, gametes that carry the directly induced

epigenetic marks become the next generation. In a second process often called “transgenerational” inheritance, induced histone PTMs travel across multiple generations without the need for individuals inheriting them to be directly exposed to stress (Bošković and Rando, 2018; Mørkve Knudsen et al., 2018; Perez and Lehner, 2019; Woodhouse and Ashe, 2020). Transgenerational inheritance is especially relevant for stress-induced evolution as it extends the time that natural selection can act on epigenetically mediated phenotypic variation. Heat stress, for example, was shown to increase the global acetylation levels of histones H3 and H4 in the brine shrimp (*Artemia spec.*). After heat stress subsided, the induced histone PTM landscape could be transmitted through three subsequent generations, and it was associated with enhanced tolerance to severe heat stress in the progeny (Norouzitallab et al., 2014).

While the mechanism of transgenerational epigenetic inheritance is not yet fully elucidated, individuals can directly receive modified histones from the gametes that form them. This process is relatively straightforward regarding maternal transfer, but epigenetic reprogramming represents a hurdle to paternal transfer. During spermatogenesis, histone proteins are replaced with protamines for an even tighter packaging of DNA (Bao and Bedford, 2016). Some species such as mice only retain 1-2% of histones in sperm; however, this value is widely variable between species (Champroux et al., 2018). For example, the percentage of retained histones is approximately 5-10% in humans (Champroux et al., 2018), 37% in nematode worms (Samson et al., 2014), 45% in marsupials (Soon et al., 1997), and 100% in lampreys and hagfish (Saperas et al., 1997). In this way, it is possible that some species have a much higher propensity for the transgenerational inheritance of histone PTMs.

Histone PTMs offer individuals a mechanism to rapidly modify gene expression patterns and their phenotypes to better tolerate their environment. Such altered phenotypes (and the

underlying genotypes of corresponding individuals) are acted upon by natural selection and, therefore, represent targets of stress-induced adaptation. Selection on these targets may be prolonged over multiple generations since individuals exposed to stress can transmit histone PTMs, gene expression patterns, and the resulting phenotypes they acquire to their progeny. The adaptive value of retaining phenotypes that confer tolerance to short periods of stress in the absence of persistent stress may seem questionable (Nilsson et al., 2018). However, what natural selection favors under such conditions are individuals with the ability to tolerate transient periods of stress best while also performing best during intermittent periods of low stress. For this reason, histone PTMs and corresponding gene expression patterns and phenotypes are reversible, and their persistence within a lineage can depend on the intensity and duration of stress experienced by their ancestors. In this way, epigenetic mechanisms can facilitate trial runs of new phenotypes and integrate stochasticity and periodicity in environmental conditions into the process of natural selection (Burggren, 2016; Walker and Burggren, 2020). Through this mechanism (and epigenetic inheritance of DNA methylation), natural selection assesses the adaptive value of corresponding phenotype variants in a particular lineage under variable environmental conditions over longer periods of time.

Stress alters heritable (epigenetic) DNA methylation patterns

DNA methylation is a heritable epigenetic mark characterized as a methyl group attached to the fifth carbon of cytosine. When DNA methylation occurs in a promoter, it typically silences the gene by preventing the binding of transcription factors and prompting the formation of heterochromatin. Conversely, when methylation occurs in an open reading frame, it typically activates the gene (Greenberg and Bourc'his, 2019; Jones, 2012; Moore et al., 2013). De novo

DNA methylation is facilitated by the DNA methyltransferase enzymes DNMT3a and DNMT3b, which can be targeted to specific genes through the guidance of piwi-interacting RNA (Flores et al., 2013; Okano et al., 1999). Stress is well documented to induce de novo DNA methylation, leading to differentially methylated regions (DMRs). Due to their influence on gene expression, DMRs can impact morphology, physiology, behavior, and development (Angers et al., 2010).

Stress-induced DMRs have been reported across taxa, from plants to insects to humans (Ou et al., 2012; Shi et al., 2011; Martin and Fry, 2018). Through this epigenetic mechanism, the environment generates new phenotypes in individuals that, for better or worse, affect their fitness (Table 4.3). Many putatively adaptive responses have been observed. For example, the spiny chromis damselfish (*Acanthochromis polyacanthus*) was recently shown to accumulate 193 DMRs after exposure to increased temperature (Ryu et al., 2018). Those DMRs correlated with increased aerobic scope, which enhanced tolerance to heat stress (Ryu et al., 2018). Similarly, purple sea urchins (*Strongylocentrotus purpuratus*) that experienced upwelling conditions during gametogenesis induced DMRs in their progeny that were associated with increased body size (Strader et al., 2019; Wong et al., 2019). However, stress can sometimes also lead to transgenerational transmission of traits that reduce fitness. Ionizing radiation in zebrafish (*Danio rerio*), for example, was shown to induce 5658 DMRs; 19 of these were passed through one generation, and 5 were passed through two generations (Kamstra et al., 2018). In this case, the DMRs were localized to genes involved in cancer and apoptosis, which could help explain the developmental defects observed in the progeny inheriting these epigenetic marks (Kamstra et al., 2018).

Whether adaptive or maladaptive, phenotypes generated through stress-induced DMRs can be inherited within individuals and across generations. Within individuals, patterns of DNA

methylation are often stably maintained through mitosis by the DNMT1 enzyme (Smith and Meissner, 2013). DNMT1 itself, however, has a relatively high error rate of about 5% (Bird, 2002). As a result, additional variation in DNA methylation patterns can emerge through time within an individual's cell population, which affects organismal phenotype. The mechanism of transgenerational inheritance of DNA methylation is not yet fully understood. A natural limitation to this process is that widespread reprogramming of DNA methylation takes place during gametogenesis and shortly after fertilization, but some genetic loci are protected during these events (Angers et al., 2010; Engmann and Mansuy, 2020). Even so, it has been observed on many occasions that stress-induced DMRs can be transferred through multiple generations, including in the examples mentioned above.

As an epigenetic mark, DNA methylation rapidly elicits phenotypic variation that can equip some individuals and their progeny to better cope with stress they experience. Importantly, DNA methylation functions beyond an epigenetic mark as well, in a much more permanent manner. Namely, it increases rates of mutation by frequently causing cytosine to thymine transitions (Zhou et al., 2020; Yang et al., 2021; Holliday and Grigg, 1993). This pattern is so apparent that species with widespread DNA methylation exhibit global depletion of CpG dinucleotides, because this is where DNA methylation most often occurs (Gruenbaum et al., 1982). In humans, 60-80% of all CpG sites are methylated (Smith and Meissner, 2013). With such extensive DNA methylation, the human genome only has 20% of the expected amount of CpG dinucleotides, presumably because many cytosines in these sequences have been mutated into thymines (Bird, 1980). In contrast, fruit flies (*Drosophila melanogaster*), which display a very low level of DNA methylation, still have >90% of the expected amount of CpG sites (Capuano et al., 2014; Lyko, 2001; Bird, 1980). Because DNA methylation is targeted, C→T

mutation can be targeted as well. Therefore, when stress induces DMRs, resulting phenotypic advantages can potentially be fixed in a lineage by nonrandom mutation to specific genetic loci (Angers et al., 2010).

Stress impacts genome structure through chromoanagenesis

Of all the physiological mechanisms of stress-induced evolution, changes to genome structure are the most dramatic. In a process called chromoanagenesis (also known as genome chaos), severe stress causes cells to rapidly shatter the genome and rearrange its contents (Heng and Heng, 2020). Structural genomic variants are the outcome of this process, and they can include any combination of copy number variants, chromosomal fusions, fissions, translocations, inversions, and reshuffling (Mérot et al., 2020; Heng, 2009). These structural changes strongly affect organismal fitness by changing gene regulatory networks, altering gene dosage, functionally deleting genes, or even creating new genes from previously non-coding DNA (Mérot et al., 2020; Pellestor and Gatinois, 2020; Ye et al., 2018). Most often, the effects of chromoanagenesis are deleterious. On the rare occasion, however, the generated phenotypic diversity is lifesaving (Figure 4.2).

Stress-induced changes in genome structure are well studied in the context of human disease. It has been discovered within the past 20 years that structural genomic variants are a universal feature of cancer, and they are frequently associated with additional diseases such as Alzheimer's (Heng, 2009; Horne et al., 2014). Using disease study systems, three categories of chromoanagenesis have been identified: chromothripsis, chromoanasythesis, and chromoplexy (Koltsova et al., 2019). Chromothripsis refers to a single event where one chromosome is shattered and randomly stitched back together. The process is triggered by a high load of DNA

double-strand breaks, which result under the pressure of numerous environmental stresses (Koltsova et al., 2019). Additional forces including telomere attrition, abortive apoptosis, and mitotic errors also prompt chromothripsis (Pellestor and Gatinois, 2020). Chromoanagenesis is a process that specifically leads to the generation of copy number variants, and it is triggered by DNA replication and repair errors (Koltsova et al., 2019). Finally, chromoplexy describes the reshuffling of several chromosomes over the course of multiple events, and it is often caused by replication stress, mitotic errors, and premature chromosome compaction (Shen, 2013).

Beyond causing disease states of somatic cells, chromoanagenesis proceeds within the germline and within embryos during early development (Pellestor and Gatinois, 2020). In this context, chromoanagenesis can be adaptive and lead to rapid speciation in asexually reproducing organisms and even in heterogametic species, as long as both parents experience compatible genome changes for sexual reproduction (Heng, 2009). Every type of structural genomic variant has been implicated in driving speciation (Campbell et al., 2018; Feulner and De-Kayne, 2017). Accordingly, both the morphology and number of chromosomes vary widely across taxa (Ferguson-Smith and Trifonov, 2007). For example, the number of chromosome pairs in eukaryotes ranges from one to 720 (Schubert and Vu, 2016; Khandelwal, 1990). In light of evolutionary history, chromoanagenesis could be a large contributor to this structural genomic variation because periods of major evolutionary change tend to occur during periods of severe stress. For example, the “Big Five” mass extinctions and their subsequent events of adaptive radiation corresponded to large changes in temperature, sea-level, volcanic and tectonic activity, and meteor impacts (Condamine et al., 2013). During such periods, eurytopic species are favored over stenotopic species while the opposite is the case during long, stable geological periods

(Kültz, 2003). Corresponding patterns of evolutionary history have been interpreted by the theory of punctuated equilibrium (Gould, 1982).

Structural genomic variants can be adaptive under various contexts (Table 4.4). When challenged by the widely used herbicide glyphosate, palmer amaranth (*Amaranthus palmeri*) developed a copy number variant that enabled resistance to the herbicide (Gaines et al., 2010). Similarly, the codling moth (*Cydia pomonella*) developed a sex-linked resistance to insecticides through a chromosome fusion (Nguyen et al., 2013). Chromosome inversions have been adaptive in the context of behavior, mating strategies, and morphology (Wellenreuther and Bernatchez, 2018). For example, inversions produced cryptic color phenotypes in stick insects (*Timema cristinae*) and facilitated appropriate migratory behaviors in rainbow trout (*Oncorhynchus mykiss*) (Lindtke et al., 2017; Wellenreuther and Bernatchez, 2018).

Whether the process occurs in somatic cells or gametes, chromoanagenesis elicits major phenotypic changes by altering genome structure in individuals facing severe stress. Most of the time, the outcomes are deleterious – either a disease emerges, or individuals generate gametes that are incompatible with potential mates, rendering the individuals sterile. On the lucky occasion, structural genomic variants enable successful survival and reproduction, and they do so within one generation.

Stress affects the activity of transposable elements

Transposable elements (TEs) have long been considered an engine of evolutionary change fueled by stress (McClintock, 1984), and they make up a large portion of eukaryotic genomes. In mammals, about 40% of the genome is comprised of TEs, and in plants, that value can be as high as 85% (Chénais et al., 2012). TEs are sequences of DNA, sometimes called

“jumping genes,” that can readily move throughout the genome. The process of their transposition can proceed through “copy and paste” or “cut and paste” strategies. In the copy and paste strategy, class I TEs are transcribed into an RNA intermediate then reverse transcribed back into DNA at a new location. In the cut and paste strategy, many class II TEs have their DNA sequence broken out of its position, then relocated (Wicker et al., 2007). Oftentimes, all the information needed for transposition is encoded within the TE. If this is the case, then they are called autonomous TEs, and depending on their family, they encode enzymes such as reverse transcriptase, proteinase, RNase, integrase, and transposase. Nonautonomous TEs have also evolved, and they lack some of the necessary components for transposition. As a result, they rely on autonomous TEs for their mobilization (Wicker et al., 2007).

When activated, TEs can quickly produce distinctive phenotypes by impacting gene expression, gene products, and genome structure. The expression of genes can be affected when newly incorporated TEs provide *cis*-regulatory elements (CREs), change the context of existing CREs, or alter the local epigenetic landscape (Chénais et al., 2012; Lanciano and Mirouze, 2018). Similarly, transposition can alter gene products when inserted TEs cause alternative transcription start sites, alternative splicing, or premature termination. New exons and introns can even be created in the process (Lanciano and Mirouze, 2018). For transposition to occur, DNA double-strand breaks (DSBs) are needed to cut out and insert TEs. This form of DNA damage increases rates of mutation, specifically at the sites of deletion and insertion (Biémont and Vieira, 2006). Furthermore, transposition-induced DSBs can produce structural genomic variants by feeding into the chromothripsis pathway, which leads to chromosome inversions and chromosome reshuffling (Figure 4.2) (Pellestor and Gatinois, 2020). TEs generate additional structural genomic variants as a consequence of the high sequence similarity between TEs of the

same family, in particular at their flanking sequences such as inverted terminal repeats (ITRs). This similarity enables non-allelic homologous recombination, which can cause chromosome inversions, duplications, translocations, and deletions (Kent et al., 2017).

Numerous stresses can alter TE activity, including cold and heat stresses, UV irradiation, salinity stress, and pollution (Miousse et al., 2015; Rey et al., 2016). However, the pattern of alteration is context dependent. In response to stress, TEs may be activated, repressed, activated then repressed, or repressed then activated (Horváth et al., 2017). Furthermore, when TEs are activated, it can be at the transcriptional level, the transpositional level, or both (Horváth et al., 2017). Epigenetic regulation is one major force that mediates this change (Biéumont and Vieira, 2006). TEs are repressed under the control of DNA methylation and histone PTMs (Zemach et al., 2010). When stress alters these epigenetic marks, TEs can be released from repression and freed to transcribe their contents and/or mobilize to other parts of the genome (Pappalardo et al., 2021). Another stress-sensitive mechanism of TE activation involves the heat shock protein 90 family (HSP90). While HSP90 silences TEs under optimal environmental conditions, moderate stress can limit this function when HSP90 is instead needed to protect protein conformation (Ryan et al., 2016). Notably, the limitation of available HSP90 also increases phenotypic diversity by releasing cryptic genetic variation (CGV) from suppression (Paaby and Rockman, 2014). Therefore, HSP90 has been considered a key evolutionary capacitor (Rutherford and Lindquist, 1998).

Stress-induced changes in TEs have been observed across eukaryotic taxa (Table 4.5), and on many occasions, they have proven to be adaptive. For example, insecticide exposure has altered TE activity in insects. In the fruit fly (*Drosophila melanogaster*), this led to the overexpression of an insecticide detoxifying gene (Chung et al., 2007). In the common house

mosquito (*Culex pipiens*), this led to the alternative splicing of a toxin receptor gene (Darboux et al., 2007). In both instances, the TEs induced by insecticides resulted in insecticide resistance. Similarly, climate has been shown to induce potentially adaptive TEs in the Asian tiger mosquito (*Aedes albopictus*). The frequency of TE insertions varies between a native population in a tropical environment and an invasive population in a temperate environment. In the invasive population, TEs of multiple families are inserted at higher frequencies, and they are positioned within the proximity of genes that likely facilitate overwintering (Goubert et al., 2017). Altered regulation of these genes could increase the fitness of mosquitoes living in colder climates.

Through the alteration of TE activity, stress generates rapid phenotypic variation. The variation can be significant because TE activation has the power to affect gene expression, gene products, and genome structure. When these changes happen in the germline, they can be passed from parent to offspring indefinitely. This standard form of transmission is referred to as “vertical transfer.” However, “horizontal transfer” of TEs can happen as well, where TEs jump between species. In the evolutionary history of vertebrates, for example, at least 975 events of horizontal transfer of TEs have occurred (Zhang et al., 2020).

Life experience and physiology shape evolution

Contrary to the principles of the Modern Synthesis of evolutionary theory, stress that an individual encounters throughout its lifetime is now known to induce heritable phenotypic variation (Burggren, 2014b; Jablonka and Lamb, 2020; Noble, 2013; Skinner, 2015). This concept of stress-induced evolution (SIE) has been accepted for decades in regard to prokaryotes (Radman, 1975; Bjedov et al., 2003; Foster, 2007; Rosenberg et al., 2012). In prokaryotes, stress significantly increases rates of mutation, largely through the activation of the SOS system and

RpoS stress response (Radman, 1975; Foster, 2007). Although these systems do not exist in eukaryotes, more recent studies have demonstrated that eukaryotes employ several powerful mechanisms to increase phenotypic variation in response to stress. Beyond the increased rates of mutation via DNA damage and lowered DNA repair fidelity that occur outside of the prokaryotic SOS and RpoS systems, variation is achieved through histone PTMs, DNA methylation, chromoanagenesis, and transposable element activity.

In multicellular eukaryotes, the mechanisms of SIE can proceed in both the soma and the germline. Somatic cell evolution has been studied intensively in the context of disease (Anway et al., 2006; Heng, 2009; Rajesh Kumar et al., 2002), proving that the outcome of these mechanisms can be maladaptive. Considering that many multicellular organisms consist of millions, billions, or even trillions of cells, e.g., 37 trillion cells in humans (Bianconi et al., 2013), the large population of cells provides a sufficient pool of beneficial alterations that selection can act on. A classic example of adaptive somatic cell evolution is the production of antibodies in vertebrates. After organisms are exposed to new antigens, the variable regions of immunoglobulin genes in B cells become hypermutated (Diaz and Flajnik, 1998; Wysocki et al., 1986). This mechanism ultimately increases the affinity of antibodies to circulating antigens, thereby strengthening the immune system. While these changes to somatic cells easily impact the fitness of individuals by affecting their ability to survive and reproduce, stress arguably has the strongest influence over organismal evolution when alterations happen within the germline. Each of the physiological mechanisms of SIE can proceed within the germline, although this happens less frequently than in somatic cells because germ cell chromatin is transcriptionally silent and better protected from damage (Bao and Yan, 2012; Engmann and Mansuy, 2020; Heng, 2009; Milholland et al., 2017). Nonetheless, critical windows of development exist where stress is

more likely to induce stably transmitted epigenetic marks in the germline (Skinner, 2011). Embryonic gonadal sex determination is the first critical window, and gametogenesis is the second (Hanson and Skinner, 2016).

Despite the popularity of the idea that the soma and the germline are completely isolated, i.e., the Weismann Barrier (Weismann, 1890), this barrier can be bypassed through microvesicles. Microvesicles, in the form of either shedding vesicles or exosomes, are released from all cell types (Camussi et al., 2010; Doyle and Wang, 2019). Once released, they can remain in the extracellular matrix within the proximity of the cell of origin, or they can travel through biological fluids to reach distant target cells (Camussi et al., 2010). These microvesicles contain components of the origin cell, including RNA and proteins. By delivering both of these components, microvesicles have the power to epigenetically reprogram target cells (Engmann and Mansuy, 2020; Sharma, 2014). This important transfer of information can take place between two somatic cells, or between somatic and germ cells. A recent study clearly demonstrated this phenomenon in mice xenografted with human tumor cells. RNA from the xenografted cells traveled through the bloodstream in exosomes until being finally received by spermatozoa (Cossetti et al., 2014). Therefore, germ cells do not necessarily need to be directly altered by stress; it is possible for information from affected somatic cells to reach and modify the germline. Impressively, Charles Darwin essentially predicted the existence of microvesicles. He described them as “gemmules” in 1868, before they could have possibly been detected (Noble, 2021).

Through all the physiological mechanisms discussed in this brief essay, eukaryotic organisms can establish heritable phenotypic variation in response to stress. Notably, DNA base mutation is not the only driver of this variation. Rapid phenotypic diversity can be achieved by

histone PTMs, DNA methylation, chromoanagenesis, and transposable element activity. The induced variation can be adaptive, maladaptive, or neutral in specific contexts. In any case, it is produced at a time when homeostasis cannot be maintained, and the system is forced to explore novelty.

Conclusions and future perspectives

This essay summarizes five physiological mechanisms of stress-induced evolution (SIE), which serve to generate novelty in populations experiencing altered environmental conditions. Due to their widespread presence across the phylogenetic web of life, these mechanisms have likely been favored during evolution by conferring significant selective advantages that outweigh potential disadvantages, such as the increased susceptibility to pathologies. A better understanding of the profound implications of these mechanisms for cells, organisms, and populations represents an exciting frontier in biology. Many open questions that should be of great interest to comparative physiologists remain, including the following. Is there a correlation between the prevalence of SIE mechanisms, incidence of proliferative disease, and average lifespan across different species? How does the magnitude of stress impact the proportion of favorable to unfavorable phenotypes produced through SIE mechanisms in a population? To what extent has SIE driven punctuated equilibrium throughout evolutionary history? How does SIE impact ecosystem succession during geological periods of rapid environmental change? SIE represents an exciting new paradigm in comparative evolutionary physiology that challenges long-standing dogmas and stimulates the creative intellect of current and future physiologists. In this brief essay, we share our enthusiasm for this fascinating area of biology to inspire future research on SIE by a broader scientific community.

Competing interests

No competing interests declared

Funding

This work was supported by the National Science Foundation Grant MCB-2127516 to D.K.

Figure Legends

Figure 4.1. The modes of epigenetic inheritance of histone PTMs. Stress induces changes in the relative abundance of histone PTMs in somatic cells (represented by white stars) and/or germ cells (represented by black stars). When an epigenetic mark persists through time within the F_0 individual, it is intragenerationally inherited. If the mark is passed through one generation due to direct gamete exposure, it is intergenerationally inherited. In the case of transgenerational inheritance, the mark can be passed through multiple generations, and progeny inheriting the mark never need to experience the stress.

Figure 4.2. Stress-induced effects on genome structure. First, stress causes strain on cellular systems. These perturbations lead to chromoanagenesis in the form of chromothripsis, chromoplexy, or chromoanasythesis. Each subset of chromoanagenesis produces a set of structural genomic variants. These structural genomic variants can be maladaptive or adaptive. It should be noted that not all activators of chromoanagenesis are included in this diagram.

Figures

Figure 4.1

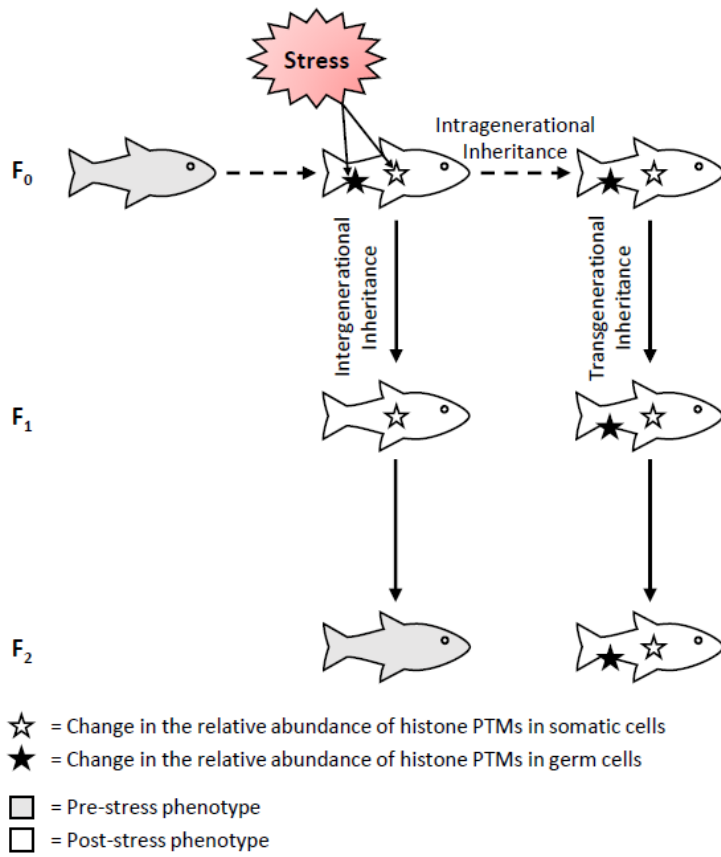
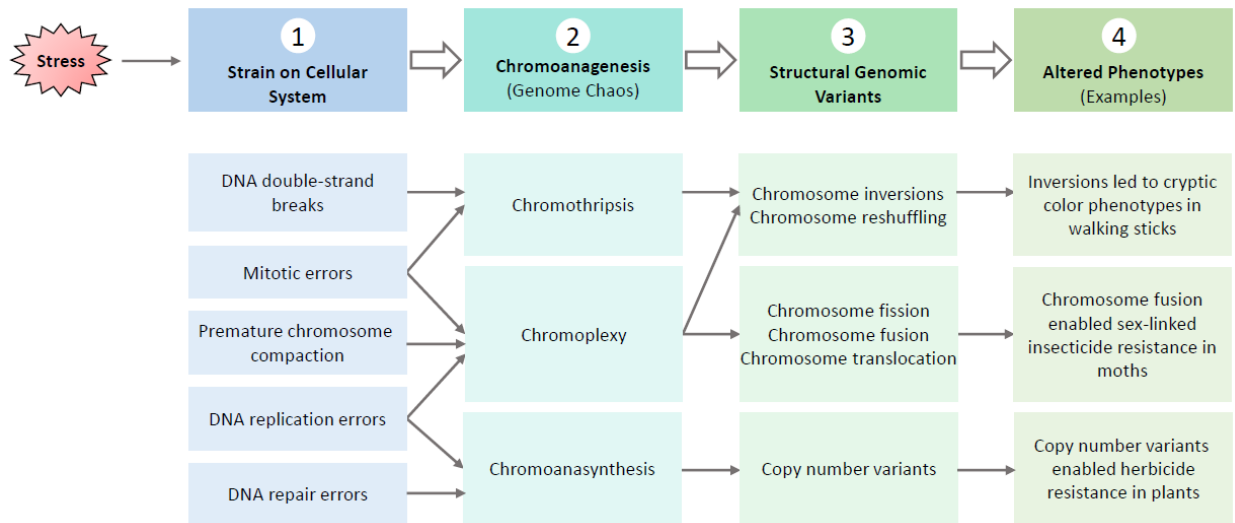


Figure 4.2



Tables

Table 4.1

Table 4.1. Examples of stress-induced DNA damage.

| Stress | DNA Damage | Species | Reference |
|--------------------------------------|-------------------------------------|--|---------------------------------|
| Oxidative stress | Strand breaks | Human (<i>Homo sapiens</i>) | (Honda et al., 2001) |
| | | Mouse (<i>Mus musculus</i>) | (Rajesh Kumar et al., 2002) |
| | | Chub (<i>Leuciscus cephalus</i>) | (Aniagu et al., 2006) |
| | Thymine glycol | Rat (<i>Rattus norvegicus</i>) | (Cathcart et al., 1984) |
| | | Human (<i>Homo sapiens</i>) | (Yoon et al., 2010) |
| | 8-oxo-deoxyguanosine | Gilt-head bream (<i>Sparus aurata</i>) | (Diaz-Mendez et al., 1997) |
| Mouse (<i>Mus musculus</i>) | | (Yamanaka et al., 2001) | |
| Human (<i>Homo sapiens</i>) | | (Matsui et al., 1999) | |
| Hypoxia | Single-strand breaks | Rainbow trout (<i>Oncorhynchus mykiss</i>) | (Liepelt et al., 1995) |
| | | Human (<i>Homo sapiens</i>) | (Møller et al., 2001) |
| Salinity stress | Double-strand breaks | Mouse (<i>Mus musculus</i>) | (Kültz and Chakravarty, 2001) |
| | | Thale cress (<i>Arabidopsis thaliana</i>) | (Boyko et al., 2010b) |
| | Single-strand breaks | Strawberry (<i>Fragaria x ananassa</i>) | (Tanou et al., 2009) |
| Extreme pH | Strand breaks | Pacific white shrimp (<i>Litopenaeus vannamei</i>) | (Wang et al., 2009) |
| | AP sites | Human (<i>Homo sapiens</i>) | (Chatterjee and Walker, 2017) |
| Heat stress | Strand breaks | Pufferfish (<i>Takifugu obscurus</i>) | (Cheng et al., 2018) |
| | AP sites | Human (<i>Homo sapiens</i>) | (Chatterjee and Walker, 2017) |
| | Deaminated cytosine | Mammals (multiple species) | (Fryxell and Zuckerkandl, 2000) |
| UV irradiation | Strand breaks | Human (<i>Homo sapiens</i>) | (Lankinen et al., 1996) |
| | | Pig (<i>Sus sp.</i>) | (Choy et al., 2005) |
| | Cyclobutane pyrimidine dimers | Human (<i>Homo sapiens</i>) | (Clingen et al., 1995) |
| | | Mouse (<i>Mus musculus</i>) | (Garinis et al., 2005) |
| | | Rockcress (<i>Arabidopsis sp.</i>) | (Chen et al., 1994) |
| | Pyrimidine-pyrimidone photoproducts | Human (<i>Homo sapiens</i>) | (Mitchell et al., 1990) |
| | | Prussian carp (<i>Carassius auratus gibelio</i>) | (Bagdonas and Zukas, 2004) |
| Rockcress (<i>Arabidopsis sp.</i>) | | (Chen et al., 1994) | |

Table 4.2

Table 4.2. Examples of stress-induced change in histone PTMs.

| Stress | Change in Histone PTMs | Species | Associated Phenotype (if reported) | Reference |
|-----------------|--|---|---|------------------------------|
| Heat stress | Increase in H3K27me3 | Chicken (<i>Gallus gallus domesticus</i>) | Increased glucocorticoid production | (Zheng et al., 2021) |
| | Increase in H3K4me2/3 | Thale cress (<i>Arabidopsis thaliana</i>) | Transcriptional memory of heat stress | (Lämke et al., 2016) |
| | Decrease in H3K9me2/3** | Fruit fly (<i>Drosophila melanogaster</i>) | Not reported | (Seong et al., 2011) |
| | Decrease in H3K9me3** | Nematode worm (<i>Caenorhabditis elegans</i>) | Altered gene expression** | (Klosin et al., 2017) |
| | Acetylation of histones H3 and H4** | Brine shrimp (<i>Artemia</i>) | Enhanced tolerance to lethal heat stress; resistance to <i>Vibrio campbellii</i> ** | (Norouzitallab et al., 2014) |
| Cold stress | Decrease in H3K9me2 | Mouse (<i>Mus musculus</i>) | Long-term tolerance to cold stress | (Abe et al., 2018) |
| | Decrease in H3K27me3 | Thale cress (<i>Arabidopsis thaliana</i>) | Activation of cold stress genes | (Kwon et al., 2009) |
| | Increase in H3K27ac and H3K36ac | Rice (<i>Oryza sativa</i>) | Not reported | (Xue et al., 2018) |
| Salinity stress | Decrease in H3K9me2/3** | Fruit fly (<i>Drosophila melanogaster</i>) | Not reported | (Seong et al., 2011) |
| | Increase in H3K4me3 and H3K9K14ac; decrease in H3K9me2 | Thale cress (<i>Arabidopsis thaliana</i>) | Activation of salinity-induced genes | (Chen et al., 2010) |
| Drought stress | Increase in H3K4me3 and H3K9ac | Thale cress (<i>Arabidopsis thaliana</i>) | Activation of drought-induced genes | (Kim et al., 2008) |
| Toxin exposure | Decrease in H3K4me2, H3K18ac, H3K27me2, and H3K20me2; increase in H3K14ac* | Rat (<i>Rattus norvegicus</i>) | Desensitization to toxin (cocaine)* | (Wimmer et al., 2019) |
| | Increase in H3K4me2 and H3K9ac | Human (<i>Homo sapiens</i>) | Increased risk of lung cancer | (Cantone et al., 2011) |

*Effect observed in next generation

**Effect observed through multiple generations

Table 4.3

Table 4.3. Examples of stress-induced change in DNA methylation.

| Stress | Species | Associated Phenotype (if reported) | Reference |
|--------------------|---|---|---|
| Heat stress | Spiny chromis damselfish (<i>Acanthochromis polyacanthus</i>) | Increased aerobic scope* | (Ryu et al., 2018) |
| | Brine shrimp (<i>Artemia</i>) | Enhanced tolerance to lethal heat stress; resistance to <i>Vibrio campbellii</i> ** | (Norouzitallab et al., 2014) |
| Cold stress | Mouse (<i>Mus musculus</i>) | Increased tolerance to cold stress; reduced risk of obesity* | (Sun et al., 2018) |
| | Tartary buckwheat (<i>Fagopyrum tataricum</i>) | Altered expression of genes involved in cold memory | (Song et al., 2020) |
| | Turnip (<i>Brassica rapa</i>) | Increased growth rate and heat tolerance | (Liu et al., 2017) |
| | Three-spined stickleback (<i>Gasterosteus aculeatus</i>) | Not reported | (Metzger and Schulte, 2017) |
| Salinity stress | Rice (<i>Oryza sativa</i>) | Tolerance to salinity stress* | (Feng et al., 2012) |
| | Thale cress (<i>Arabidopsis thaliana</i>) | Tolerance to salinity stress* | (Boyko et al., 2010a) |
| | Water flea (<i>Daphnia magna</i>) | Altered expression of genes involved in the cellular stress response** | (Jeremias et al., 2018) |
| | Three-spined stickleback (<i>Gasterosteus aculeatus</i>) | Not reported | (Heckwolf et al., 2020) |
| Upwelling | Purple sea urchin (<i>Strongylocentrotus purpuratus</i>) | Increased body size* | (Strader et al., 2019; Wong et al., 2019) |
| Drought stress | Rice (<i>Oryza sativa</i>) | Altered gene expression** | (Zheng et al., 2013) |
| Pesticides | Rat (<i>Rattus norvegicus</i>) | Risk of obesity** | (Skinner et al., 2013) |
| | | Reduced male fertility** | (Anway et al., 2005) |
| | | Adult-onset disease** | (Anway et al., 2006) (Manikkam et al., 2014) |
| Ionizing radiation | Zebrafish (<i>Danio rerio</i>) | Developmental defects** | (Kamstra et al., 2018) |
| Toxin exposure | Water flea (<i>Daphnia magna</i>) | Altered gene expression* | (Vandegehuchte et al., 2010) |

*Effect observed in next generation

**Effect observed through multiple generations

Table 4.4

Table 4.4. Examples of stress-induced change in genome structure.

| Stress | Change in Genome Structure | Species | Associated Phenotype | Reference |
|-------------------------------|----------------------------|--|---|-----------------------------|
| Altered climate | Chromosome inversion | Mosquito (<i>Anopheles gambiae</i>) | Increased thermotolerance in larvae | (Rocca et al., 2009) |
| | | Fruit fly (<i>Drosophila subobscura</i>) | Altered optimal temperature | (Rego et al., 2010) |
| | Chromosome reshuffling | Buckler mustard (<i>Biscutella laevigata</i>) | Heightened tolerance to abiotic stresses | (Geiser et al., 2016) |
| | | Yellow arctic whitlow grass (<i>Draba nivalis</i>) | Increased tolerance to cold, drought, and oxidative stresses | (Nowak et al., 2021) |
| Altered nutrient availability | Copy number variant | Human (<i>Homo sapiens</i>) | Increased abundance of salivary amylase protein | (Perry et al., 2007) |
| | | Baker's yeast (<i>Saccharomyces cerevisiae</i>) | Increased efficiency of glucose metabolism | (Brown et al., 1998) |
| Hyposaline stress | Chromosome inversion | Atlantic cod (<i>Gadus morhua</i>) | Reduced recombination in genes necessary to tolerate low salinity | (Barth et al., 2017) |
| Pathogens | Copy number variant | Soybean (<i>Glycine max</i>) | Pathogen resistance | (Cook et al., 2012) |
| Toxin exposure | Chromosome inversion | Mosquito (<i>Anopheles atroparvus</i>) | DDT resistance | (D'Alessandro et al., 1957) |
| | Copy number variant | Barley (<i>Hordeum vulgare</i>) | Boron-toxicity tolerance | (Sutton et al., 2007) |
| | | Palmer amaranth (<i>Amaranthus palmeri</i>) | Herbicide resistance | (Gaines et al., 2010) |

Table 4.5

Table 4.5. Examples of stress-induced change in transposable elements.

| Stress | Species | Change in Transposable Elements | Associated Phenotype (if reported) | Reference |
|------------------|---|--|---|---|
| Heat stress | Thale cress (<i>Arabidopsis thaliana</i>) | Activation of <i>ONSEN</i> retrotransposon | Not reported | (Cavrak et al., 2014) |
| | Fruit fly (<i>Drosophila melanogaster</i>) | <i>P element</i> transposition disrupting heat shock protein gene <i>hsp70Ba</i> | Altered thermotolerance | (Lerman et al., 2003) |
| | Rice blast fungus (<i>Magnaporthe oryzae</i>) | Activation of <i>Pyret</i> , <i>MAGGY</i> , <i>Pot2</i> , <i>MINE</i> , <i>Mg-SINE</i> , <i>Grasshopper</i> , and <i>MGLR3</i> | Genomic instability | (Chadha and Sharma, 2014) |
| | Nematode worms (<i>Caenorhabditis elegans</i> and <i>Caenorhabditis briggsae</i>) | Activation of <i>CemaT1</i> and <i>Tc1</i> | Genomic instability | (Ryan et al., 2016) |
| | Mouse (<i>Mus musculus</i>) | Activation of <i>MERV-L</i> and <i>IAPEz</i> | Altered gene expression | (Hummel et al., 2017) |
| Cold stress | Asian tiger mosquito (<i>Aedes albopictus</i>) | Altered insertion frequency of <i>Lian1</i> , <i>RTE4</i> , <i>RTE5</i> , <i>L2B</i> , and <i>IL1</i> | Localization of TEs to genes potentially involved in overwintering | (Goubert et al., 2017) |
| | Rice (<i>Oryza sativa</i>) | Activation of <i>mPing</i> | Altered gene expression | (Naito et al., 2009) |
| | Common snapdragon (<i>Antirrhinum majus</i>) | Activation of <i>Tam3</i> | Not reported | (Hashida et al., 2003) |
| UV irradiation | Human (<i>Homo sapiens</i>) | Activation of <i>L1</i> | Malignant transformation of keratinocytes | (Banerjee et al., 2005) |
| Pollution | Amazon cichlid (<i>Cichlasoma amazonarum</i>) | Differential insertion patterns of <i>Rex 1</i> , <i>Rex 3</i> , and <i>Rex 6</i> | Not reported | (da Silva et al., 2020) |
| Oxidative stress | Mouse (<i>Mus musculus</i>) | Activation of <i>L1</i> | Not reported | (Van Meter et al., 2014) |
| | Nematode worms (<i>Caenorhabditis elegans</i> and <i>Caenorhabditis briggsae</i>) | Activation of <i>CemaT1</i> and <i>Tc1</i> | Genomic instability | (Ryan et al., 2016) |
| Pesticides | Fruit fly (<i>Drosophila melanogaster</i>) | Activation of <i>Accord</i> retrotransposon | Insecticide resistance via overexpression of insecticide detoxifying gene | (Chung et al., 2007) |
| | Common house mosquito (<i>Culex pipiens</i>) | Insertion of TE-like DNA into coding region of <i>cmp1</i> | Insecticide resistance via alternative splicing of toxin receptor | (Darboux et al., 2007) |
| Salinity stress | Rice (<i>Oryza sativa</i>) | Activation of <i>mPing</i> | Higher salinity stress tolerance via overexpression of ZFP252 | (Naito et al., 2009; Yasuda et al., 2013) |

BIBLIOGRAPHY

- Abbatiello, S., Ackermann, B. L., Borchers, C., Bradshaw, R. A., Carr, S. A., Chalkley, R., Choi, M., Deutsch, E., Domon, B., Hoofnagle, A. N., et al. (2017). New guidelines for publication of manuscripts describing development and application of targeted mass spectrometry measurements of peptides and proteins. *Mol Cell Proteomics* 16, 327–328.
- Abe, Y., Fujiwara, Y., Takahashi, H., Matsumura, Y., Sawada, T., Jiang, S., Nakaki, R., Uchida, A., Nagao, N., Naito, M., et al. (2018). Histone demethylase JMJD1A coordinates acute and chronic adaptation to cold stress via thermogenic phospho-switch. *Nat. Commun.* 9, 1566.
- Alabert, C. and Groth, A. (2012). Chromatin replication and epigenome maintenance. *Nat. Rev. Mol. Cell Biol.* 13, 153–167.
- Alabert, C., Barth, T. K., Reverón-Gómez, N., Sidoli, S., Schmidt, A., Jensen, O. N., Imhof, A. and Groth, A. (2015). Two distinct modes for propagation of histone PTMs across the cell cycle. *Genes Dev.* 29, 585–590.
- Angers, B., Castonguay, E. and Massicotte, R. (2010). Environmentally induced phenotypes and DNA methylation: how to deal with unpredictable conditions until the next generation and after. *Mol. Ecol.* 19, 1283–1295.
- Aniagu, S. O., Day, N., Chipman, J. K., Taylor, E. W., Butler, P. J. and Winter, M. J. (2006). Does exhaustive exercise result in oxidative stress and associated DNA damage in the Chub (*Leuciscus cephalus*)? *Environ. Mol. Mutagen.* 47, 616–623.
- Anway, M. D., Cupp, A. S., Uzumcu, M. and Skinner, M. K. (2005). Epigenetic Transgenerational Actions of Endocrine Disruptors and Male Fertility. *Science* 308, 1466–1469.
- Anway, M. D., Leathers, C. and Skinner, M. K. (2006). Endocrine Disruptor Vinclozolin Induced Epigenetic Transgenerational Adult-Onset Disease. *Endocrinology* 147, 5515–5523.
- Artemov, A. V., Mague, N. S., Rastorguev, S. M., Zhenilo, S., Mazur, A. M., Tsygankova, S. V., Boulygina, E. S., Kaplun, D., Nedoluzhko, A. V., Medvedeva, Y. A., et al. (2017). Genome-Wide DNA Methylation Profiling Reveals Epigenetic Adaptation of Stickleback to Marine and Freshwater Conditions. *Mol. Biol. Evol.* 34, 2203–2213.
- Atlasi, Y. and Stunnenberg, H. G. (2017). The interplay of epigenetic marks during stem cell differentiation and development. *Nat. Rev. Genet.* 18, 643–658.
- Audia, J. E. and Campbell, R. M. (2016). Histone Modifications and Cancer. *Cold Spring Harb. Perspect. Biol.* 8, a019521.
- Bagdonas, E. and Zukas, K. (2004). Repair of UVC induced DNA lesions in erythrocytes from *Carassius auratus gibelio*. *Sveik. Moksl.* 22–24.

- Banerjee, G., Gupta, N., Tiwari, J. and Raman, G. (2005). Ultraviolet-induced transformation of keratinocytes: possible involvement of long interspersed element-1 reverse transcriptase. *Photodermatol. Photoimmunol. Photomed.* 21, 32–39.
- Bao, J. and Bedford, M. T. (2016). Epigenetic regulation of the histone-to-protamine transition during spermiogenesis. *Reprod. Camb. Engl.* 151, R55–R70.
- Bao, J. and Yan, W. (2012). Male Germline Control of Transposable Elements. *Biol. Reprod.* 86,.
- Barth, J. M. I., Berg, P. R., Jonsson, P. R., Bonanomi, S., Corell, H., Hemmer-Hansen, J., Jakobsen, K. S., Johannesson, K., Jorde, P. E., Knutsen, H., et al. (2017). Genome architecture enables local adaptation of Atlantic cod despite high connectivity. *Mol. Ecol.* 26, 4452–4466.
- Barzilai, A. and Yamamoto, K.-I. (2004). DNA damage responses to oxidative stress. *DNA Repair* 3, 1109–1115.
- Belova, G. I., Postnikov, Y. V., Furusawa, T., Birger, Y. and Bustin, M. (2008). Chromosomal Protein HMGN1 Enhances the Heat Shock-induced Remodeling of Hsp70 Chromatin *. *J. Biol. Chem.* 283, 8080–8088.
- Benjamini, Y. and Hochberg, Y. (1995). Controlling the False Discovery Rate: A Practical and Powerful Approach to Multiple Testing. *J. R. Stat. Soc. Ser. B Methodol.* 57, 289–300.
- Bianconi, E., Piovesan, A., Facchin, F., Beraudi, A., Casadei, R., Frabetti, F., Vitale, L., Pelleri, M. C., Tassani, S., Piva, F., et al. (2013). An estimation of the number of cells in the human body. *Ann. Hum. Biol.* 40, 463–471.
- Biémont, C. and Vieira, C. (2006). Junk DNA as an evolutionary force. *Nature* 443, 521–524.
- Bilichak, A., Illynskyy, Y., Hollunder, J. and Kovalchuk, I. (2012). The Progeny of Arabidopsis thaliana Plants Exposed to Salt Exhibit Changes in DNA Methylation, Histone Modifications and Gene Expression. *PLOS ONE* 7, e30515.
- Bird, A. P. (1980). DNA methylation and the frequency of CpG in animal DNA. *Nucleic Acids Res.* 8, 1499–1504.
- Bird, A. (2002). DNA methylation patterns and epigenetic memory. *Genes Dev.* 16, 6–21.
- Bjedov, I., Tenaillon, O., Gérard, B., Souza, V., Denamur, E., Radman, M., Taddei, F. and Matic, I. (2003). Stress-Induced Mutagenesis in Bacteria. *Science* 300, 1404–1409.
- Bošković, A. and Rando, O. J. (2018). Transgenerational Epigenetic Inheritance. *Annu. Rev. Genet.* 52, 21–41.
- Bostick, M., Kim, J. K., Estève, P.-O., Clark, A., Pradhan, S. and Jacobsen, S. E. (2007). UHRF1 Plays a Role in Maintaining DNA Methylation in Mammalian Cells. *Science* 317, 1760–1764.

- Boyko, A., Blevins, T., Yao, Y., Golubov, A., Bilichak, A., Ilnytsky, Y., Hollander, J., Jr, F. M. and Kovalchuk, I. (2010a). Transgenerational Adaptation of Arabidopsis to Stress Requires DNA Methylation and the Function of Dicer-Like Proteins. *PLOS ONE* 5, e9514.
- Boyko, A., Golubov, A., Bilichak, A. and Kovalchuk, I. (2010b). Chlorine Ions but not Sodium Ions Alter Genome Stability of Arabidopsis thaliana. *Plant Cell Physiol.* 51, 1066–1078.
- Brown, C. J., Todd, K. M. and Rosenzweig, R. F. (1998). Multiple duplications of yeast hexose transport genes in response to selection in a glucose-limited environment. *Mol. Biol. Evol.* 15, 931–942.
- Burdge, G. C. and Lillycrop, K. A. (2010). Nutrition, Epigenetics, and Developmental Plasticity: Implications for Understanding Human Disease. *Annu. Rev. Nutr.* 30, 315–339.
- Burggren, W. W. (2014a). Epigenetics as a source of variation in comparative animal physiology - or - Lamarck is lookin' pretty good these days. *J. Exp. Biol.* 217, 682–689.
- Burggren, W. W. (2014b). Epigenetics as a source of variation in comparative animal physiology – or – Lamarck is lookin' pretty good these days. *J. Exp. Biol.* 217, 682–689.
- Burggren, W. (2016). Epigenetic Inheritance and Its Role in Evolutionary Biology: Re-Evaluation and New Perspectives. *Biology* 5, 24.
- Call, E., Jones, R., DeMonja, K., Burton, J. N., Jellum, S., Bernkopf, A. and Oberg, C. (2017). “The elastic limit”: Introducing a novel concept in communicating excessive shear and tissue deformation. *World Counc. Enteros. Ther. J.* 37, 16–20.
- Campbell, C. R., Poelstra, J. W. and Yoder, A. D. (2018). What is Speciation Genomics? The roles of ecology, gene flow, and genomic architecture in the formation of species. *Biol. J. Linn. Soc.* 124, 561–583.
- Camussi, G., Deregibus, M.-C., Bruno, S., Grange, C., Fonsato, V. and Tetta, C. (2010). Exosome/microvesicle-mediated epigenetic reprogramming of cells. *Am. J. Cancer Res.* 1, 98–110.
- Cantone, L., Nordio, F., Hou, L., Apostoli, P., Bonzini, M., Tarantini, L., Angelici, L., Bollati, V., Zanobetti, A., Schwartz, J., et al. (2011). Inhalable metal-rich air particles and histone H3K4 dimethylation and H3K9 acetylation in a cross-sectional study of steel workers. *Environ. Health Perspect.* 119, 964–969.
- Capuano, F., Mülleder, M., Kok, R., Blom, H. J. and Ralser, M. (2014). Cytosine DNA Methylation Is Found in Drosophila melanogaster but Absent in Saccharomyces cerevisiae, Schizosaccharomyces pombe, and Other Yeast Species. *Anal. Chem.* 86, 3697–3702.
- Carrer, A., Parris, J. L. D., Trefely, S., Henry, R. A., Montgomery, D. C., Torres, A., Viola, J. M., Kuo, Y.-M., Blair, I. A., Meier, J. L., et al. (2017). Impact of a High-fat Diet on Tissue Acyl-CoA and Histone Acetylation Levels *. *J. Biol. Chem.* 292, 3312–3322.

- Cathcart, R., Schwiers, E., Saul, R. L. and Ames, B. N. (1984). Thymine glycol and thymidine glycol in human and rat urine: a possible assay for oxidative DNA damage. *Proc. Natl. Acad. Sci.* 81, 5633–5637.
- Cavrak, V. V., Lettner, N., Jamge, S., Kosarewicz, A., Bayer, L. M. and Scheid, O. M. (2014). How a Retrotransposon Exploits the Plant's Heat Stress Response for Its Activation. *PLOS Genet.* 10, e1004115.
- Chadha, S. and Sharma, M. (2014). Transposable Elements as Stress Adaptive Capacitors Induce Genomic Instability in Fungal Pathogen *Magnaporthe oryzae*. *PLOS ONE* 9, e94415.
- Chakarov, S., Petkova, R., Russev, G. C. and Zhelev, N. (2014). DNA damage and mutation. Types of DNA damage. *BioDiscovery* 11, e8957.
- Champagne, F. A. (2013). Epigenetics and developmental plasticity across species. *Dev. Psychobiol.* 55, 33–41.
- Champroux, A., Cocquet, J., Henry-Berger, J., Drevet, J. R. and Kocer, A. (2018). A Decade of Exploring the Mammalian Sperm Epigenome: Paternal Epigenetic and Transgenerational Inheritance. *Front. Cell Dev. Biol.* 6, 50.
- Chang, H. H. Y., Pannunzio, N. R., Adachi, N. and Lieber, M. R. (2017). Non-homologous DNA end joining and alternative pathways to double-strand break repair. *Nat. Rev. Mol. Cell Biol.* 18, 495–506.
- Chappell, K., Graw, S., Washam, C. L., Storey, A. J., Bolden, C., Peterson, E. C. and Byrum, S. D. (2021). PTMViz: a tool for analyzing and visualizing histone post translational modification data. *BMC Bioinformatics* 22, 275.
- Chatterjee, N. and Walker, G. C. (2017). Mechanisms of DNA damage, repair, and mutagenesis. *Environ. Mol. Mutagen.* 58, 235–263.
- Chen, J. J., Mitchell, D. L. and Britt, A. B. (1994). A Light-Dependent Pathway for the Elimination of UV-Induced Pyrimidine (6-4) Pyrimidinone Photoproducts in *Arabidopsis*. *Plant Cell* 6, 1311–1317.
- Chen, L.-T., Luo, M., Wang, Y.-Y. and Wu, K. (2010). Involvement of *Arabidopsis* histone deacetylase HDA6 in ABA and salt stress response. *J. Exp. Bot.* 61, 3345–3353.
- Chénais, B., Caruso, A., Hiard, S. and Casse, N. (2012). The impact of transposable elements on eukaryotic genomes: From genome size increase to genetic adaptation to stressful environments. *Gene* 509, 7–15.
- Cheng, C.-H., Guo, Z.-X., Luo, S.-W. and Wang, A.-L. (2018). Effects of high temperature on biochemical parameters, oxidative stress, DNA damage and apoptosis of pufferfish (*Takifugu obscurus*). *Ecotoxicol. Environ. Saf.* 150, 190–198.
- Cheng, L., Trenberth, K. E., Gruber, N., Abraham, J. P., Fasullo, J. T., Li, G., Mann, M. E., Zhao, X. and Zhu, J. (2020). Improved Estimates of Changes in Upper Ocean Salinity and the Hydrological Cycle. *J. Clim.* 33, 10357–10381.

- Choy, C. K. M., Benzie, I. F. F. and Cho, P. (2005). UV-Mediated DNA Strand Breaks in Corneal Epithelial Cells Assessed Using the Comet Assay Procedure. *Photochem. Photobiol.* 81, 493–497.
- Christensen, M. E., Rattner, J. B. and Dixon, G. H. (1984). Hyperacetylation of histone H4 promotes chromatin decondensation prior to histone replacement by protamines during spermatogenesis in rainbow trout. *Nucleic Acids Res.* 12, 4575–4592.
- Chung, H., Bogwitz, M. R., McCart, C., Andrianopoulos, A., French-Constant, R. H., Batterham, P. and Daborn, P. J. (2007). Cis-Regulatory Elements in the Accord Retrotransposon Result in Tissue-Specific Expression of the *Drosophila melanogaster* Insecticide Resistance Gene Cyp6g1. *Genetics* 175, 1071–1077.
- Clingen, P. H., Arlett, C. F., Roza, L., Mori, T., Nikaido, O. and Green, M. H. L. (1995). Induction of Cyclobutane Pyrimidine Dimers, Pyrimidine(6-4)pyrimidone Photoproducts, and Dewar Valence Isomers by Natural Sunlight in Normal Human Mononuclear Cells. *Cancer Res.* 55, 2245–2248.
- Condamine, F. L., Rolland, J. and Morlon, H. (2013). Macroevolutionary perspectives to environmental change. *Ecol. Lett.* 16, 72–85.
- Cook, D. E., Lee, T. G., Guo, X., Melito, S., Wang, K., Bayless, A. M., Wang, J., Hughes, T. J., Willis, D. K., Clemente, T. E., et al. (2012). Copy Number Variation of Multiple Genes at Rhg1 Mediates Nematode Resistance in Soybean. *Science* 338, 1206–1209.
- Cossetti, C., Lugini, L., Astrologo, L., Saggio, I., Fais, S. and Spadafora, C. (2014). Soma-to-Germline Transmission of RNA in Mice Xenografted with Human Tumour Cells: Possible Transport by Exosomes. *PLOS ONE* 9, e101629.
- Covington, H. E., Maze, I., LaPlant, Q. C., Vialou, V. F., Ohnishi, Y. N., Berton, O., Fass, D. M., Renthal, W., Rush, A. J., Wu, E. Y., et al. (2009). Antidepressant Actions of Histone Deacetylase Inhibitors. *J. Neurosci.* 29, 11451–11460.
- Creyghton, M. P., Cheng, A. W., Welstead, G. G., Kooistra, T., Carey, B. W., Steine, E. J., Hanna, J., Lodato, M. A., Frampton, G. M., Sharp, P. A., et al. (2010). Histone H3K27ac separates active from poised enhancers and predicts developmental state. *Proc. Natl. Acad. Sci.* 107, 21931–21936.
- Cruz Vieira, A. B., Weber, A. A., Ribeiro, Y. M., Luz, R. K., Bazzoli, N. and Rizzo, E. (2019). Influence of salinity on spermatogenesis in adult Nile tilapia (*Oreochromis niloticus*) testis. *Theriogenology* 131, 1–8.
- da Silva, F. A., Guimarães, E. M. C., Carvalho, N. D. M., Ferreira, A. M. V., Schneider, C. H., Carvalho-Zilse, G. A., Feldberg, E. and Gross, M. C. (2020). Transposable DNA Elements in Amazonian Fish: From Genome Enlargement to Genetic Adaptation to Stressful Environments. *Cytogenet. Genome Res.* 160, 148–155.
- Daled, S., Willems, S., Van Puyvelde, B., Corveleyn, L., Verhelst, S., De Clerck, L., Deforce, D. and Dhaenens, M. (2021). Histone Sample Preparation for Bottom-Up Mass Spectrometry: A Roadmap to Informed Decisions. *Proteomes* 9, 17.

- D'Alessandro, G., Frizzi, G. and Mariani, M. (1957). Effect of DDT selection pressure on the frequency of chromosomal structures in *Anopheles atroparvus*. *Bull. World Health Organ.* 16, 859–864.
- Darboux, I., Charles, J.-F., Pauchet, Y., Warot, S. and Pauron, D. (2007). Transposon-mediated resistance to *Bacillus sphaericus* in a field-evolved population of *Culex pipiens* (Diptera: Culicidae). *Cell. Microbiol.* 9, 2022–2029.
- de Lima, L. P., Poubel, S. B., Yuan, Z.-F., Rosón, J. N., Vitorino, F. N. de L., Holetz, F. B., Garcia, B. A. and da Cunha, J. P. C. (2020). Improvements on the quantitative analysis of *Trypanosoma cruzi* histone post translational modifications: Study of changes in epigenetic marks through the parasite's metacyclogenesis and life cycle. *J. Proteomics* 225, 103847.
- Di Cerbo, V., Mohn, F., Ryan, D. P., Montellier, E., Kacem, S., Tropberger, P., Kallis, E., Holzner, M., Hoerner, L., Feldmann, A., et al. (2014). Acetylation of histone H3 at lysine 64 regulates nucleosome dynamics and facilitates transcription. *eLife* 3, e01632.
- Diaz, M. and Flajnik, M. E. (1998). Evolution of somatic hypermutation and gene conversion in adaptive immunity. *Immunol. Rev.* 162, 13–24.
- Diaz-Mendez, I., Alhama, J., Pueyo, C. and Lopez-Barea, J. (1997). Fish 8-oxo-dG levels as biomarker of oxidative damages by environmental pollutants. *Mutat. Res. Fundam. Mol. Mech. Mutagen.* 379, S168.
- DiFiore, J. V., Ptacek, T. S., Wang, Y., Li, B., Simon, J. M. and Strahl, B. D. (2020). Unique and Shared Roles for Histone H3K36 Methylation States in Transcription Regulation Functions. *Cell Rep.* 31, 107751.
- Doyle, L. M. and Wang, M. Z. (2019). Overview of Extracellular Vesicles, Their Origin, Composition, Purpose, and Methods for Exosome Isolation and Analysis. *Cells* 8, 727.
- Drake, J., Petroze, R., Castegna, A., Ding, Q., Keller, J. N., Markesbery, W. R., Lovell, M. A. and Butterfield, D. A. (2004). 4-Hydroxynonenal oxidatively modifies histones: implications for Alzheimer's disease. *Neurosci. Lett.* 356, 155–158.
- Du, P., Zhang, X., Huang, C.-C., Jafari, N., Kibbe, W. A., Hou, L. and Lin, S. M. (2010). Comparison of Beta-value and M-value methods for quantifying methylation levels by microarray analysis. *BMC Bioinformatics* 11, 587.
- Duncan, B. K. and Miller, J. H. (1980). Mutagenic deamination of cytosine residues in DNA. *Nature* 287, 560–561.
- Eirin-Lopez, J. M. and Putnam, H. M. (2019a). Marine Environmental Epigenetics. *Annu. Rev. Mar. Sci.* 11, 335–368.
- Eirin-Lopez, J. M. and Putnam, H. M. (2019b). Marine Environmental Epigenetics. *Annu. Rev. Mar. Sci.* 11, 335–368.
- Engmann, O. and Mansuy, I. M. (2020). Chapter 18 - Stress and its effects across generations. In *Stress Resilience* (ed. Chen, A.), pp. 269–290. Academic Press.

- Fan, J., Krautkramer, K. A., Feldman, J. L. and Denu, J. M. (2015a). Metabolic Regulation of Histone Post-Translational Modifications. *ACS Chem. Biol.* 10, 95–108.
- Fan, J., Krautkramer, K. A., Feldman, J. L. and Denu, J. M. (2015b). Metabolic Regulation of Histone Post-Translational Modifications. *ACS Chem. Biol.* 10, 95–108.
- Febry, R. and Lutz, P. (1987). Energy Partitioning in Fish: The Activity-related Cost of Osmoregulation in a Euryhaline Cichlid. *J. Exp. Biol.* 128, 63–85.
- Feng, Q., Yang, C., Lin, X., Wang, J., Ou, X., Zhang, C., Chen, Y. and Liu, B. (2012). Salt and alkaline stress induced transgenerational alteration in DNA methylation of rice ('*Oryza sativa*'). *Aust. J. Crop Sci.* 6, 877–883.
- Ferguson-Smith, M. A. and Trifonov, V. (2007). Mammalian karyotype evolution. *Nat. Rev. Genet.* 8, 950–962.
- Ferrari, K. J., Scelfo, A., Jammula, S., Cuomo, A., Barozzi, I., Stützer, A., Fischle, W., Bonaldi, T. and Pasini, D. (2014). Polycomb-Dependent H3K27me1 and H3K27me2 Regulate Active Transcription and Enhancer Fidelity. *Mol. Cell* 53, 49–62.
- Feulner, P. G. D. and De-Kayne, R. (2017). Genome evolution, structural rearrangements and speciation. *J. Evol. Biol.* 30, 1488–1490.
- Flores, K. B., Wolschin, F. and Amdam, G. V. (2013). The Role of Methylation of DNA in Environmental Adaptation. *Integr. Comp. Biol.* 53, 359–372.
- Foster, P. L. (2007). Stress-Induced Mutagenesis in Bacteria. *Crit. Rev. Biochem. Mol. Biol.* 42, 373–397.
- Fryxell, K. J. and Zuckerkandl, E. (2000). Cytosine Deamination Plays a Primary Role in the Evolution of Mammalian Isochores. *Mol. Biol. Evol.* 17, 1371–1383.
- Gaines, T. A., Zhang, W., Wang, D., Bukun, B., Chisholm, S. T., Shaner, D. L., Nissen, S. J., Patzoldt, W. L., Tranel, P. J., Culpepper, A. S., et al. (2010). Gene amplification confers glyphosate resistance in *Amaranthus palmeri*. *Proc. Natl. Acad. Sci.* 107, 1029–1034.
- Galhardo, R. S., Hastings, P. J. and Rosenberg, S. M. (2007). Mutation as a Stress Response and the Regulation of Evolvability. *Crit. Rev. Biochem. Mol. Biol.* 42, 399–435.
- Garcia, B. A., Thomas, C. E., Kelleher, N. L. and Mizzen, C. A. (2008). Tissue-Specific Expression and Post-Translational Modification of Histone H3 Variants. *J. Proteome Res.* 7, 4225–4236.
- García-Giménez, J.-L., Garcés, C., Romá-Mateo, C. and Pallardó, F. V. (2021). Oxidative stress-mediated alterations in histone post-translational modifications. *Free Radic. Biol. Med.* 170, 6–18.
- Gardell, A. M., Qin, Q., Rice, R. H., Li, J. and Kültz, D. (2014). Derivation and Osmotolerance Characterization of Three Immortalized Tilapia (*Oreochromis mossambicus*) Cell Lines. *PLOS ONE* 9, e95919.

- Garinis, G. A., Mitchell, J. R., Moorhouse, M. J., Hanada, K., de Waard, H., Vandeputte, D., Jans, J., Brand, K., Smid, M., van der Spek, P. J., et al. (2005). Transcriptome analysis reveals cyclobutane pyrimidine dimers as a major source of UV-induced DNA breaks. *EMBO J.* 24, 3952–3962.
- Geiser, C., Mandáková, T., Arrigo, N., Lysak, M. A. and Parisod, C. (2016). Repeated Whole-Genome Duplication, Karyotype Reshuffling, and Biased Retention of Stress-Responding Genes in Buckler Mustard. *Plant Cell* 28, 17–27.
- Gerlach, V. L., Aravind, L., Gotway, G., Schultz, R. A., Koonin, E. V. and Friedberg, E. C. (1999). Human and mouse homologs of Escherichia coli DinB (DNA polymerase IV), members of the UmuC/DinB superfamily. *Proc. Natl. Acad. Sci. U. S. A.* 96, 11922–11927.
- Gluckman, P. D., Hanson, M. A., Buklijas, T., Low, F. M. and Beedle, A. S. (2009). Epigenetic mechanisms that underpin metabolic and cardiovascular diseases. *Nat. Rev. Endocrinol.* 5, 401–408.
- Godfrey, K. M., Costello, P. M. and Lillycrop, K. A. (2016). Development, Epigenetics and Metabolic Programming. *Prev. Asp. Early Nutr.* 85, 71–80.
- Goubert, C., Henri, H., Minard, G., Moro, C. V., Mavingui, P., Vieira, C. and Boulesteix, M. (2017). High-throughput sequencing of transposable element insertions suggests adaptive evolution of the invasive Asian tiger mosquito towards temperate environments. *Mol. Ecol.* 26, 3968–3981.
- Gould, S. J. (1982). The meaning of punctuated equilibrium and its role in validating a hierarchical approach to macroevolution. In *Perspectives in Evolution* (ed. Milkman, R.), pp. 83–104. Sunderland, MA: Sinauer Associates Inc.
- Govaert, E., Van Steendam, K., Scheerlinck, E., Vossaert, L., Meert, P., Stella, M., Willems, S., De Clerck, L., Dhaenens, M. and Deforce, D. (2016). Extracting histones for the specific purpose of label-free MS. *Proteomics* 16, 2937–2944.
- Greenberg, M. V. C. and Bourc'his, D. (2019). The diverse roles of DNA methylation in mammalian development and disease. *Nat. Rev. Mol. Cell Biol.* 20, 590–607.
- Grollman, A. P. and Moriya, M. (1993). Mutagenesis by 8-oxoguanine: an enemy within. *Trends Genet.* 9, 246–249.
- Groner, A. C., Cato, L., de Tribolet-Hardy, J., Bernasocchi, T., Janouskova, H., Melchers, D., Houtman, R., Cato, A. C. B., Tschopp, P., Gu, L., et al. (2016). TRIM24 Is an Oncogenic Transcriptional Activator in Prostate Cancer. *Cancer Cell* 29, 846–858.
- Gruenbaum, Y., Cedar, H. and Razin, A. (1982). Substrate and sequence specificity of a eukaryotic DNA methylase. *Nature* 295, 620–622.
- Hanson, M. A. and Skinner, M. K. (2016). Developmental origins of epigenetic transgenerational inheritance. *Environ. Epigenetics* 2, dvw002.
- Harrison, J. S., Cornett, E. M., Goldfarb, D., DaRosa, P. A., Li, Z. M., Yan, F., Dickson, B. M., Guo, A. H., Cantu, D. V., Kaustov, L., et al. Hemi-methylated DNA regulates DNA methylation inheritance through allosteric activation of H3 ubiquitylation by UHRF1. *eLife* 5, e17101.

- Hashida, S., Kitamura, K., Mikami, T. and Kishima, Y. (2003). Temperature Shift Coordinately Changes the Activity and the Methylation State of Transposon Tam3 in *Antirrhinum majus*. *Plant Physiol.* 132, 1207–1216.
- He, Y., Gorkin, D. U., Dickel, D. E., Nery, J. R., Castanon, R. G., Lee, A. Y., Shen, Y., Visel, A., Pennacchio, L. A., Ren, B., et al. (2017). Improved regulatory element prediction based on tissue-specific local epigenomic signatures. *Proc. Natl. Acad. Sci.* 114, E1633–E1640.
- Heckwolf, M. J., Meyer, B. S., Häsler, R., Höppner, M. P., Eizaguirre, C. and Reusch, T. B. H. (2020). Two different epigenetic information channels in wild three-spined sticklebacks are involved in salinity adaptation. *Sci. Adv.* 6, eaaz1138.
- Heintzman, N. D., Hon, G. C., Hawkins, R. D., Kheradpour, P., Stark, A., Harp, L. F., Ye, Z., Lee, L. K., Stuart, R. K., Ching, C. W., et al. (2009). Histone modifications at human enhancers reflect global cell-type-specific gene expression. *Nature* 459, 108–112.
- Heng, H. H. Q. (2009). The genome-centric concept: resynthesis of evolutionary theory. *BioEssays* 31, 512–525.
- Heng, J. and Heng, H. H. (2020). Genome chaos: Creating new genomic information essential for cancer macroevolution. *Semin. Cancer Biol.*
- Ho, D. H. and Burggren, W. W. (2010). Epigenetics and transgenerational transfer: a physiological perspective. *J. Exp. Biol.* 213, 3–16.
- Hoegh-Guldberg, O., Mumby, P. J., Hooten, A. J., Steneck, R. S., Greenfield, P., Gomez, E., Harvell, C. D., Sale, P. F., Edwards, A. J., Caldeira, K., et al. (2007). Coral Reefs Under Rapid Climate Change and Ocean Acidification. *Science* 318, 1737–1742.
- Holliday, R. and Grigg, G. W. (1993). DNA methylation and mutation. *Mutat. Res. Mol. Mech. Mutagen.* 285, 61–67.
- Höllmüller, E., Geigges, S., Niedermeier, M. L., Kammer, K.-M., Kienle, S. M., Rösner, D., Scheffner, M., Marx, A. and Stengel, F. (2021). Site-specific ubiquitylation acts as a regulator of linker histone H1. *Nat. Commun.* 12, 3497.
- Holt, W. V. and Comizzoli, P. (2022). Conservation Biology and Reproduction in a Time of Developmental Plasticity. *Biomolecules* 12, 1297.
- Honda, S., Hjelmeland, L. M. and Handa, J. T. (2001). Oxidative Stress–Induced Single-Strand Breaks in Chromosomal Telomeres of Human Retinal Pigment Epithelial Cells In Vitro. *Invest. Ophthalmol. Vis. Sci.* 42, 2139–2144.
- Horne, S. D., Chowdhury, S. K. and Heng, H. H. (2014). Stress, genomic adaptation, and the evolutionary trade-off. *Front Genet* 5, 92.
- Horváth, V., Merenciano, M. and González, J. (2017). Revisiting the Relationship between Transposable Elements and the Eukaryotic Stress Response. *Trends Genet.* 33, 832–841.

- Hottiger, M. O. (2011). ADP-ribosylation of histones by ARTD1: An additional module of the histone code? *FEBS Lett.* 585, 1595–1599.
- Hsu, K.-F., Wilkins, S. E., Hopkinson, R. J., Sekirnik, R., Flashman, E., Kawamura, A., McCullagh, J. S. O., Walport, L. J. and Schofield, C. J. (2021). Hypoxia and hypoxia mimetics differentially modulate histone post-translational modifications. *Epigenetics* 16, 14–27.
- Hu, J., Wuitchik, S. J. S., Barry, T. N., Jamniczky, H. A., Rogers, S. M. and Barrett, R. D. H. (2021). Heritability of DNA methylation in threespine stickleback (*Gasterosteus aculeatus*). *Genetics* 217, iyab001.
- Hummel, B., Hansen, E. C., Yoveva, A., Aprile-Garcia, F., Hussong, R. and Sawarkar, R. (2017). The evolutionary capacitor HSP90 buffers the regulatory effects of mammalian endogenous retroviruses. *Nat. Struct. Mol. Biol.* 24, 234–242.
- Hwang, P. P., Sun, C. M. and Wu, S. M. (1989). Changes of plasma osmolality, chloride concentration and gill Na-K-ATPase activity in tilapia *Oreochromis mossambicus* during seawater acclimation. *Mar. Biol.* 100, 295–299.
- Hwang, P., Lee, T., Weng, C., Fang, M. and Cho, G. (1999). Presence of Na-K-ATPase in Mitochondria-Rich Cells in the Yolk-Sac Epithelium of Larvae of the Teleost *Oreochromis mossambicus*. *Physiol. Biochem. Zool.* 72, 138–144.
- Ikeuchi, M., Iwase, A. and Sugimoto, K. (2015). Control of plant cell differentiation by histone modification and DNA methylation. *Curr. Opin. Plant Biol.* 28, 60–67.
- Isogawa, A., Fuchs, R. P. and Fujii, S. (2020). Chromatin Pull-Down Methodology Based on DNA Triple Helix Formation. *Methods Mol. Biol. Clifton NJ* 2119, 183–199.
- Jablonka, E. (2004). Epigenetic epidemiology. *Int. J. Epidemiol.* 33, 929–935.
- Jablonka, E. and Lamb, M. J. (2020). Inheritance Systems and the Extended Evolutionary Synthesis. *Elem. Philos. Biol.*
- Jamieson, K., Rountree, M. R., Lewis, Z. A., Stajich, J. E. and Selker, E. U. (2013). Regional control of histone H3 lysine 27 methylation in *Neurospora*. *Proc. Natl. Acad. Sci.* 110, 6027–6032.
- Janssen, K. A., Coradin, M., Lu, C., Sidoli, S. and Garcia, B. A. (2019). Quantitation of Single and Combinatorial Histone Modifications by Integrated Chromatography of Bottom-up Peptides and Middle-down Polypeptide Tails. *J. Am. Soc. Mass Spectrom.* 30, 2449–2459.
- Jeremias, G., Barbosa, J., Marques, S. M., De Schamphelaere, K. A. C., Van Nieuwerburgh, F., Deforce, D., Goncalves, F. J. M., Pereira, J. L. and Asselman, J. (2018). Transgenerational Inheritance of DNA Hypomethylation in *Daphnia magna* in Response to Salinity Stress. *Environ. Sci. Technol.* 52, 10114–10123.
- Jones, P. A. (2012). Functions of DNA methylation: islands, start sites, gene bodies and beyond. *Nat. Rev. Genet.* 13, 484–492.

- Kalli, A., Sweredoski, M. J. and Hess, S. (2013). Data-Dependent Middle-Down Nano-Liquid Chromatography–Electron Capture Dissociation–Tandem Mass Spectrometry: An Application for the Analysis of Unfractionated Histones. *Anal. Chem.* 85, 3501–3507.
- Kammerer, B. D., Sardella, B. A. and Kültz, D. (2009). Salinity stress results in rapid cell cycle changes of tilapia (*Oreochromis mossambicus*) gill epithelial cells. *J. Exp. Zool. Part Ecol. Genet. Physiol.* 311A, 80–90.
- Kamstra, J. H., Hurem, S., Martin, L. M., Lindeman, L. C., Legler, J., Oughton, D., Salbu, B., Brede, D. A., Lyche, J. L. and Aleström, P. (2018). Ionizing radiation induces transgenerational effects of DNA methylation in zebrafish. *Sci. Rep.* 8, 15373.
- Kantidze, O. L., Velichko, A. K., Luzhin, A. V. and Razin, S. V. (2016). Heat stress-induced DNA damage. *Acta Naturae Англоязычная Версия* 8, 75–78.
- Karen, C. and Rajan, K. E. (2019). Social Behaviour and Epigenetic Status in Adolescent and Adult Rats: The Contribution of Early-Life Stressful Social Experience. *Cell. Mol. Neurobiol.* 39, 371–385.
- Karger, D. N., Schmatz, D. R., Dettling, G. and Zimmermann, N. E. (2020). High-resolution monthly precipitation and temperature time series from 2006 to 2100. *Sci. Data* 7, 248.
- Kent, T. V., Uzunović, J. and Wright, S. I. (2017). Coevolution between transposable elements and recombination. *Philos. Trans. R. Soc. B Biol. Sci.* 372, 20160458.
- Khandelwal, S. (1990). Chromosome evolution in the genus *Ophioglossum* L. *Bot. J. Linn. Soc.* 102, 205–217.
- Kienel, U., Plessen, B., Schettler, G., Weise, S., Pinkerneil, S., Böhnelt, H., Englebrecht, A. and Haug, G. (2013). Sensitivity of a hypersaline crater lake to the seasonality of rainfall, evaporation, and guano supply. *Fundam. Appl. Limnol. Arch. Für Hydrobiol.* 183, 135–152.
- Kim, J.-M., To, T. K., Ishida, J., Morosawa, T., Kawashima, M., Matsui, A., Toyoda, T., Kimura, H., Shinozaki, K. and Seki, M. (2008). Alterations of Lysine Modifications on the Histone H3 N-Tail under Drought Stress Conditions in *Arabidopsis thaliana*. *Plant Cell Physiol.* 49, 1580–1588.
- Klein, B. J., Jang, S. M., Lachance, C., Mi, W., Lyu, J., Sakuraba, S., Krajewski, K., Wang, W. W., Sidoli, S., Liu, J., et al. (2019). Histone H3K23-specific acetylation by MORF is coupled to H3K14 acylation. *Nat. Commun.* 10, 4724.
- Klosin, A., Casas, E., Hidalgo-Carcedo, C., Vavouri, T. and Lehner, B. (2017). Transgenerational transmission of environmental information in *C. elegans*. *Science* 356, 320–323.
- Koltsova, A. S., Pendina, A. A., Efimova, O. A., Chiryayeva, O. G., Kuznetsova, T. V. and Baranov, V. S. (2019). On the Complexity of Mechanisms and Consequences of Chromothripsis: An Update. *Front. Genet.* 10, 393.
- Kong, A. T., Leprevost, F. V., Avtonomov, D. M., Mellacheruvu, D. and Nesvizhskii, A. I. (2017). MSFragger: ultrafast and comprehensive peptide identification in shotgun proteomics. *Nat. Methods* 14, 513–520.

- Korthauer, K., Kimes, P. K., Duvallet, C., Reyes, A., Subramanian, A., Teng, M., Shukla, C., Alm, E. J. and Hicks, S. C. (2019). A practical guide to methods controlling false discoveries in computational biology. *Genome Biol.* 20, 118.
- Kouzarides, T. (2007). Chromatin Modifications and Their Function. *Cell* 128, 693–705.
- Kugler, J. E., Deng, T. and Bustin, M. (2012). The HMGN family of chromatin-binding proteins: Dynamic modulators of epigenetic processes. *Biochim. Biophys. Acta BBA - Gene Regul. Mech.* 1819, 652–656.
- Kültz, D. (2003). Evolution of the cellular stress proteome: from monophyletic origin to ubiquitous function. *J Exp Biol* 206, 3119–24.
- Kültz, D. (2005). Molecular and evolutionary basis of the cellular stress response. *Annu Rev Physiol* 67, 225–57.
- Kültz, D. (2015). Physiological mechanisms used by fish to cope with salinity stress. *J. Exp. Biol.* 218, 1907–1914.
- Kültz, D. (2020a). Defining biological stress and stress responses based on principles of physics. *J. Exp. Zool. Part Ecol. Integr. Physiol.* 333, 350–358.
- Kültz, D. (2020b). Evolution of cellular stress response mechanisms. *J. Exp. Zool. Part Ecol. Integr. Physiol.* 333, 359–378.
- Kültz, D. and Chakravarty, D. (2001). Hyperosmolality in the form of elevated NaCl but not urea causes DNA damage in murine kidney cells. *Proc. Natl. Acad. Sci.* 98, 1999–2004.
- Kültz, D. and Jürss, K. (1991). Acclimation of chloride cells and Na/K-ATPase to energy deficiency in tilapia (*Oreochromis mossambicus*). *Zool. Jahrb. Abt. Für Allg. Zool. Physiol. Tiere* 95, 39–50.
- Kültz, D., Madhany, S. and Burg, M. B. (1998). Hyperosmolality Causes Growth Arrest of Murine Kidney Cells: INDUCTION OF GADD45 AND GADD153 BY OSMOSENSING VIA STRESS-ACTIVATED PROTEIN KINASE 2 *. *J. Biol. Chem.* 273, 13645–13651.
- Kültz, D., Li, J., Gardell, A. and Sacchi, R. (2013). Quantitative Molecular Phenotyping of Gill Remodeling in a Cichlid Fish Responding to Salinity Stress. *Mol. Cell. Proteomics* 12, 3962–3975.
- Kuo, M. H., Brownell, J. E., Sobel, R. E., Ranalli, T. A., Cook, R. G., Edmondson, D. G., Roth, S. Y. and Allis, C. D. (1996). Transcription-linked acetylation by Gcn5p of histones H3 and H4 at specific lysines. *Nature* 383, 269–272.
- Kwon, C. S., Lee, D., Choi, G. and Chung, W.-I. (2009). Histone occupancy-dependent and -independent removal of H3K27 trimethylation at cold-responsive genes in Arabidopsis. *Plant J.* 60, 112–121.
- Lämke, J., Brzezinka, K., Altmann, S. and Bäurle, I. (2016). A hit-and-run heat shock factor governs sustained histone methylation and transcriptional stress memory. *EMBO J.* 35, 162–175.

- Lanciano, S. and Mirouze, M. (2018). Transposable elements: all mobile, all different, some stress responsive, some adaptive? *Curr. Opin. Genet. Dev.* 49, 106–114.
- Lankinen, M. H., Vilpo, L. M. and Vilpo, J. A. (1996). UV- and γ -irradiation-induced DNA single-strand breaks and their repair in human blood granulocytes and lymphocytes. *Mutat. Res. Mol. Mech. Mutagen.* 352, 31–38.
- Lee, L. R., Wengier, D. L. and Bergmann, D. C. (2019). Cell-type-specific transcriptome and histone modification dynamics during cellular reprogramming in the Arabidopsis stomatal lineage. *Proc. Natl. Acad. Sci.* 116, 21914–21924.
- Leek, J. T., Jager, L., Boca, S. M. and Konopka, T. (2022). swfdr: Estimation of the science-wise false discovery rate and the false discovery rate conditional on covariates.
- Leelatian, N., Doxie, D. B., Greenplate, A. R., Sinnaeve, J., Ihrie, R. A. and Irish, J. M. (2017). Preparing Viable Single Cells from Human Tissue and Tumors for Cytomic Analysis Current Protocols in Molecular Biology UNIT 25C.1. *Curr. Protoc. Mol. Biol.* 118, 25C.1.1-25C.1.23.
- Lerman, D. N., Michalak, P., Helin, A. B., Bettencourt, B. R. and Feder, M. E. (2003). Modification of Heat-Shock Gene Expression in *Drosophila melanogaster* Populations via Transposable Elements. *Mol. Biol. Evol.* 20, 135–144.
- Li, H., Yan, S., Zhao, L., Tan, J., Zhang, Q., Gao, F., Wang, P., Hou, H. and Li, L. (2014). Histone acetylation associated up-regulation of the cell wall related genes is involved in salt stress induced maize root swelling. *BMC Plant Biol.* 14, 105.
- Liepelt, A., Karbe, L. and Westendorf, J. (1995). Induction of DNA strand breaks in rainbow trout *Oncorhynchus mykiss* under hypoxic and hyperoxic conditions. *Aquat. Toxicol.* 33, 177–181.
- Lin, S. and Garcia, B. A. (2012). Examining Histone Posttranslational Modification Patterns by High Resolution Mass Spectrometry. *Methods Enzymol.* 512, 3–28.
- Lindtke, D., Lucek, K., Soria-Carrasco, V., Villoutreix, R., Farkas, T. E., Riesch, R., Dennis, S. R., Gompert, Z. and Nosil, P. (2017). Long-term balancing selection on chromosomal variants associated with cypsis in a stick insect. *Mol. Ecol.* 26, 6189–6205.
- Liu, T., Li, Y., Duan, W., Huang, F. and Hou, X. (2017). Cold acclimation alters DNA methylation patterns and confers tolerance to heat and increases growth rate in *Brassica rapa*. *J. Exp. Bot.* 68, 1213–1224.
- Lothrop, A. P., Torres, M. P. and Fuchs, S. M. (2013). Deciphering post-translational modification codes. *FEBS Lett.* 587, 1247–1257.
- Lu, L., Chen, X., Sanders, D., Qian, S. and Zhong, X. (2015). High-resolution mapping of H4K16 and H3K23 acetylation reveals conserved and unique distribution patterns in Arabidopsis and rice. *Epigenetics* 10, 1044–1053.

- Luense, L. J., Wang, X., Schon, S. B., Weller, A. H., Lin Shiao, E., Bryant, J. M., Bartolomei, M. S., Coutifaris, C., Garcia, B. A. and Berger, S. L. (2016). Comprehensive analysis of histone post-translational modifications in mouse and human male germ cells. *Epigenetics Chromatin* 9, 24.
- Luger, K., Mäder, A. W., Richmond, R. K., Sargent, D. F. and Richmond, T. J. (1997). Crystal structure of the nucleosome core particle at 2.8 Å resolution. *Nature* 389, 251–260.
- Lyko, F. (2001). DNA methylation learns to fly. *Trends Genet.* 17, 169–172.
- Ma, L., Yuan, L., An, J., Barton, M. C., Zhang, Q. and Liu, Z. (2016). Histone H3 lysine 23 acetylation is associated with oncogene TRIM24 expression and a poor prognosis in breast cancer. *Tumor Biol.* 37, 14803–14812.
- Maegawa, S., Hinkal, G., Kim, H. S., Shen, L., Zhang, L., Zhang, J., Zhang, N., Liang, S., Donehower, L. A. and Issa, J.-P. J. (2010). Widespread and tissue specific age-related DNA methylation changes in mice. *Genome Res.* 20, 332–340.
- Mahalingaiah, P. K. S., Ponnusamy, L. and Singh, K. P. (2016). Oxidative stress-induced epigenetic changes associated with malignant transformation of human kidney epithelial cells. *Oncotarget* 8, 11127–11143.
- Makova, K. D. and Hardison, R. C. (2015). The effects of chromatin organization on variation in mutation rates in the genome. *Nat. Rev. Genet.* 16, 213–223.
- Manikkam, M., Haque, M. M., Guerrero-Bosagna, C., Nilsson, E. E. and Skinner, M. K. (2014). Pesticide Methoxychlor Promotes the Epigenetic Transgenerational Inheritance of Adult-Onset Disease through the Female Germline. *PLOS ONE* 9, e102091.
- Martin, E. M. and Fry, R. C. (2018). Environmental Influences on the Epigenome: Exposure-Associated DNA Methylation in Human Populations. *Annu. Rev. Public Health* 39, 309–333.
- Masuda, Y., Hanaoka, F. and Masutani, C. (2016). Translesion DNA Synthesis and Damage Tolerance Pathways. In *DNA Replication, Recombination, and Repair: Molecular Mechanisms and Pathology* (ed. Hanaoka, F.) and Sugawara, K.), pp. 249–304. Tokyo: Springer Japan.
- Matsui, M., Nishigori, C., Imamura, S., Miyachi, Y., Toyokuni, S., Takada, J., Akaboshi, M. and Ishikawa, M. (1999). The Role of Oxidative DNA Damage in Human Arsenic Carcinogenesis: Detection of 8-Hydroxy-2'-Deoxyguanosine in Arsenic-Related Bowen's Disease. *J. Invest. Dermatol.* 113, 26–31.
- McClintock, B. (1984). The significance of responses of the genome to challenge. *Science* 226, 792–801.
- Meagher, R. B. (2014). 'Memory and molecular turnover,' 30 years after inception. *Epigenetics Chromatin* 7, 37.
- Mérot, C., Oomen, R. A., Tigano, A. and Wellenreuther, M. (2020). A Roadmap for Understanding the Evolutionary Significance of Structural Genomic Variation. *Trends Ecol. Evol.* 35, 561–572.

- Metzger, D. C. H. and Schulte, P. M. (2017). Persistent and plastic effects of temperature on DNA methylation across the genome of threespine stickleback (*Gasterosteus aculeatus*). *Proc. R. Soc. B Biol. Sci.* 284, 20171667.
- Michieletto, D., Chiang, M., Coli, D., Papantonis, A., Orlandini, E., Cook, P. R. and Marenduzzo, D. (2018). Shaping epigenetic memory via genomic bookmarking. *Nucleic Acids Res.* 46, 83–93.
- Mihaylova, V. T., Bindra, R. S., Yuan, J., Campisi, D., Narayanan, L., Jensen, R., Giordano, F., Johnson, R. S., Rockwell, S. and Glazer, P. M. (2003). Decreased Expression of the DNA Mismatch Repair Gene Mlh1 under Hypoxic Stress in Mammalian Cells. *Mol. Cell. Biol.* 23, 3265–3273.
- Milholland, B., Dong, X., Zhang, L., Hao, X., Suh, Y. and Vijg, J. (2017). Differences between germline and somatic mutation rates in humans and mice. *Nat. Commun.* 8, 15183.
- Millán-Zambrano, G., Burton, A., Bannister, A. J. and Schneider, R. (2022). Histone post-translational modifications — cause and consequence of genome function. *Nat. Rev. Genet.* 23, 563–580.
- Miller, G. M., Watson, S.-A., Donelson, J. M., McCormick, M. I. and Munday, P. L. (2012). Parental environment mediates impacts of increased carbon dioxide on a coral reef fish. *Nat. Clim. Change* 2, 858–861.
- Miousse, I. R., Chalbot, M.-C. G., Lumen, A., Ferguson, A., Kavouras, I. G. and Koturbash, I. (2015). Response of transposable elements to environmental stressors. *Mutat. Res. Mutat. Res.* 765, 19–39.
- Mitchell, D. L., Nguyen, T. D. and Cleaver, J. E. (1990). Nonrandom induction of pyrimidine-pyrimidone (6-4) photoproducts in ultraviolet-irradiated human chromatin. *J. Biol. Chem.* 265, 5353–5356.
- Moczek, A. P. (2015). Developmental plasticity and evolution—quo vadis? *Heredity* 115, 302–305.
- Mojica, E. A. and Kültz, D. (2022). Physiological mechanisms of stress-induced evolution. *J. Exp. Biol.* 225, jeb243264.
- Mojica, E. A. and Kültz, D. (2023a). A Strategy to Characterize the Global Histone PTM Landscape Within Tissues of Non-Model Organisms. *Rev.*
- Mojica, E. A. and Kültz, D. (2023b). H3K14ac, H3K18ub, and H1K16ub Identified as Salinity-Responsive Histone PTMs in Mozambique Tilapia (*Oreochromis mossambicus*). *Rev.*
- Møller, P., Loft, S., Lundby, C. and Olsen, N. V. (2001). Acute hypoxia and hypoxic exercise induce DNA strand breaks and oxidative DNA damage in humans. *FASEB J.* 15, 1181–1186.
- Moore, L. D., Le, T. and Fan, G. (2013). DNA Methylation and Its Basic Function. *Neuropsychopharmacology* 38, 23–38.
- Moorman, B. P., Inokuchi, M., Yamaguchi, Y., Lerner, D. T., Grau, E. G. and Seale, A. P. (2014). The osmoregulatory effects of rearing Mozambique tilapia in a tidally changing salinity. *Gen. Comp. Endocrinol.* 207, 94–102.

- Moorman, B. P., Lerner, D. T., Grau, E. G. and Seale, A. P. (2015). The effects of acute salinity challenges on osmoregulation in Mozambique tilapia reared in a tidally changing salinity. *J. Exp. Biol.* 218, 731–739.
- Morán, P., Marco-Rius, F., Megías, M., Covelo-Soto, L. and Pérez-Figueroa, A. (2013). Environmental induced methylation changes associated with seawater adaptation in brown trout. *Aquaculture* 392–395, 77–83.
- Morgan, J. D., Sakamoto, T., Grau, E. G. and Iwama, G. K. (1997). Physiological and Respiratory Responses of the Mozambique Tilapia (*Oreochromis mossambicus*) to Salinity Acclimation. *Comp. Biochem. Physiol. A Physiol.* 117, 391–398.
- Moriya, M. (1993). Single-stranded shuttle phagemid for mutagenesis studies in mammalian cells: 8-oxoguanine in DNA induces targeted G.C→T.A transversions in simian kidney cells. *Proc. Natl. Acad. Sci.* 90, 1122–1126.
- Mørkve Knudsen, T., Rezwan, F. I., Jiang, Y., Karmaus, W., Svanes, C. and Holloway, J. W. (2018). Transgenerational and intergenerational epigenetic inheritance in allergic diseases. *J. Allergy Clin. Immunol.* 142, 765–772.
- Naito, K., Zhang, F., Tsukiyama, T., Saito, H., Hancock, C. N., Richardson, A. O., Okumoto, Y., Tanisaka, T. and Wessler, S. R. (2009). Unexpected consequences of a sudden and massive transposon amplification on rice gene expression. *Nature* 461, 1130–1134.
- Nakamura, M. and Takahashi, H. (1973). Gonadal Sex Differentiation in *Tilapia mossambica*, with Special Regard to the Time of Estrogen Treatment Effective in Inducing Complete Feminization of Genetic Males. *Bull. Fac. Fish. Hokkaido Univ.* 24, 13.
- Nettle, D. and Bateson, M. (2015). Adaptive developmental plasticity: what is it, how can we recognize it and when can it evolve? *Proc. R. Soc. B Biol. Sci.* 282, 20151005.
- Nguyen, P., Sýkorová, M., Šíchová, J., Kůta, V., Dalíková, M., Čapková Frydrychová, R., Neven, L. G., Sahara, K. and Marec, F. (2013). Neo-sex chromosomes and adaptive potential in tortricid pests. *Proc. Natl. Acad. Sci.* 110, 6931–6936.
- Nilsson, E. E., Sadler-Riggelman, I. and Skinner, M. K. (2018). Environmentally induced epigenetic transgenerational inheritance of disease. *Environ. Epigenetics* 4, dvy016.
- Noberini, R., Robusti, G. and Bonaldi, T. (2022). Mass spectrometry-based characterization of histones in clinical samples: applications, progress, and challenges. *FEBS J.* 289, 1191–1213.
- Noble, D. (2013). Physiology is rocking the foundations of evolutionary biology. *Exp. Physiol.* 98, 1235–1243.
- Noble, D. (2021). The Illusions of the Modern Synthesis. *Biosemitics* 14, 5–24.
- Norouzitalab, P., Baruah, K., Vandegehuchte, M., Stappen, G. V., Catania, F., Bussche, J. V., Vanhaecke, L., Sorgeloos, P. and Bossier, P. (2014). Environmental heat stress induces epigenetic

- transgenerational inheritance of robustness in parthenogenetic *Artemia* model. *FASEB J.* 28, 3552–3563.
- Norouzitalab, P., Baruah, K., Vanrompay, D. and Bossier, P. (2019). Can epigenetics translate environmental cues into phenotypes? *Sci. Total Environ.* 647, 1281–1293.
- Norton, V. G., Imai, B. S., Yau, P. and Bradbury, E. M. (1989). Histone acetylation reduces nucleosome core particle linking number change. *Cell* 57, 449–457.
- Nowak, M. D., Birkeland, S., Mandáková, T., Choudhury, R. R., Guo, X., Gustafsson, A. L. S., Gizaw, A., Schrøder-Nielsen, A., Fracassetti, M., Brysting, A. K., et al. (2021). The genome of *Draba nivalis* shows signatures of adaptation to the extreme environmental stresses of the Arctic. *Mol. Ecol. Resour.* 21, 661–676.
- Okano, M., Bell, D. W., Haber, D. A. and Li, E. (1999). DNA Methyltransferases Dnmt3a and Dnmt3b Are Essential for De Novo Methylation and Mammalian Development. *Cell* 99, 247–257.
- Önder, Ö., Sidoli, S., Carroll, M. and Garcia, B. A. (2015). Progress in epigenetic histone modification analysis by mass spectrometry for clinical investigations. *Expert Rev. Proteomics* 12, 499–517.
- Ortega-Recalde, O., Goikoetxea, A., Hore, T., Todd, E. and Gemmell, N. (2020). The Genetics and Epigenetics of Sex Change in Fish. *Annu. Rev. Anim. Biosci.* 8,.
- Østrup, O., Reiner, A. H., Aleström, P. and Collas, P. (2014). The specific alteration of histone methylation profiles by DZNep during early zebrafish development. *Biochim. Biophys. Acta BBA - Gene Regul. Mech.* 1839, 1307–1315.
- Ou, X., Zhang, Y., Xu, C., Lin, X., Zang, Q., Zhuang, T., Jiang, L., Wettstein, D. von and Liu, B. (2012). Transgenerational Inheritance of Modified DNA Methylation Patterns and Enhanced Tolerance Induced by Heavy Metal Stress in Rice (*Oryza sativa* L.). *PLOS ONE* 7, e41143.
- Paaby, A. B. and Rockman, M. V. (2014). Cryptic genetic variation, evolution's hidden substrate. *Nat. Rev. Genet.* 15, 247–258.
- Pappalardo, A. M., Ferrito, V., Biscotti, M. A., Canapa, A. and Capriglione, T. (2021). Transposable Elements and Stress in Vertebrates: An Overview. *Int. J. Mol. Sci.* 22, 1970.
- Park, P. J. (2009). ChIP–seq: advantages and challenges of a maturing technology. *Nat. Rev. Genet.* 10, 669–680.
- Paul, A., Dasgupta, P., Roy, D. and Chaudhuri, S. (2017). Comparative analysis of Histone modifications and DNA methylation at OsBZ8 locus under salinity stress in IR64 and Nonabokra rice varieties. *Plant Mol. Biol.* 95, 63–88.
- Pellestor, F. and Gatinois, V. (2020). Chromoanagenesis: a piece of the macroevolution scenario. *Mol. Cytogenet.* 13, 3.
- Perez, M. F. and Lehner, B. (2019). Intergenerational and transgenerational epigenetic inheritance in animals. *Nat. Cell Biol.* 21, 143–151.

- Perry, G. H., Dominy, N. J., Claw, K. G., Lee, A. S., Fiegler, H., Redon, R., Werner, J., Villanea, F. A., Mountain, J. L., Misra, R., et al. (2007). Diet and the evolution of human amylase gene copy number variation. *Nat. Genet.* 39, 1256–1260.
- Pham, A.-D. and Sauer, F. (2000). Ubiquitin-Activating/Conjugating Activity of TAFII250, a Mediator of Activation of Gene Expression in *Drosophila*. *Science* 289, 2357–2360.
- Pilzecker, B. and Jacobs, H. (2019). Mutating for Good: DNA Damage Responses During Somatic Hypermutation. *Front. Immunol.* 10, 438.
- Pilzecker, B., Buoninfante, O. A. and Jacobs, H. (2019). DNA damage tolerance in stem cells, ageing, mutagenesis, disease and cancer therapy. *Nucleic Acids Res.* 47, 7163–7181.
- Pino, L. K., Searle, B. C., Bollinger, J. G., Nunn, B., MacLean, B. and MacCoss, M. J. (2017). The Skyline ecosystem: Informatics for quantitative mass spectrometry proteomics. *Mass Spectrom Rev* 39, 229–244.
- Porter, E. G., Dhiman, A., Chowdhury, B., Carter, B. C., Lin, H., Stewart, J. C., Kazemian, M., Wendt, M. K. and Dykhuizen, E. C. (2019). PBRM1 Regulates Stress Response in Epithelial Cells. *iScience* 15, 196–210.
- Qin, W., Wolf, P., Liu, N., Link, S., Smets, M., Mastra, F. L., Forné, I., Pichler, G., Hörl, D., Fellingner, K., et al. (2015). DNA methylation requires a DNMT1 ubiquitin interacting motif (UIM) and histone ubiquitination. *Cell Res.* 25, 911–929.
- R Core Team (2022). R: A Language and Environment for Statistical Computing.
- Radman, M. (1975). SOS Repair Hypothesis: Phenomenology of an Inducible DNA Repair Which is Accompanied by Mutagenesis. In *Molecular Mechanisms for Repair of DNA: Part A* (ed. Hanawalt, P. C.) and Setlow, R. B.), pp. 355–367. Boston, MA: Springer US.
- Raisner, R., Kharbanda, S., Jin, L., Jeng, E., Chan, E., Merchant, M., Haverty, P. M., Bainer, R., Cheung, T., Arnott, D., et al. (2018). Enhancer Activity Requires CBP/P300 Bromodomain-Dependent Histone H3K27 Acetylation. *Cell Rep.* 24, 1722–1729.
- Rajesh Kumar, T., Doreswamy, K., Shrilatha, B., and Muralidhara (2002). Oxidative stress associated DNA damage in testis of mice: induction of abnormal sperms and effects on fertility. *Mutat. Res. Toxicol. Environ. Mutagen.* 513, 103–111.
- Rashid, Md. M., Vaishnav, A., Verma, R. K., Sharma, P., Suprasanna, P. and Gaur, R. K. (2022). Epigenetic regulation of salinity stress responses in cereals. *Mol. Biol. Rep.* 49, 761–772.
- Rego, C., Balanyà, J., Fragata, I., Matos, M., Rezende, E. L. and Santos, M. (2010). Clinal Patterns of Chromosomal Inversion Polymorphisms in *Drosophila Subobscura* Are Partly Associated with Thermal Preferences and Heat Stress Resistance. *Evolution* 64, 385–397.
- Rey, O., Danchin, E., Mirouze, M., Loot, C. and Blanchet, S. (2016). Adaptation to Global Change: A Transposable Element–Epigenetics Perspective. *Trends Ecol. Evol.* 31, 514–526.

- Rocca, K. A., Gray, E. M., Costantini, C. and Besansky, N. J. (2009). 2La chromosomal inversion enhances thermal tolerance of *Anopheles gambiae* larvae. *Malar. J.* 8, 147.
- Root, L. and Kültz, D. (2022). *Gill proteome networks explain energy homeostasis during salinity stress in Oreochromis mossambicus*. Preprints.
- Root, L., Campo, A., MacNiven, L., Cnaani, A. and Kültz, D. (2021a). A data-independent acquisition (DIA) assay library for quantitation of environmental effects on the kidney proteome of *Oreochromis niloticus*. *Mol Ecol Approaches* 21, 2486–2503.
- Root, L., Campo, A., MacNiven, L., Con, P., Cnaani, A. and Kültz, D. (2021b). Nonlinear effects of environmental salinity on the gill transcriptome versus proteome of *Oreochromis niloticus* modulate epithelial cell turnover. *Genomics* 113, 3235–3249.
- Rosenberg, S. M., Shee, C., Frisch, R. L. and Hastings, P. J. (2012). Stress-induced mutation via DNA breaks in *Escherichia coli*: A molecular mechanism with implications for evolution and medicine. *BioEssays* 34, 885–892.
- Rugg-Gunn, P. J., Cox, B. J., Ralston, A. and Rossant, J. (2010). Distinct histone modifications in stem cell lines and tissue lineages from the early mouse embryo. *Proc. Natl. Acad. Sci.* 107, 10783–10790.
- Rusk, N. (2009). Reverse CHIP. *Nat. Methods* 6, 187–187.
- Rutherford, S. L. and Lindquist, S. (1998). Hsp90 as a capacitor for morphological evolution. *Nature* 396, 336–342.
- Ryan, C. P., Brownlie, J. C. and Whyard, S. (2016). Hsp90 and Physiological Stress Are Linked to Autonomous Transposon Mobility and Heritable Genetic Change in Nematodes. *Genome Biol. Evol.* 8, 3794–3805.
- Ryu, T., Veilleux, H. D., Donelson, J. M., Munday, P. L. and Ravasi, T. (2018). The epigenetic landscape of transgenerational acclimation to ocean warming. *Nat. Clim. Change* 8, 504–509.
- Salinas, S. and Munch, S. B. (2012). Thermal legacies: transgenerational effects of temperature on growth in a vertebrate. *Ecol. Lett.* 15, 159–163.
- Sallmyr, A., Fan, J. and Rassool, F. V. (2008). Genomic instability in myeloid malignancies: Increased reactive oxygen species (ROS), DNA double strand breaks (DSBs) and error-prone repair. *Cancer Lett.* 270, 1–9.
- Samodova, D., Hosfield, C. M., Cramer, C. N., Giuli, M. V., Cappellini, E., Franciosa, G., Rosenblatt, M. M., Kelstrup, C. D. and Olsen, J. V. (2020). ProAlanase is an Effective Alternative to Trypsin for Proteomics Applications and Disulfide Bond Mapping. *Mol. Cell. Proteomics* 19, 2139–2157.
- Samson, M., Jow, M. M., Wong, C. C. L., Fitzpatrick, C., Aslanian, A., Saucedo, I., Estrada, R., Ito, T., Park, S. R., Iijima, J. R. Y., et al. (2014). The Specification and Global Reprogramming of Histone Epigenetic Marks during Gamete Formation and Early Embryo Development in *C. elegans*. *PLOS Genet.* 10, e1004588.

- Sani, E., Herzyk, P., Perrella, G., Colot, V. and Amtmann, A. (2013). Hyperosmotic priming of Arabidopsis seedlings establishes a long-term somatic memory accompanied by specific changes of the epigenome. *Genome Biol.* 14, R59.
- Saperas, N., Chiva, M., Pfeiffer, D. C., Kasinsky, H. E. and Ausió, J. (1997). Sperm Nuclear Basic Proteins (SNBPs) of Agnathans and Chondrichthyans: Variability and Evolution of Sperm Proteins in Fish. *J. Mol. Evol.* 44, 422–431.
- Sardella, B. A. and Brauner, C. J. (2008). The effect of elevated salinity on ‘California’ Mozambique tilapia (*Oreochromis mossambicus* x *O. urolepis hornorum*) metabolism. *Comp. Biochem. Physiol. Part C Toxicol. Pharmacol.* 148, 430–436.
- Sardella, B. A. and Brauner, C. J. (2016). The Osmo-respiratory Compromise in Fish: The Effects of Physiological State and the Environment. In *Fish Respiration and Environment* (ed. Fernandes, M. N.), Rantin, F. T.), Glass, M. L.), and Kapoor, B. G.), pp. 147–166. CRC Press.
- Schaefer, J. and Ryan, A. (2006). Developmental plasticity in the thermal tolerance of zebrafish *Danio rerio*. *J. Fish Biol.* 69, 722–734.
- Schermelleh, L., Haemmer, A., Spada, F., Rösing, N., Meilinger, D., Rothbauer, U., Cardoso, M. C. and Leonhardt, H. (2007). Dynamics of Dnmt1 interaction with the replication machinery and its role in postreplicative maintenance of DNA methylation. *Nucleic Acids Res.* 35, 4301–4312.
- Schiltz, R. L., Mizzen, C. A., Vassilev, A., Cook, R. G., Allis, C. D. and Nakatani, Y. (1999). Overlapping but Distinct Patterns of Histone Acetylation by the Human Coactivators p300 and PCAF within Nucleosomal Substrates *. *J. Biol. Chem.* 274, 1189–1192.
- Schneider-Poetsch, T. and Yoshida, M. (2018). Along the Central Dogma—Controlling Gene Expression with Small Molecules. *Annu. Rev. Biochem.* 87, 391–420.
- Schreck, C. B. and Tort, L. (2016). The Concept of Stress in Fish. In *Fish Physiology*, pp. 1–34. Elsevier.
- Schubert, I. and Vu, G. T. H. (2016). Genome Stability and Evolution: Attempting a Holistic View. *Trends Plant Sci.* 21, 749–757.
- Searle, B. C., Pino, L. K., Egertson, J. D., Ting, Y. S., Lawrence, R. T., MacLean, B. X., Villén, J. and MacCoss, M. J. (2018). Chromatogram libraries improve peptide detection and quantification by data independent acquisition mass spectrometry. *Nat. Commun.* 9, 5128.
- Searle, B. C., Swearingen, K. E., Barnes, C. A., Schmidt, T., Gessulat, S., Küster, B. and Wilhelm, M. (2020). Generating high quality libraries for DIA MS with empirically corrected peptide predictions. *Nat. Commun.* 11, 1548.
- Seong, K.-H., Li, D., Shimizu, H., Nakamura, R. and Ishii, S. (2011). Inheritance of Stress-Induced, ATF-2-Dependent Epigenetic Change. *Cell* 145, 1049–1061.
- Sharma, A. (2014). Bioinformatic analysis revealing association of exosomal mRNAs and proteins in epigenetic inheritance. *J. Theor. Biol.* 357, 143–149.

- Shechter, D., Dormann, H. L., Allis, C. D. and Hake, S. B. (2007). Extraction, purification and analysis of histones. *Nat. Protoc.* 2, 1445–1457.
- Shen, M. M. (2013). Chromoplexy: A New Category of Complex Rearrangements in the Cancer Genome. *Cancer Cell* 23, 567–569.
- Shi, Y. Y., Huang, Z. Y., Zeng, Z. J., Wang, Z. L., Wu, X. B. and Yan, W. Y. (2011). Diet and Cell Size Both Affect Queen-Worker Differentiation through DNA Methylation in Honey Bees (*Apis mellifera*, Apidae). *PLOS ONE* 6, e18808.
- Sievers, F. and Higgins, D. G. (2018). Clustal Omega for making accurate alignments of many protein sequences. *Protein Sci. Publ. Protein Soc.* 27, 135–145.
- Skinner, M. K. (2011). Environmental epigenetic transgenerational inheritance and somatic epigenetic mitotic stability. *Epigenetics* 6, 838–842.
- Skinner, M. K. (2015). Environmental Epigenetics and a Unified Theory of the Molecular Aspects of Evolution: A Neo-Lamarckian Concept that Facilitates Neo-Darwinian Evolution. *Genome Biol. Evol.* 7, 1296–1302.
- Skinner, M. K., Manikkam, M., Tracey, R., Guerrero-Bosagna, C., Haque, M. and Nilsson, E. E. (2013). Ancestral dichlorodiphenyltrichloroethane (DDT) exposure promotes epigenetic transgenerational inheritance of obesity. *BMC Med.* 11, 228.
- Slowikowski, K. (2021). ggrepel: Automatically Position Non-Overlapping Text Labels with “ggplot2.”
- Smith, Z. D. and Meissner, A. (2013). DNA methylation: roles in mammalian development. *Nat. Rev. Genet.* 14, 204–220.
- Sokol, A., Kwiatkowska, A., Jerzmanowski, A. and Prymakowska-Bosak, M. (2007). Up-regulation of stress-inducible genes in tobacco and Arabidopsis cells in response to abiotic stresses and ABA treatment correlates with dynamic changes in histone H3 and H4 modifications. *Planta* 227, 245–254.
- Song, Y., Jia, Z., Hou, Y., Ma, X., Li, L., Jin, X. and An, L. (2020). Roles of DNA Methylation in Cold Priming in Tartary Buckwheat. *Front. Plant Sci.* 11, 2022.
- Soon, L. L. L., Ausio, J., Breed, W. G., Power, J. H. T. and Muller, S. (1997). Isolation of histones and related chromatin structures from spermatozoa nuclei of a dasyurid marsupial, *Sminthopsis crassicaudata*. *J. Exp. Zool.* 278, 322–332.
- Stickney, R. R. (1986). Tilapia Tolerance of Saline Waters: A Review. *Progress. Fish-Cult.* 48, 161–167.
- Strader, M. E., Wong, J. M., Kozal, L. C., Leach, T. S. and Hofmann, G. E. (2019). Parental environments alter DNA methylation in offspring of the purple sea urchin, *Strongylocentrotus purpuratus*. *J. Exp. Mar. Biol. Ecol.* 517, 54–64.

- Sun, W., Dong, H., Becker, A. S., Dapito, D. H., Modica, S., Grandl, G., Opitz, L., Efthymiou, V., Straub, L. G., Sarker, G., et al. (2018). Cold-induced epigenetic programming of the sperm enhances brown adipose tissue activity in the offspring. *Nat. Med.* 24, 1372–1383.
- Sutton, T., Baumann, U., Hayes, J., Collins, N. C., Shi, B.-J., Schnurbusch, T., Hay, A., Mayo, G., Pallotta, M., Tester, M., et al. (2007). Boron-Toxicity Tolerance in Barley Arising from Efflux Transporter Amplification. *Science* 318, 1446–1449.
- Tanou, G., Molassiotis, A. and Diamantidis, G. (2009). Induction of reactive oxygen species and necrotic death-like destruction in strawberry leaves by salinity. *Environ. Exp. Bot.* 65, 270–281.
- Thorslund, T., Ripplinger, A., Hoffmann, S., Wild, T., Uckelmann, M., Villumsen, B., Narita, T., Sixma, T. K., Choudhary, C., Bekker-Jensen, S., et al. (2015). Histone H1 couples initiation and amplification of ubiquitin signalling after DNA damage. *Nature* 527, 389–393.
- Tian, L., Cheng, Y.-Q., Shan, Z.-W., Li, J., Wang, C.-C., Han, X.-D., Sun, J. and Ma, E. (2012). Approaching the ideal elastic limit of metallic glasses. *Nat. Commun.* 3, 609.
- Tousson, E., Ali, E. M. M., Ibrahim, W. and Mansour, M. A. (2011). Proliferating Cell Nuclear Antigen as a Molecular Biomarker for Spermatogenesis in PTU-Induced Hypothyroidism of Rats. *Reprod. Sci.* 18, 679–686.
- Tsui, C., Inouye, C., Levy, M., Lu, A., Florens, L., Washburn, M. P. and Tjian, R. (2018). dCas9-targeted locus-specific protein isolation method identifies histone gene regulators. *Proc. Natl. Acad. Sci.* 115, E2734–E2741.
- Van Meter, M., Kashyap, M., Rezazadeh, S., Geneva, A. J., Morello, T. D., Seluanov, A. and Gorbunova, V. (2014). SIRT6 represses LINE1 retrotransposons by ribosylating KAP1 but this repression fails with stress and age. *Nat. Commun.* 5, 5011.
- Vandegheuchte, M. B., De Coninck, D., Vandenbrouck, T., De Coen, W. M. and Janssen, C. R. (2010). Gene transcription profiles, global DNA methylation and potential transgenerational epigenetic effects related to Zn exposure history in *Daphnia magna*. *Environ. Pollut.* 158, 3323–3329.
- Visel, A., Blow, M. J., Li, Z., Zhang, T., Akiyama, J. A., Holt, A., Plajzer-Frick, I., Shoukry, M., Wright, C., Chen, F., et al. (2009). ChIP-seq accurately predicts tissue-specific activity of enhancers. *Nature* 457, 854–858.
- Walker, C. and Burggren, W. (2020). Remodeling the epigenome and (epi)cytoskeleton: a new paradigm for co-regulation by methylation. *J. Exp. Biol.* 223, jeb220632.
- Wang, W.-N., Zhou, J., Wang, P., Tian, T.-T., Zheng, Y., Liu, Y., Mai, W. and Wang, A.-L. (2009). Oxidative stress, DNA damage and antioxidant enzyme gene expression in the Pacific white shrimp, *Litopenaeus vannamei* when exposed to acute pH stress. *Comp. Biochem. Physiol. Part C Toxicol. Pharmacol.* 150, 428–435.
- Wapenaar, H. and Dekker, F. J. (2016). Histone acetyltransferases: challenges in targeting bi-substrate enzymes. *Clin. Epigenetics* 8, 59.

- Weaver, I. C. G., Cervoni, N., Champagne, F. A., D'Alessio, A. C., Sharma, S., Seckl, J. R., Dymov, S., Szyf, M. and Meaney, M. J. (2004). Epigenetic programming by maternal behavior. *Nat. Neurosci.* 7, 847–854.
- Weishaupt, H., Sigvardsson, M. and Attema, J. L. (2010). Epigenetic chromatin states uniquely define the developmental plasticity of murine hematopoietic stem cells. *Blood* 115, 247–256.
- Weismann, A. (1890). Prof. Weismann's Theory of Heredity. *Nature* 41, 317–323.
- Wellenreuther, M. and Bernatchez, L. (2018). Eco-Evolutionary Genomics of Chromosomal Inversions. *Trends Ecol. Evol.* 33, 427–440.
- Whitfield, A. K. (2015). Why are there so few freshwater fish species in most estuaries? *J. Fish Biol.* 86, 1227–1250.
- Whitfield, A. K. and Blaber, S. J. M. (1979). The distribution of the freshwater cichlid *Sarotherodon mossambicus* in estuarine systems. *Environ. Biol. Fishes* 4, 77–81.
- Whittle, C. A., Otto, S. P., Johnston, M. O. and Krochko, J. E. (2009). Adaptive epigenetic memory of ancestral temperature regime in *Arabidopsis thaliana*. *Botany* 87, 650–657.
- Wicker, T., Sabot, F., Hua-Van, A., Bennetzen, J. L., Capy, P., Chalhoub, B., Flavell, A., Leroy, P., Morgante, M., Panaud, O., et al. (2007). A unified classification system for eukaryotic transposable elements. *Nat. Rev. Genet.* 8, 973–982.
- Wickham, H. (2016). *ggplot2: Elegant Graphics for Data Analysis*. Springer-Verlag New York.
- Wickham, H., Averick, M., Bryan, J., Chang, W., McGowan, L. D., François, R., Grolemund, G., Hayes, A., Henry, L., Hester, J., et al. (2019). Welcome to the Tidyverse. *J. Open Source Softw.* 4, 1686.
- Wilke, C. (2020). cowplot: Streamlined Plot Theme and Plot Annotations for “ggplot2.”
- Wimmer, M. E., Vassoler, F. M., White, S. L., Schmidt, H. D., Sidoli, S., Han, Y., Garcia, B. A. and Pierce, R. C. (2019). Impaired cocaine-induced behavioral plasticity in the male offspring of cocaine-experienced sires. *Eur. J. Neurosci.* 49, 1115–1126.
- Wong, J. M., Kozal, L. C., Leach, T. S., Hoshijima, U. and Hofmann, G. E. (2019). Transgenerational effects in an ecological context: Conditioning of adult sea urchins to upwelling conditions alters maternal provisioning and progeny phenotype. *J. Exp. Mar. Biol. Ecol.* 517, 65–77.
- Woodhouse, R. M. and Ashe, A. (2020). How do histone modifications contribute to transgenerational epigenetic inheritance in *C. elegans*? *Biochem. Soc. Trans.* 48, 1019–1034.
- Wu, T., Pi, E.-X., Tsai, S.-N., Lam, H.-M., Sun, S.-M., Kwan, Y. W. and Ngai, S.-M. (2011). GmPHD5 acts as an important regulator for crosstalk between histone H3K4 di-methylation and H3K14 acetylation in response to salinity stress in soybean. *BMC Plant Biol.* 11, 178.

- Wu, Z. E., Kruger, M. C., Cooper, G. J. S., Sequeira, I. R., McGill, A.-T., Poppitt, S. D. and Fraser, K. (2022). Dissecting the relationship between plasma and tissue metabolome in a cohort of women with obesity: Analysis of subcutaneous and visceral adipose, muscle, and liver. *FASEB J.* 36, e22371.
- Wysocki, L., Manser, T. and Gefter, M. L. (1986). Somatic evolution of variable region structures during an immune response. *Proc. Natl. Acad. Sci.* 83, 1847–1851.
- Xie, L., Korkmaz, K. S., Braun, K. and Bock, J. (2013). Early life stress-induced histone acetylations correlate with activation of the synaptic plasticity genes *Arc* and *Egr1* in the mouse hippocampus. *J. Neurochem.* 125, 457–464.
- Xue, C., Liu, S., Chen, C., Zhu, J., Yang, X., Zhou, Y., Guo, R., Liu, X. and Gong, Z. (2018). Global Proteome Analysis Links Lysine Acetylation to Diverse Functions in *Oryza Sativa*. *Proteomics* 18, 1700036.
- Yamanaka, K., Takabayashi, F., Mizoi, M., An, Y., Hasegawa, A. and Okada, S. (2001). Oral Exposure of Dimethylarsinic Acid, a Main Metabolite of Inorganic Arsenics, in Mice Leads to an Increase in 8-Oxo-2'-deoxyguanosine Level, Specifically in the Target Organs for Arsenic Carcinogenesis. *Biochem. Biophys. Res. Commun.* 287, 66–70.
- Yang, J., Horton, J. R., Akdemir, K. C., Li, J., Huang, Y., Kumar, J., Blumenthal, R. M., Zhang, X. and Cheng, X. (2021). Preferential CEBP binding to T:G mismatches and increased C-to-T human somatic mutations. *Nucleic Acids Res.* 49, 5084–5094.
- Yaschenko, A. E., Fenech, M., Mazzoni-Putman, S., Alonso, J. M. and Stepanova, A. N. (2022). Deciphering the molecular basis of tissue-specific gene expression in plants: Can synthetic biology help? *Curr. Opin. Plant Biol.* 68, 102241.
- Yasuda, K., Ito, M., Sugita, T., Tsukiyama, T., Saito, H., Naito, K., Teraishi, M., Tanisaka, T. and Okumoto, Y. (2013). Utilization of transposable element mPing as a novel genetic tool for modification of the stress response in rice. *Mol. Breed.* 32, 505–516.
- Ye, C. J., Liu, G. and Heng, H. H. (2018). Experimental Induction of Genome Chaos. In *Chromothripsis: Methods and Protocols* (ed. Pellestor, F.), pp. 337–352. Totowa: Humana Press Inc.
- Yoon, J.-H., Bhatia, G., Prakash, S. and Prakash, L. (2010). Error-free replicative bypass of thymine glycol by the combined action of DNA polymerases κ and ζ in human cells. *Proc. Natl. Acad. Sci.* 107, 14116–14121.
- Yuan, L., Liu, X., Luo, M., Yang, S. and Wu, K. (2013). Involvement of Histone Modifications in Plant Abiotic Stress Responses. *J. Integr. Plant Biol.* 55, 892–901.
- Zee, B. M., Levin, R. S., DiMaggio, P. A. and Garcia, B. A. (2010). Global turnover of histone post-translational modifications and variants in human cells. *Epigenetics Chromatin* 3, 22.
- Zemach, A., McDaniel, I. E., Silva, P. and Zilberman, D. (2010). Genome-Wide Evolutionary Analysis of Eukaryotic DNA Methylation. *Science* 328, 916–919.
- Zempleni, J., Chew, Y. C., Bao, B., Pestinger, V. and Wijeratne, S. S. K. (2009). Repression of Transposable Elements by Histone Biotinylation. *J. Nutr.* 139, 2389–2392.

- Zhang, L., Eugeni, E. E., Parthun, M. R. and Freitas, M. A. (2003). Identification of novel histone post-translational modifications by peptide mass fingerprinting. *Chromosoma* 112, 77–86.
- Zhang, Y., Zhang, S., Liu, Z., Zhang, L. and Zhang, W. (2013). Epigenetic Modifications During Sex Change Repress Gonadotropin Stimulation of Cyp19a1a in a Teleost Ricefield Eel (*Monopterus albus*). *Endocrinology* 154, 2881–2890.
- Zhang, D., Tang, Z., Huang, H., Zhou, G., Cui, C., Weng, Y., Liu, W., Kim, S., Lee, S., Perez-Neut, M., et al. (2019). Metabolic regulation of gene expression by histone lactylation. *Nature* 574, 575–580.
- Zhang, H.-H., Peccoud, J., Xu, M.-R.-X., Zhang, X.-G. and Gilbert, C. (2020). Horizontal transfer and evolution of transposable elements in vertebrates. *Nat. Commun.* 11, 1362.
- Zhang, W., Tan, X., Lin, S., Gou, Y., Han, C., Zhang, C., Ning, W., Wang, C. and Xue, Y. (2022). CPLM 4.0: an updated database with rich annotations for protein lysine modifications. *Nucleic Acids Res.* 50, D451–D459.
- Zhao, Y. and Garcia, B. A. (2015). Comprehensive Catalog of Currently Documented Histone Modifications. *Cold Spring Harb. Perspect. Biol.* 7, a025064.
- Zheng, X., Chen, L., Li, M., Lou, Q., Xia, H., Wang, P., Li, T., Liu, H. and Luo, L. (2013). Transgenerational Variations in DNA Methylation Induced by Drought Stress in Two Rice Varieties with Distinguished Difference to Drought Resistance. *PLOS ONE* 8, e80253.
- Zheng, M., Liu, X., Lin, J., Liu, X., Wang, Z., Xin, M., Yao, Y., Peng, H., Zhou, D.-X., Ni, Z., et al. (2019). Histone acetyltransferase GCN5 contributes to cell wall integrity and salt stress tolerance by altering the expression of cellulose synthesis genes. *Plant J.* 97, 587–602.
- Zheng, H.-T., Zhuang, Z.-X., Chen, C.-J., Liao, H.-Y., Chen, H.-L., Hsueh, H.-C., Chen, C.-F., Chen, S.-E. and Huang, S.-Y. (2021). Effects of acute heat stress on protein expression and histone modification in the adrenal gland of male layer-type country chickens. *Sci. Rep.* 11, 6499.
- Zhou, H.-L., Luo, G., Wise, J. A. and Lou, H. (2014). Regulation of alternative splicing by local histone modifications: potential roles for RNA-guided mechanisms. *Nucleic Acids Res.* 42, 701–713.
- Zhou, Y., He, F., Pu, W., Gu, X., Wang, J. and Su, Z. (2020). The Impact of DNA Methylation Dynamics on the Mutation Rate During Human Germline Development. *G3 GenesGenomesGenetics* 10, 3337–3346.
- Zhu, J., Adli, M., Zou, J. Y., Verstappen, G., Coyne, M., Zhang, X., Durham, T., Miri, M., Deshpande, V., De Jager, P. L., et al. (2013). Genome-wide Chromatin State Transitions Associated with Developmental and Environmental Cues. *Cell* 152, 642–654.